Stability improvement of plant extracts by modification of the manufacturing process with special focus on *Sennae fructus*

Dissertation

with the aim of achieving a doctoral degree

at the Faculty of Mathematics, Informatics and Natural Sciences

Department of Chemistry

Universität Hamburg

submitted by

Kira-Isabel Zier

Hamburg 2020

The experimental studies and the preparation of this thesis were carried out between January 2015 and October 2019 in the Department of Chemistry at the University of Hamburg, in the division of Pharmaceutical Technology, on the initiative and under supervision of Professor Dr. Claudia S. Leopold.

Zusammenfassung

Arzneimittel, deren Wirkstoffe aus Pflanzen oder Pflanzenteilen gewonnen werden, sind als vollwertige Arzneimittel zu betrachten und müssen dieselben rechtlichen Anforderungen hinsichtlich Wirksamkeit, Unbedenklichkeit und gleichbleibender Qualität erfüllen wie Arzneimittel mit chemisch definierten Wirkstoffen. Die analytischen Prüfmethoden entwickeln sich stetig weiter, wodurch die Qualität von pflanzlichen Arzneimitteln immer genauer definiert werden kann. Aufgrund dessen müssen die Monografien des Europäischen Arzneibuchs immer wieder an den aktuellen Wissenstand angepasst werden. Das Ziel der vorliegenden Dissertation war es, an dem aktuellen Beispiel der laxierend wirkenden Arzneipflanze Senna durch die Untersuchung geeigneter analytischer Methoden und Herstellungs-prozesse eine stabile Darreichungsform nach dem aktuellen wissenschaftlichen Erkenntnisstand zu entwickeln.

Zur Bestimmung der Hydroxyanthracenderivate (Sennoside), welche die wirksamen Inhaltsstoffe von Senna darstellen, schlugen Mitglieder der Expertengruppe 13 A der Europäischen Arzneibuchkommission 2015 vor, den spektralphotometrischen Assay durch eine HPLC-Methode zu ersetzen. Daher wurden in der vorliegenden Arbeit HPLC-UV(DAD)-ESI/MS- und HPLC-ESI/MS/MS-Messungen durchgeführt, um die Effizienz dieser vorgeschlagenen Methode hinsichtlich Trennung und Zuordnung der Bestandteile von Extrakten aus Sennesfrüchten zu bewerten. Eine Auswertung aller Hydroxyanthracenderivate wurde durchgeführt, um ausreichende Informationen über die Qualität der Extrakte zu erlangen. Eine Unterscheidung zwischen den Extrakten der Arten Cassia angustifolia und Cassia acutifolia mittels Tinnevellin, Tinnevellin-6-glucosid, 6-Hydroxymusicin-glucosid und eine geringe Menge einer unbekannten Substanz war möglich. Gegenwärtig stammt der Hauptanteil der Sennesfrüchte

aufgrund ihres geringen Aflatoxingehalts aus neu erschlossenen Anbaugebieten in Nordindien. Dieses Pflanzenmaterial weist hinsichtlich Morphologie und Inhaltsstoffzusammensetzung die Eigenschaften von beiden Arten auf.

Stabilitätstests wurden mit sprühgetrockneten wässrigen Extrakten aus Sennesfrüchten durchgeführt. Die Herstellung erfolgte hierbei mit unterschiedlichen Zerstäubungsdrücken, Pumpraten und Einlasstemperaturen. Diese Prozessparameter hatten Auswirkungen auf die Partikelgröße, die Partikeloberfläche (glatt, faltig), die Partikelform (Golfball, Doughnut, Scherbe), die wahre Dichte sowie die Restfeuchte. Stabilitätsmindernde Faktoren waren der Feuchtigkeitsgehalt der Proben und deren Hygroskopizität, sowie die Partikelmorphologie. Eine Erhöhung des Zerstäubungsdrucks hatte den größten Einfluss auf die Abnahme der Partikelgröße und Restfeuchte. Eine Erhöhung der Einlasstemperatur führte ebenfalls zu einer Verringerung der Restfeuchte sowie zu einer Erhöhung des Anteils der Partikel mit glatter Oberfläche. Ein Anstieg der Pumpgeschwindigkeit ließ stabile Hohlkugeln entstehen, jedoch mit erhöhter Restfeuchte. Somit hatte die Einlasstemperatur während der Sprühtrocknung den größten positiven Effekt auf die Partikeleigenschaften und die Stabilität der Sennoside als wirksame Bestandteile der Sennesfrüchte.

Des Weiteren wurden sprühgetrocknete und gefriergetrocknete Extrakte aus Sennesfrüchten hinsichtlich der Sennosidstabilität und des Einflusses des Hilfsstoffes Maltodextrin auf die Produktqualität miteinander verglichen. Die Zugabe des Maltodextrins erfolgte vor den Trocknungsprozessen und während einer Wirbelschichtgranulierung. Die Bestimmung der Hygroskopizität, die Auswertung von TGA-DSC-MS-Daten und die Gehaltsbestimmung mittels HPLC ergaben, dass sprühgetrocknete Extrakte stabiler sind als gefriergetrocknete. Der Zusatz von Maltodextrin führte zu einer besseren Stabilität der Extrakte, wobei geringe Mengen

an Maltodextrin ausreichend waren, wenn sie durch eine Wirbelschichtgranulation von außen aufgebracht wurden.

Zur Verbesserung der Stabilität von hygroskopischen Tabletten, die einen sprüh-getrockneten Extrakt aus Sennesfrüchten enthielten, wurde der Feuchtigkeitsschutz von Hot Melt-Coatings allein sowie in Kombination mit einem magensaftresistenten Überzug untersucht. Verwendet wurden mittelkettige Triglyceride, Stearinsäure, Glycerolpalmitostearat und Glycerolbehenat. Analysiert wurden die Feuchtigkeits-aufnahme, der Zerfall und die Wirkstofffreisetzung der Tabletten. Gegenüber den Tablettenkernen konnte mit Tabletten, die mit einer Kombination aus Glycerol-palmitostearat und einem magensaftresistenten Überzug beschichtet waren, die Feuchtigkeitsaufnahme bei 75 % relativer Luftfeuchtigkeit um 85 % reduziert werden. Diese Kombination war effizienter als größere Mengen des magensaftresistenten Überzugs. Das Hot Melt-Coating erwies sich als geeignete Technik zum Aufbringen von Beschichtungsmaterial, das als Barriere gegen das Eindringen von Wasser in hygroskopische Tablettenkerne dienen soll, ohne von den Anforderungen des Arzneibuches an Zerfall und Freisetzung abzuweichen.

Abstract

Drug products, the active ingredients of which are derived from plant materials, are regarded as full-featured drug products and need to meet the same legal requirements in terms of effectiveness, safety, and consistent quality as with chemically defined active substances. The test methods for the analysis of herbal drugs undergo permanent development, whereby the quality of herbal drug products may be improved constantly. Therefore, the monographs of the European Pharmacopoeia have to be continuously adapted to the current state of knowledge. The aim of the present thesis was to develop a stable dosage form of the laxative herbal drug *Sennae fructus* based on its dry extracts by examining and modifying manufacturing processes and suitable analytical methods.

To determine the active ingredients of Senna, which are hydroxyanthracene derivatives (sennosides), members of the expert group 13 A of the European Pharmacopoeia Commission suggested replacing the spectrophotometric assay by an HPLC method. Therefore, in the present work HPLC-UV(DAD)-ESI/MS and HPLC-ESI/MS/MS measurements were carried out to evaluate the efficiency of this proposed method with regard to the separation of the ingredients of Sennae fructus extracts and their assignment. An evaluation of all hydroxyanthracene derivatives was carried out to obtain sufficient information for the assessment of the respective extract quality. A distinction between the extracts of the species Cassia angustifolia and Cassia acutifolia based on tinnevellin, tinnevellin-6-glucoside, 6-hydroxymusicin-glucoside, and a small amount of an unknown substance was possible. Currently, the majority of Sennae fructus is obtained from newly developed cultivation areas in northern India because of their low aflatoxin content. The obtained plant material has the properties of both, Cassia angustifolia and Cassia acutifolia, in terms of morphology and ingredient composition.

Abstract

In the present thesis, stability tests were carried out with spray-dried aqueous Sennae fructus extracts. Spray-drying was carried out with different atomizing gas pressures, pump feed rates, and inlet temperatures. These process parameters had an impact on the particle size, the particle surface (smooth, wrinkled), the particle shape (golf ball, doughnut, shard), the absolute density, and the residual moisture. Stability-reducing factors were the moisture content of the samples and their hygroscopicity as well as the particle morphology. An increase of the atomizing gas pressure led to the most pronounced decrease of both, the particle size and the residual moisture content. An increase of the inlet temperature also resulted in a decrease of the residual moisture content and moreover, in an increase of the proportion of particles with a smooth surface. An increase of the pump feed rate caused stable hollow spheres, but with increased residual moisture content. Thus, during spray-drying the inlet temperature had the greatest positive effect on the particle properties and the stability of the sennosides.

Furthermore, spray-dried and freeze-dried extracts of Sennae fructus were compared with respect to the sennoside stability and the influence of the excipient maltodextrin on the product quality. Maltodextrin was added either before the drying processes or during fluidized bed granulation. The determination of the extract hygroscopicity, the evaluation of TGA-DSC-MS data, and the determination of the sennoside content by HPLC showed that spray-dried extracts are more stable than freeze-dried extracts. The addition of maltodextrin led to an improved stability of the extracts, whereby small amounts of maltodextrin were sufficient if they were applied during fluidized bed granulation.

To improve the stability of tablets containing a hygroscopic spray-dried extract of Sennae fructus, the moisture protection of hot-melt coatings was investigated separately as well as in combination with an enteric coating. Medium-chain

triglycerides, stearic acid, glycerol palmitostearate, and glycerol behenate were used. Moisture absorption, disintegration, and dissolution of the tablets were analysed. Compared to the tablet cores, tablets coated with a combination of glycerol palmitostearate and the enteric coating reduced the moisture absorption by 85 % at 75 % relative humidity. This combination was more efficient than the application of larger amounts of the enteric coating. Hot-melt coating proved to be a suitable technique to apply lipophilic coating materials to hygroscopic tablet cores serving as a barrier against the penetration of water into the tablets while still complying with the requirements of the Pharmacopoeia regarding disintegration and dissolution.

List of Abbreviations

BET — Brunauer-Emmet-Teller

Cp — Compritol$^®$ 888 ATO

DAD — Diode array detector

DSC — Differential scanning calorimetry

ESI — Electrospray ionization

EuL55 — Eudragit$^®$ L 30 D-55

Fig. — Figure

FTIR — Fourier-transform infrared spectroscopy

HMC — Hot melt coating

HPLC — High performance liquid chromatography

MCT — Medium chain triglyceride

MD — Maltodextrin

MS — Mass spectrometry

Ph. Eur. — European Pharmacopoeia

Q-TOF — Quadrupole – time of flight

RH — Relative humidity

Pr — Precirol$^®$ ATO 5

RT — room temperature

SD   Standard deviation

SEM   Scanning electron microscopy

StA   Stearic acid

TGA   Thermogravimetric analysis

UV   Ultraviolet

CONTENTS

CONTENTS

CONTENTS

XIII

1. Introduction

1.1. Pharmaceutical quality of herbal drug formulations

1.1.1. General aspects

Drug formulations must be approved and controlled by the responsible regulatory authorities. The approval of pharmaceuticals is not only based on the therapeutic efficacy and safety, but also on the warrantee of the pharmaceutical quality. Therefore, during the application for approval the applicant must provide information on topics such as the shelf life, the storage conditions, the results of stability tests, methods of quality testing, and if necessary, the method of preservation. These details of the German Medicinal Products Act are based on the guidelines of the international conference on harmonisation of technical requirements for registration of pharmaceuticals for human use (ICH). The ICH develops uniform guidelines on harmonization of the assessment criteria of pharmaceuticals for human use as the basis for drug approval in the European Union, the USA, and Japan to ensure that safe, effective and high-quality medicines are developed and approved.

In the European Union, the approval procedure is regulated by Annex 1 of Commission Directive 2003/63/EC [1] and is specified by the Committee for Human Medicinal Products (CHMP) appointed by the European Medicines Agency (EMA). The Committee for Proprietary Medicinal Products (CPMP) has published various quality guidelines for stability testing with a main part dealing with chemically defined drug substances, but also applicable to herbal substances and herbal preparations [2; 3]. The "Guideline on quality of herbal medicinal products/traditional herbal medicinal products" [4] determines the requirements especially for herbal products. The stability studies should consider the physical, chemical, and microbiological changes over the storage time period. The requirement is to develop a medicinal product specification for the quality characteristics of the product such as limits for

drug content, impurities and degradation products. If there is an official pharmaco-poeia monograph available for the substance, the testing should comply with the monograph. The stability studies should include the effects of temperature, humidity and oxygen, all depending on the climate zone [2]. Characterization of drug release, water content, and undesired discolorations are also important. To recognize degradation pathways, the identification and quantification of the degradation products under stress conditions is useful but requires suitable analytical methods. The analysed data from long-term, intermediate or accelerated testing decides on the expiration date.

1.1.2. Special aspects of herbal drug formulations

While the analytics of chemically defined substances are usually straightforward, herbal drug formulations are mixtures of various ingredients and require a more complex analytical effort. According to the "Guideline on quality of herbal medicinal products / traditional herbal medicinal products" [4] the respective herbal compound or herbal preparation in its entirety is regarded as the active substance. An analysis of only the known therapeutic active ingredients is not sufficient. A fingerprint chromatogram may give additional information of the composition of the herbal drug preparation and may serve as a proof of stability in comparison to the initial fingerprint [5]. The required control procedure of the shelf life is described as an on-going stability test in Chapter 6 of the "EU Guideline for good manufacturing practice for medicinal products for human and veterinary Use" [6]. During the required storage time periods, the content of the known active ingredients of a plant should not deviate more than ± 5 % from the initial value. If the ingredients are unknown, the deviation of the content of a selected lead substance during the proposed shelf life must not exceed ± 10 % of the initial value.

1.2. Preparation and characterization of plant extracts

1.2.1. General aspects

Herbal drugs and herbal drug preparations are defined in the general monographs of the European Pharmacopoeia (Ph. Eur.). Herbal drug preparations include powdered plant parts, extracts, tinctures, as well as fatty and essential oils produced by extraction, fractionation, or purification. According to the Ph. Eur., extracts are preparations either in the liquid (fluid extracts and tinctures), the semisolid (thick extracts) or the solid (dry extracts) state, which are usually prepared from dried plant parts.

The German and the European Pharmacopoeia currently distinguish between the following three types of extract: standardised, quantified, and others. This classification system is based on the knowledge about the respective active ingredient(s) and their therapeutic efficacy. Standardised extracts are adjusted to a specific level of ingredient(s) of known therapeutic efficacy by the addition of inert excipients or by mixing of different extract batches. Quantified extracts are adjusted to a defined content range of one or more lead substances mostly by mixing different extract batches. Other extracts are mainly assessed by the quality of the starting material and the suitability of the manufacturing process.

1.2.2. Extraction methods

Various extraction methods are used to obtain the desired active ingredients, e.g. maceration, infusion, digestion, percolation, and hot continuous extraction (Soxhlet). The most commonly used method in the pharmaceutical industry is percolation. With appropriate process conditions such as pre-maceration, it is possible to find suitable extraction settings for the different plant parts [7]. For example, some root drugs need to be pre-soaked, while certain leaf and blossom drugs require a rapid onset of

the main extraction. During maceration, the extraction takes place only up to the extraction equilibrium, while the extraction is continuous and exhausting during percolation. For a high extraction yield, the particle size of the plant parts and the composition of the extraction agent are important. The composition of the extraction agent depends on the desired ingredients, which have to be transferred from the plant parts into the extract. Examples are water, ethanol-water mixtures, and various organic solvents. The resulting liquid extracts are usually not used directly as finished herbal drug formulations. Therefore, a reduction of the extraction agent is often necessary.

1.2.3.   Drying methods

To evaporate the extraction agent and to prepare a semisolid concentrated extract, falling film, wiped film or rotary vacuum evaporators are used. The suitable technique for each extract depends on the thermal stability of the ingredients, whereas aggregations and precipitations during the drying process should be prevented. In the case of dry extracts, the residual extraction agent needs to be removed from the semisolid extract.

1.2.3.1. *Spray-drying*

One of the most common methods for the preparation of dry extracts is spray-drying. Spray-drying is based on the evaporation of the solvent of an herbal extract by spraying in a temperature-controlled air stream. It is a continuous drying process with a low residence time of the resulting droplets within the drying zone (Fig. 1). The solution or suspension to be dried is sprayed with a nozzle into a chamber containing hot air ultimately leading to a surface increase of the volatile liquid. After evaporation of the liquid, particles are formed, separated from the air stream, and transmitted to a cyclone separator. The obtained end product is a dry powder, which

may be directly used as a pharmaceutical dosage form such as instant tea or may be further processed by granulation and/or tableting [8].

The formulation of particles with defined particle properties is crucial for the resulting product properties. It has already been observed that the shape of the obtained particles depends on the type of atomization, the drying conditions and the properties of the used material [9].
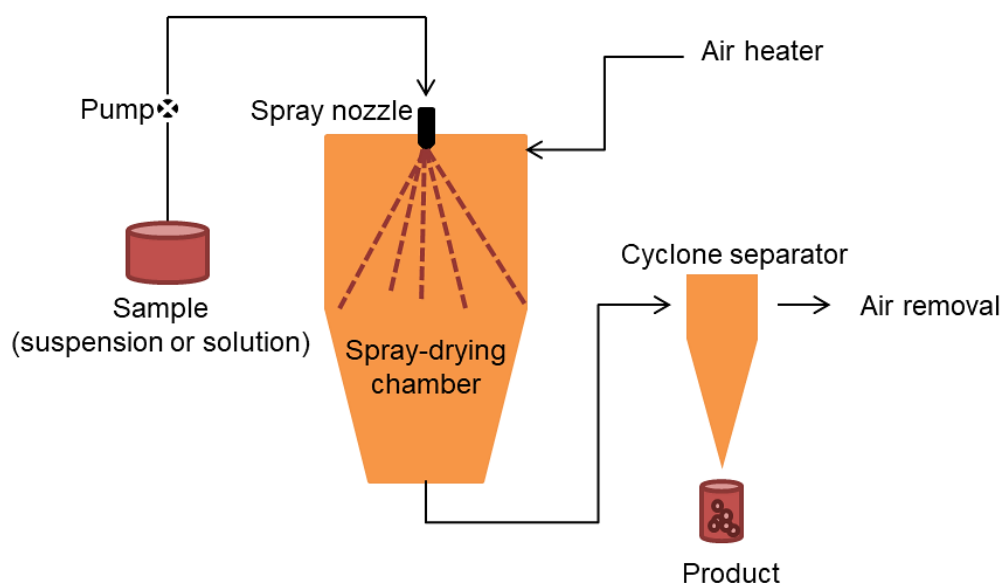
Fig. 1: Principle of a spray-dryer.

Different particle structures may be formed by spray-drying, including hollow spheres and solid spheres with a smooth or a rough surface. However, unwanted agglomeration and fragmentation of the particles might also occur [9]. It has been confirmed that the particle size and shape (spherical, ellipsoidal, and doughnut-like) may be controlled by different preparation conditions [10]. The viscosity of the sample solution or suspension and a possible addition of surfactants may affect the morphology of the particles. By this means, even spray-dried protein particles have already been prepared and investigated for their particle properties [11]. It was shown, that the shape and the morphology of the particles were influenced by the

spray-drying conditions such as the drying outlet air temperature and the composition of the protein formulation among others.

In the food industry, the effect of the spray-drying conditions on the particle properties was examined with açai powder among other model food ingredients [12]. The inlet temperature, the feed flow rate and the addition of maltodextrin influenced the residual moisture content of the powder. Furthermore, larger particles with smoother surfaces were obtained at high inlet temperatures. Other product properties, such as the wettability, the amount of insoluble solids, and the bulk density were studied after spray-drying of orange juice [13]. Increasing the atomizing gas pressure resulted in an increase of the bulk density, the average time of the wettability, and a decrease of the insoluble solids amount of the orange juice powder. Spray-drying is a process also widely used to produce dry plant extracts. During this process, the extract ingredients are being concentrated resulting in new technological product properties for further processing.

1.2.3.2. *Freeze-drying*

The solvent of native extracts may also be removed by freeze-drying, i.e. lyophilisation. Freeze-drying is based on the sublimation of a solvent of a frozen solution. This process leads to powders with a porous structure [14].

The freeze-drying process consists of three steps: freezing, primary drying, and secondary drying. During the freezing step, the material is cooled down quickly below its eutectic point to form ice crystals and to ensure a fast removal of water vapour by sublimation (Fig. 2). This is the most crucial step, as the freezing settings may impact the speed of reconstitution, the duration of the freeze-drying cycle, the resulting product stability, and the crystallization itself [15]. The primary drying step, during which ice sublimation takes place, begins whenever the chamber pressure is

reduced until the gas stage of the extracting agent is reached. This step typically takes several hours to finish and leads to a removal of approximately 95 % of the extracting agent. During the secondary drying step, the temperature is increased to enhance the drying process and to reduce the final residual extractant content. By continuously removing of gaseous water through condensation on the cooling surface in the condenser, the amount of ice in the sublimation chamber decreases.
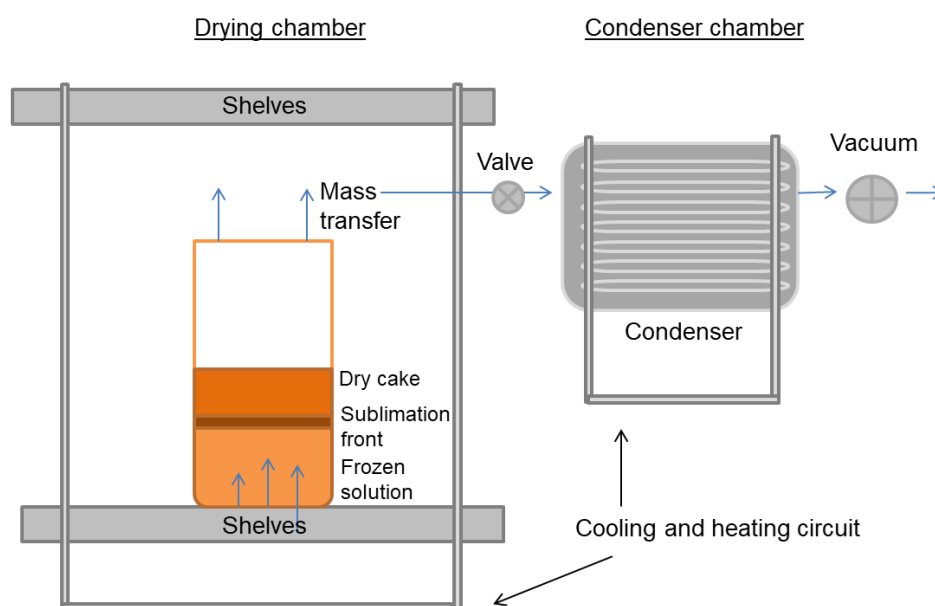
Fig. 2: Principle of a freeze-dryer.

The properties of freeze-dried powders are influenced by several factors such as the adjusted pressure, the freezing rate, the rate of growth of the ice crystals, the unfrozen amount of water, and the viscosity of the solution to be dried. Often, excipients are added to adjust the pH-value, to avoid or induce crystallization, or to protect the active substance (cryoprotectant, lyoprotectant) [16].

Freeze-drying was already of scientific interest before the twentieth century. This process was used for microscopy studies by Altman [17], who prepared and preserved sensitive materials. Also, a preparation of dry suspensions containing living bacteria was developed [18]. During the World War II, freeze-drying began to

be used in the industry resulting from the need to freeze-dry large quantities of human plasma by Flosdorf et al. [19]. Even today, scientists are still optimizing the process of freeze-drying. The focus is amongst others on novel methods such as combined spray-freeze-drying [20], stabilization of proteins during storage after freeze-drying [21], and microencapsulation of extracts during freeze-drying [22].

1.2.3.3. *Addition of drying excipients*

The suitable selection of a drying excipient is an important step to guarantee the stability and the quality of the resulting product. Drying excipients may enable or enhance the drying process to obtain stable formulations. In addition, they serve to control drug release for example from delayed or prolonged dosage forms. Also, drying excipients may assist to release the active ingredient in a certain part of the gastrointestinal tract, such as the small intestine. Another use of drying excipients may be to ensure a sufficiently long shelf life by preventing interactions with other ingredients of the formulation.

Known drying excipients are for instance gum Arabic [23], maltodextrin (MD) [24], as well as mannitol and lactose [25]. The excipient may be added to the liquid extract before the drying process or be applied to a dried extract during a fluidized bed granulation. MD is a widely used low-priced drying excipient with an inert aroma and taste, a low viscosity in solution, and an antioxidant property [23, 26, 27, 28]. Goula and Adamopoulos [29] investigated the addition of MD on the powder properties of tomato pulp after spray-drying. They noticed that the addition of MD caused a decrease of the powder hygroscopicity and thus influenced the caking tendency as well as of the water solubility. These findings were in good accordance with those of a sticking mango powder extract, which showed a decreased caking tendency and water absorption by an increase of the MD amount [30]. When studying the

physicochemical properties of cactus pear powder, Rodriguez-Hernández et al. [31] observed that not the type but the content of MD had a significant effect on the resulting powder hygroscopicity.

1.2.4. Characterization of the extract particles

Different technologies exist to characterize particles. These technologies allow a better understanding and monitoring of the particle properties, which are directly influenced by the particle size, the particle shape, the porosity, and the density. For example, shrinkage of particles as a result of drying may be assessed by measuring the porosity, determining the particle size, and characterizing the particle shape by microscopic imaging. In a study on the stability of spray-freeze-dried and freeze-dried trypsinogen particles, the investigation of the particle properties allowed the description of the complex destabilization behaviour of trypsinogen [32]. An important field for the application of particle characterization technologies is pulmonary drug delivery. It has been shown that rather large porous particles (around 5 µm) are particularly suitable for the systemic inhalation therapy (insulin) because of their high aerosolization efficiency, long-term drug release, and increased systemic bioavailability [33].

1.2.4.1. *Particle size distribution determined by laser diffraction analysis*

Laser diffraction enables the determination of the particle size and the particle size distributions. The particle sizes as well as its distribution are amongst others the most crucial parameters regarding the stability of particle formulations, as they have a direct influence on the dissolution rate, the appearance, and the flowability [34]. Laser diffraction measurements are based on different angles of light diffracted by a particle entering the light beam [35]. Small particles scatter the light at small angles in contrast to large particles, which scatter the light at large angles. This observation

leads to large alternating dark and light diffraction rings with a high light intensity in the case of small particles and to small alternating dark and light diffraction rings with a low light intensity in the case of large particles (Fig. 3).
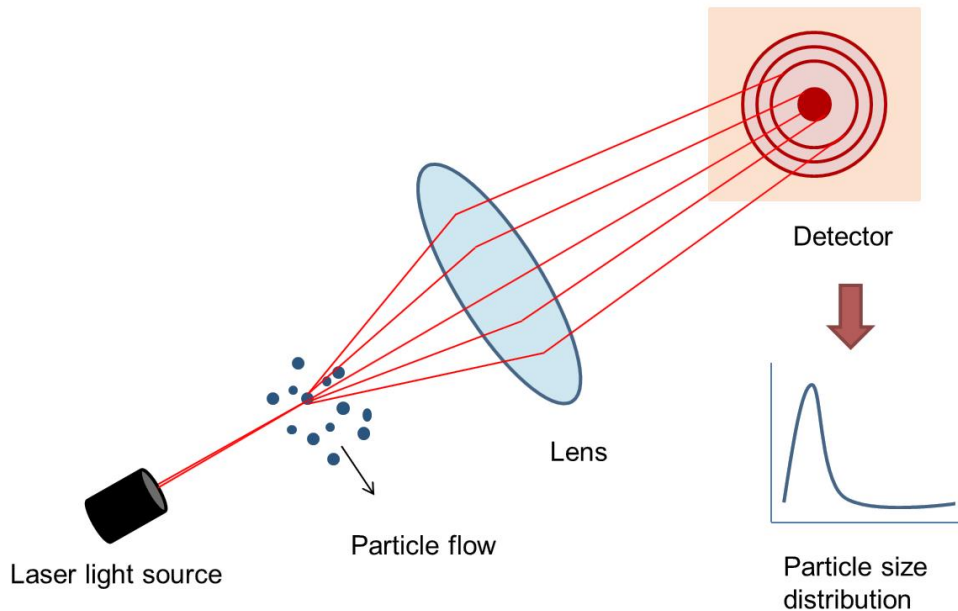
Fig. 3: Principle of a laser diffraction analysis (modified from [36]).

These diffraction rings are detected with a photo detector and the signals are converted by software into a particle size distribution. These conversions are based on the Fraunhofer approximation or the Mie theory. As the particles are moving through the measuring cell it is important to prevent aggregates [35].

1.2.4.2. *Imaging performed by scanning electron microscopy*

The particle shape also has an influence on the quality of the particle formulations. With scanning electron microscopy (SEM) additional information on the particle shape differences, the particle sizes, the aggregation tendency, and the surface structures may be obtained.

During SEM, a microscope is used that creates surface images of a sample by scanning the surface with a focused beam of electrons in a raster pattern (Fig. 4).

With this technique, a magnification of up to 100,000 times may be achieved in comparison to a light microscope, which can usually magnify up to maximum of 1,000 times [37].
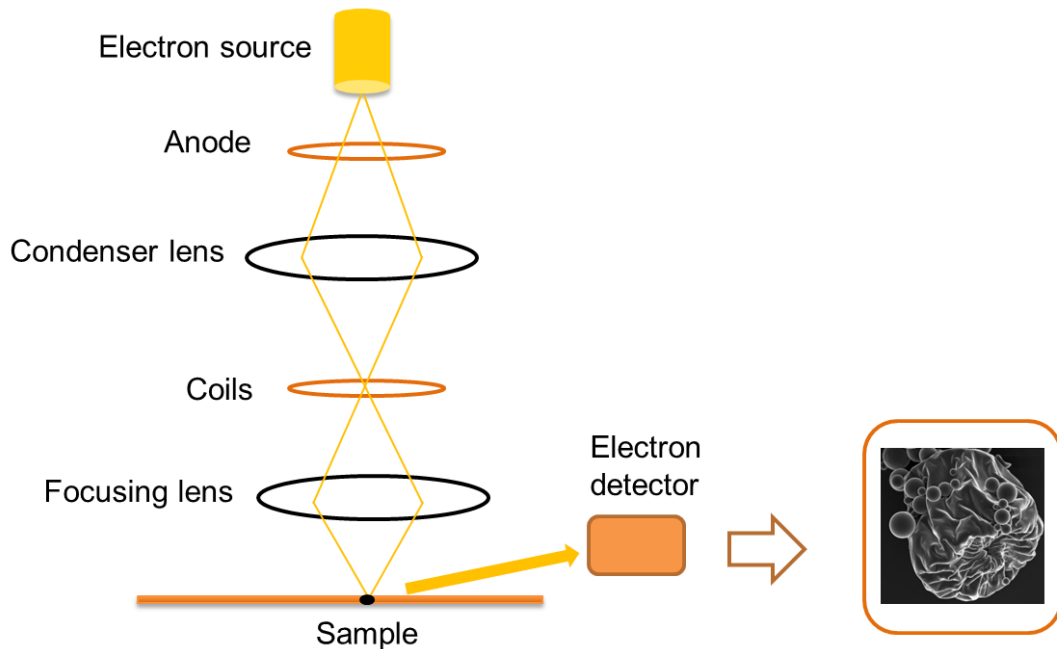
Fig. 4: Principle of a scanning electron microscope (modified from [38]).

After the electrons are generated by an electron source, primary electron beams are focused by a control cylinder and accelerated by an anode to the condenser lens, which enables to adjust the diameter of the electron beam [39]. Subsequently, the primary beams pass electromagnetic coils. Thereby, the beam undergoes a fine focusing through a second lens until it reaches the sample. This fine electron beam is necessary to scan the surface of the sample line by line. Because only conductive surfaces may be used, the samples need to be sputter coated with a thin metal film (e.g. gold). A detector registers the backscattered secondary electrons and makes a surface imaging possible.

1.2.4.3. *Pore characterization by mercury porosimetry*

Porous materials with pores between 3.5 nm and 500 µm may be characterized by mercury porosimetry [40]. The mode of operation is based on the penetration of a non-wetting liquid, such as mercury, under high pressure into a sample (Fig. 5).
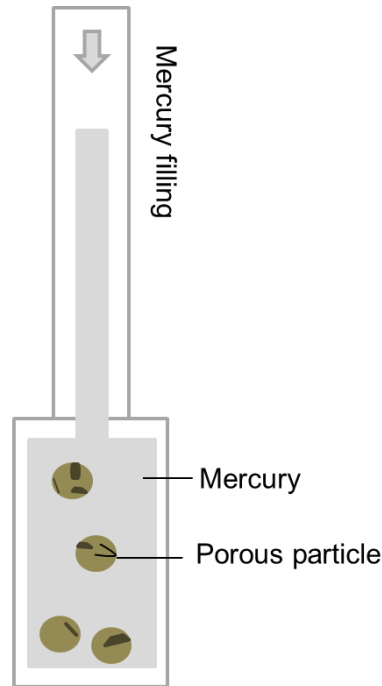
Fig. 5: Principle of a mercury porosimeter.

The external pressure is measured, which is necessary to force the liquid into a pore against the surface tension of the liquid [40]. The pore size is calculated by relationship between the pressure and the intrusion data using the Washburn Equation [41]:

$$L = \sqrt{\frac{\gamma r t \cos(\emptyset)}{2\eta}}$$ (Eq. 1)

where γ is the surface tension, r the pore radius, t the time, Ø the contact angle between the penetrating liquid and the solid, and η the dynamic viscosity.

Information on the investigated sample such as the pore size distribution, the skeletal and apparent density, the total pore volume or porosity, and the specific

surface area may be obtained. It has to be mentioned, that it is only possible to measure those pores, which the mercury has access to. Therefore, closed pores are not detectable [42].

1.2.4.4. *Surface area quantified by the BET technique*

The Brunauer, Emmett, and Teller (BET) technique is the most common method for the determination of the specific surface area of powders and porous materials. The three researchers have published their theory of multilayer adsorption in 1938 [43]. Their theory is based on the property of gases to adsorb on external and internal surfaces of porous materials. In this context, the term adsorption isotherm describes the relationship between the adsorbed gas and the relative vapour pressure at a constant temperature [44]. Most commonly, nitrogen gas is used for the BET measurements. The apparatus essentially consists of a sample and a reference chamber, which are connected with a pressure gauge [45]. These chambers are filled with nitrogen, which is passed over the sample and the amount of nitrogen adsorbed on the sample, after desorption of the residual gas by heating, is determined. As the BET analysis is undertaken at cryogenic temperature, it is possible to perform the measurement below the saturation vapour pressure to prevent condensation. During cooling, adsorption of the nitrogen gas on the particle surfaces takes place as an endothermic process. Because of the large surface area of the sample in relation to the chamber surface, there is a pressure decrease in the sample chamber in comparison to the reference chamber, which allows the determination of the BET surface area in m^2/g. In addition to the use of nitrogen and argon, carbon dioxide has been suggested as an alternative option for materials with very small pores [46].

1.2.4.5. *Determination of the extract density by helium pycnometry*

The true or absolute density describes the mass of a material per unit volume. The helium pycnometer is an instrument used to reach a close approximation to the true volume and absolute density of a material, because of the property of helium to penetrate into the smallest pores. It could be shown, that helium may be a non-adsorbing gas at room temperature and at a low pressure [47, 48]. Helium pycnometry is a suitable technique because of its easy-to-use and fully automated apparatus [49]. Furthermore, under optimal conditions an accuracy of the obtained data of 0.02 % may be achieved.

For the measurement of the volume and thus the density of a sample two chambers are necessary. One chamber is filled with a reference material of known volume, while the other chamber is filled with a sample of known weight (Fig. 6).
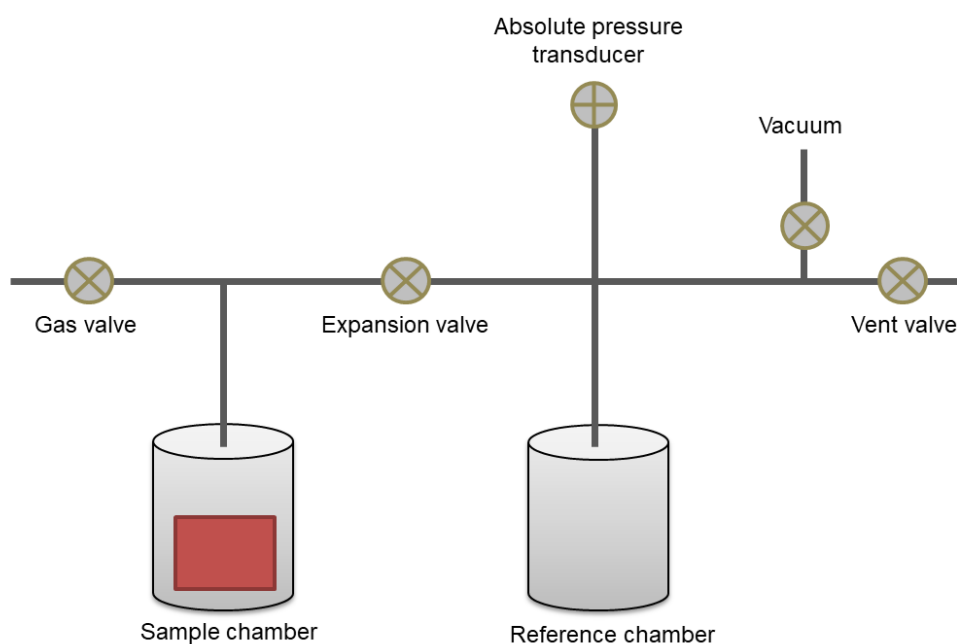
Fig. 6: Principle of a helium pycnometer (modified from [50]).

Initially, helium is added to the system and the sample chamber is rinsed several times to remove residual gases. Subsequently, the sample chamber is filled up with

helium to an initial pressure. Thereafter, the compensation valve opens and the resulting pressure is measured. The resulting equilibrium pressure is used to calculate the exact density of the sample by application of the ideal gas law [51].

1.2.5. Stability-reducing factors of plant extracts

Physicochemical instabilities may be caused by the properties of the active ingredient, the excipients, and the primary packaging material [52]. Stability-reducing factors may be distinguished into external factors and internal factors. The external factors include atmospheric oxygen, carbon dioxide, humidity, light and heat. Internal factors may be the interaction between excipients and the chemical decomposition by a change of the pH. The most common chemically-based structural changes include hydrolysis [53], oxidation [54], racemization [55], decarboxylation [56], and polymerization [57]. For herbal preparations the decomposition by hydrolysis and oxidation plays a major role because esters, lactones, epoxides or acetals are common chemical structures of many plant ingredients. Hydrolysis may be prevented by removing water or water vapour, reducing the penetration of water vapour during manufacturing processes and during storage by suitable manufacturing and storage conditions or by selection of appropriate packaging materials. Oxidation-sensitive chemical structures in plant extracts are olefins, aldehydes, alcohols, and phenols. Furthermore, the degradation of the active ingredients by enzymes present in the plant extracts may take place during storage. These plant extracts may be protected by the precipitation of the enzymes for example with ammonium sulphate [52]. In addition, the denaturation of enzymes by heating the plant extracts above 60°C may be an option to reduce the degradation processes.

1.3. Plant extract formulations

1.3.1. General aspects

Plant extract formulations contain one or more plant extracts or plant extract preparations with active ingredient(s). These active ingredient(s) are obtained by extraction and processed with different additional excipients such as fillers and flow agents. Excipients are adjunctive substances added to alter technological or pharmacological properties to guarantee the chemical and physical stability of the resulting product. Examples for plant extract formulations are syrups, ointments, granules, capsules, and tablets.

1.3.2. Interactions of excipients with plant extracts

The preparation of plant extract formulations involves the addition of excipients. However, excipients may interact physicochemically with the active ingredient [58]. Possible interactions between the active ingredient and different excipients have to be considered during preformulation studies. Most excipients are pharmacologically inert, but may interact with the active ingredient and lead to an accelerate degradation or impair bioavailability [59]. Already in 1983, drug-excipient interactions were investigated with differential scanning calorimetry (DSC) [60]. Moreover, isothermal stress tests were carried out and evaluated by high performance liquid chromatography (HPLC). DSC measurements are characterized by recording the difference in the heat flow between a sample and a reference depending on time and temperature (Fig. 7). As a result, the energy-related to thermal events such as melting or crystallization processes and glass transitions may be determined [61]. DSC measurements allow a fast assessment of interactions, which manifests themselves in the appearance, disappearance, or shifting of endothermic/exothermic peaks, which has already been described in the past e.g. by Bozdağ-Pehlivan et al.

[62]. In this study fourier-transform infrared spectroscopy (FTIR) was also applied to investigate possible interactions between the active ingredient and various excipients. Other researchers combined thermoanalytical methods with other analytical techniques and noticed that the best method to detect interactions between tricyclic ß-lactam antibiotics and various commonly used excipients turned out to be thermogravimetric analysis (TGA) coupled with DSC [63]. This combination enables the detection of interactions already at early stages by the appearance of characteristic thermal events.
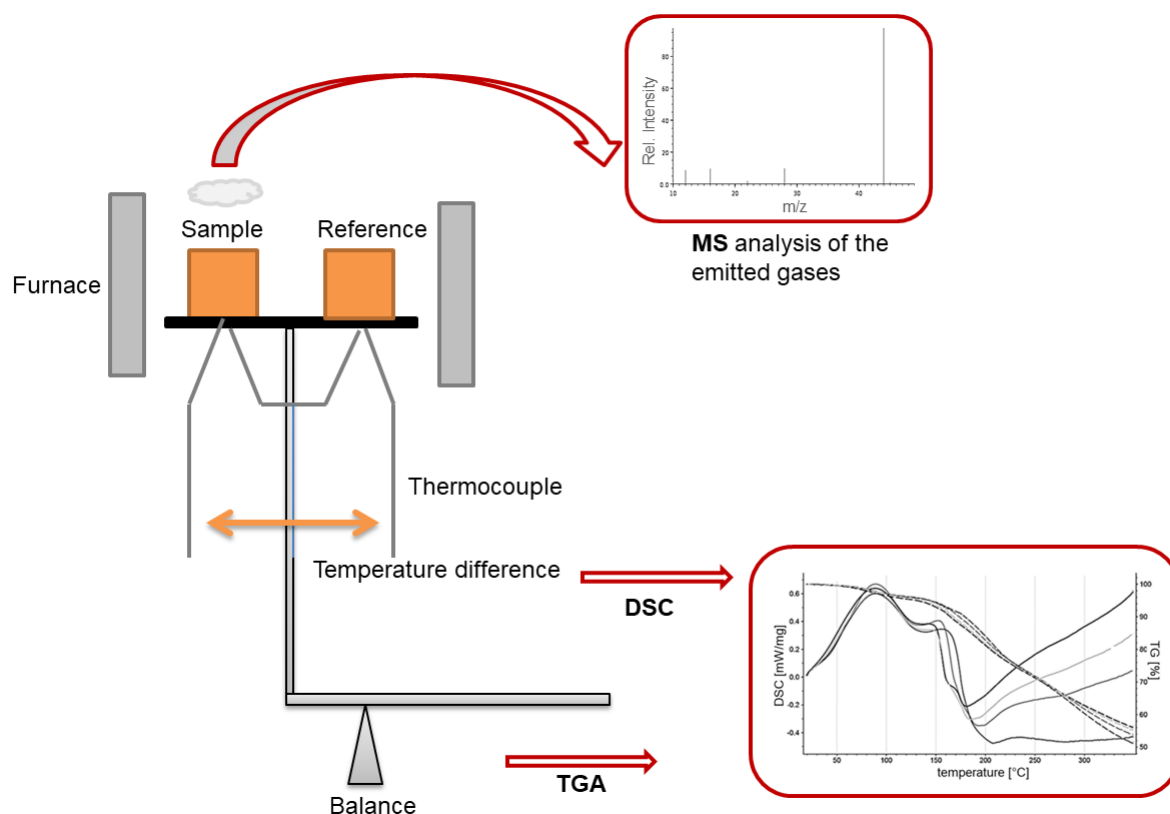
Fig. 7: Principle of simultaneous TGA-DSC-MS measurements.

Regarding TGA, the mass changes of a sample are measured as a function of temperature and time. Upon heating, the sample may emit gases environment through decomposition reactions or evaporation of volatile components which may be passed into a mass spectrometer for analysis of the sample composition. For the

qualitative and quantitative evaluation of interactions, it is necessary to couple several methods such as TGA, DSC, and mass spectrometry (MS).

1.3.3. Tableting of plant extracts

Tablets are the most common oral dosage forms consisting of a mixture of active substance(s) and excipients, compacted from a powder or granules. By an application of a compression force to a powder or to granules, a physical bond is created between the particles and the compaction process lead to a volume reduction and a particle rearrangement takes place. Usually, tablet presses are used to manufacture tablets with uniform size, shape, and weight. Thereby, an upper and a lower punch as well as a die compress the powder into a tablet. Two types of tablet presses are available: single-punch and rotary tablet presses [64]. They differ from each other in the movement of the punches, the die filling process, and the number of compressed tablets per time. Most of the known plant extracts are difficult to press into tablets because these tablets tend to tablet failures such as capping, lamination, and sticking. Furthermore, most of the plant extracts show hygroscopic behaviour and slow disintegration times. Therefore, common excipients such as fillers, flow agents, binders, disintegrants, and lubricants are necessary for a sufficient compaction as well as to increase the mechanical stability of the tablet. However, it is possible to perform a direct compression without previous granulation of the powders, which is time and cost-effective [65]. Therefore, the compression behaviour of a powder blend depends on the characteristics of the powder particles such as a low segregation tendency and a high flowability as well as on the settings of the tableting machine such as the suitable tableting speed and the compression force [66]. It is necessary to prevent tablet failures such as capping, lamination, and sticking for the development of robust tablets, which have to remain mechanically

stable over time. Additionally, a subsequent coating of tablets may help to guarantee their physical and chemical stability.

1.3.4. Coating of tablets containing plant extracts

Coating is a process used to apply an outer layer of coating material to the surface of a dosage form to obtain specific benefits [67]. Coatings are used to mask the taste or the odour and to achieve a moisture protection of the plant extracts. Especially in the 19th century, sugar-based coatings were frequently used. This process requires a time-consuming application of many layers of sugar syrup and powder blends which leads to the large size and weight of the resulting dragees. In the meantime, coatings have been developed which consist of thin polymer films available in a high variety of compositions with different functions.

1.3.4.1. *Film coating*

During the film coating process, the dissolved or dispersed coating material is sprayed onto the tablet surface and the solvent evaporates leaving behind a film on the tablet. Ionic and nonionic polymeric materials such as cellulose ethers and esters, polymethyl methacrylates, and polyvinyl derivatives may be applied to enable properties such as extended or delayed drug-release, resistance to saliva or gastric juice, and moisture protection. Moisture protection of tablet formulations is important if the active ingredient(s) or the excipients are moisture sensitive [68]. In some cases, a reduction of the moisture uptake by tablet cores is only possible through the application of coatings. Therefore, predominantly coatings of liquid coating technologies are applied. For this purpose, coating formulations such as organic polymer solutions or aqueous dispersions have been demonstrated to be suitable. However, organic polymer solutions require explosion-proof equipment and safety-trained personnel. Therefore, water has become the preferred solvent or dispersant

in the last decades. As a consequence, films from aqueous dispersions of several polymethyl methacrylates, polyvinyl alcohol, and some cellulose derivatives were investigated with regard to their water permeability and moisture protection [69]. Moreover, various studies were carried out with special aqueous polymer coatings consisting e.g. of hydroxypropylmethylcellulose with the additives microcrystalline cellulose and stearic acid [70, 71].

Enteric coated products are designed to prevent the dissolution or disintegration of an oral solid dosage form in the stomach and to cause a release of the active ingredient in the intestine. Reasons for the application of enteric coatings are the protection of the active ingredients from the acidity of the stomach or the protection of the stomach from irritating active substances. Examples for enteric coated herbal tablets are formulations with garlic extract [72], cranberry extract [73], and Sennae fructus extract [74]. Enteric coatings are polymeric acids and are therefore insoluble at the acidic pH of the stomach. They only dissolve at the alkaline pH of the intestine, after which the disintegration of the drug formulation takes place and the active ingredient(s) are released. Although the first gastro-resistant coating has already been introduced in 1884 [75], enteric coatings are still a topic of research [76, 77, 78].

1.3.4.2. *Dry coating*

Water-based coatings also have disadvantages such as the possible hydrolysis of the tablet ingredients and the energy-consuming drying process. As a result, the focus on solvent-free coating technologies has increased in recent years. Besides processes such as compression coating [79, 80], the dry powder coating [81], or the electrostatic dry coating [82], hot-melt coating (HMC) has been preferred for several years, also for the coating of plant extract tablets. This technique involves the

application of the coating material as powder onto the solid dosage form in a traditional coating pan with subsequent melting of the coating material [83] or applying it directly in its molten state [84]. The advantages of this technique are a short process time and no chemical interactions between the tablet ingredients and the usually inert coating material [85]. Disadvantages are the rather high process temperatures depending on the melting point of the HMC materials, which may affect the stability of the tablet ingredients and might lead to an increased operational risk. HMC materials are often lipids of different structures. Lipid is the generic term for a large class of materials including fatty acids, acylglycerols, phospholipids, sphingolipids, waxes, fatty oils, and sterols. The lipids used for HMC coatings may be of vegetable or animal origin. Lipid suppliers provide various types of lipids containing different chain lengths of the fatty acids or alcohols and different types of functional groups [86, 87].

1.4. The plant Senna

1.4.1. General aspects

The genus Senna belongs to the caesalpiniaceae family and comprises about 250 species. Two of them are listed in the European Pharmacopoeia: *Cassia senna* L. (syn. *Cassia acutifolia* DEL.) also called *Alexandrian* or *Khartoum senna* and *Cassia angustifolia* VAHL, which corresponds to *Tinnevelly senna*. For these two Senna species the following monographs exist: *Sennae folium* [88], *Sennae fructus acutifoliae* [89], *Sennae fructus angustifoliae* [90], and *Sennae folii extractum siccum normatum* [91]. *These* species show differences in the plant height, in the feathered leaves, in the pods, and in their ingredients (different naphthalene glycosides): *Cassia senna* can grow up to 60 cm, *Cassia angustifolia* up to 2 m. The feathered leaves of *Cassia acutifolia* are characterized by a grey-green colour whereas those of *Cassia angustifolia* are yellow-green. The kidney-shaped pods of *Cassia acutifolia* contain seeds with protruding folds in a continuous network whereas the pods of *Cassia angustifolia* contain seeds with transverse and curled folds with no continuous network (Fig. 8).
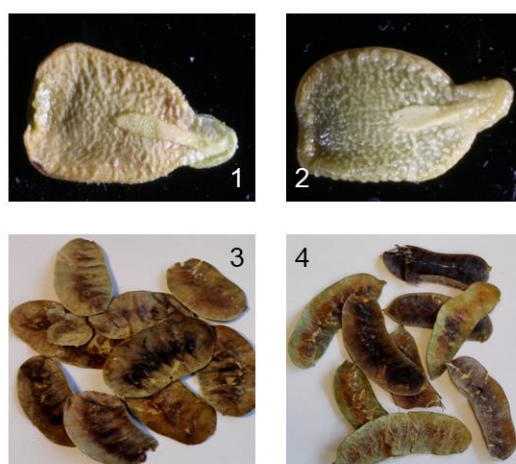
Fig. 8: Photographs of *Cassia acutifolia* seed and pods (1, 3), *Cassia angustifolia* seed and pods (2, 4).

1.4.2.   Cultivation regions of Senna

Senna is a perennial desert plant found in hot, semi-arid to arid dry zones. *Cassia angustifolia* is mainly cultivated in Tamil Nadu and Gujarat. In contrast, *Cassia acutifolia* is grown in the African Sahel zone with the main distribution centre in northern Sudan [92]. Here, the harvest mainly consists of wild collections, which is the reason for the larger amount of Cassia angustifolia on the world market, as it is obtained from plantations. Much of the traded Senna today comes from the newly tended plantations in northern India.

1.4.3.   Senna ingredients and their mechanism of action

Senna leaves and pods include a multi-component mixture consisting of sennoside A and B (Fig. 9), which contains aglycones such as sennidin A and the optically inactive meso form sennidin B [93].

10-10′ threo: Sennoside A
10-10′ erythro: Sennoside B
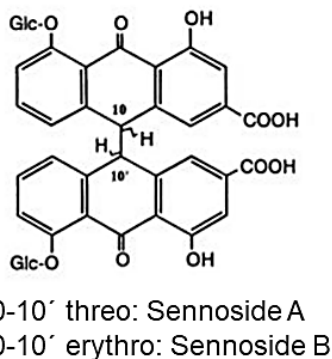
Fig. 9: Chemical formula of Sennoside A and B

In addition, anthraquinones such as rhein, aloe emodin and rhein-8-glycoside, flavonoid glycosides such as isorhamnetin, quercetin and kaempferol are contained [94]. Furthermore, mono- and sesquiterpenoids, phenylpropanoids, fatty acids and esters were identified [95]. In the living plant, the anthrone glycosides are synthesized and deposited in cell organelles. During harvest of the plant, the redox system is disturbed, so that the substrate and the enzymes are no longer present in

separate cell organelles and thus dianthrones like sennosides are formed [96, 136]. The principal active ingredients of Senna are dimeric dianthrone glycosides. Their mechanism of action is well known [97]: After hydrolysis by intestinal bacteria, a reduction to the active monoanthrone stage occurs. These lipophilic monoanthrones may pass through the intestinal wall, are absorbed, cause an active secretion of sodium and water, and inhibit the reabsorption of sodium ions, resulting in stool liquefaction. The laxative effect begins to work after 8-12 h. According to the BAH (Federal Association of Pharmaceutical Manufacturers e.V.), phytopharmaceuticals make up around 22 % of the sales with non-prescription medicines in Germany, mainly in the field of self-medication. Herbal medicines find their acceptance in the population primarily by their effectiveness accompanied with low side effects. Senna leaves and pods and their preparations are still among the most commonly used plant laxatives. Commission E of the Federal Institute of Drugs and Medical Devices and the European Association of National Phytotherapy Societies (ESCOP) describe the indication of Senna as constipation. Its designated intake is temporary and limited to a time period not exceeding 1 to 2 weeks without medical advice.

1.4.4. Quantification of the sennosides

According to the European Pharmacopoeia, the quantification of the content of 1,8-hydroxyanthraquinones in Senna is performed by a modified Bornträger reaction, determining all 1,8-dihydroxyanthraquinone derivatives, which resulted from oxidative processes. Thus, this unspecific method does not allow the recording of single compounds. Moreover, the number of separation processes of this assay affects the reproducibility of the results. These disadvantages led to the development of several HPLC methods, which not only permit a selective determination of individual anthraquinone derivatives but also prevent the use of large solvent

amounts [98]. Such HPLC methods for sennoside quantification have already been published in the past [98, 99, 100, 101, 102]. A new HPLC method was recently introduced by members of the expert group 13 A of the European Pharmacopoeia Commission and published in Pharmeuropa [103, 104]. With this method the total of hydroxyanthracene glycosides is determined as the sum of the peak areas of 6 specified peaks referring to a sennoside B standard. Additionally, the content of all anthraquinones is calculated as the sum of the peak areas of aloe emodin and rhein in relation to the rhein standard.

Problems exist in commercial trade regarding a sufficient supply of the market with authentic Senna material fulfilling the requirements of the Pharmacopoeia monographs. These problems concern the correct identification and declaration of the herbal drugs, contamination with foreign matter, deviation of the content of bioactive ingredients and contagion with pathogen fungi. Therefore, it appears to be of particular interest to introduce a reliable HPLC method for the qualitative and quantitative determination of Sennae ingredients in the European Pharmacopoeia. Especially, the qualitative determination of much as possible Sennae ingredients is necessary in addition to the sennosides. This determination is important to allow monitoring of the pharmaceutical quality of Senna. With a suitable HPLC method, a separation of the multi-substance mixture may be carried out. The most important qualitative information which is obtained from an HPLC chromatogram is the assignment of a constituent such as sennoside B according to its specific retention time and the spectra obtained by a DAD detector. This information may be manifested by injection of the reference substance sennoside B under the same chromatographic conditions. As soon as the substances are either unknown or may not be assigned on the basis of the DAD spectra, coupling to spectroscopic methods such as mass spectrometry is necessary. Mass spectrometry is an analytical

technique which involves the conversion of the sample into gaseous ions, with or without fragmentation. These ions may be characterized by their mass to charge ratio (m/z) and their relative abundances. The results are displayed as a mass spectrum, which represents a plot of the intensity of the ion signals [105]. The molecules in the sample may be identified or assigned to a specific substance class by comparing the identified masses with known masses or through characteristic strucural fragments such as an unglucosylated monoanthrone moiety for Sennoside B.

1.4.5. Stability of the sennosides

Stability issues of the sennosides may occur at each of the following stages: pulverization, extraction, drying, and during further processing e.g. in granulation and tableting. During dry heat at 70°C, oxidative reactions are predominant, whereas at 40°C / 75 % RH enzymatic processes are of higher significance [52]. Powdered herbal drugs have a higher sensitivity to decomposition than cut drugs. Laminated aluminum bags as packaging material show no advantage over paper bags at low humidity. As expected, at a high humidity they are superior to paper bags [52]. An increase of only the temperature causes no further degradation. During the cold approach of the preparation of senna leaf tea, an enzymatically induced complete degradation of the Rhein-8-glycoside was observed. During an approach, wherein the enzymes are denatured by hot water, this process does not occur. The substrate for the enzyme glucosidase is only the Rhein-8-glycoside. Simultaneously with the degradation of Rhein-8-glycoside an increase of the amount of the corresponding aglycone Rhein takes place [98]. Resulting from these observations, the following degradation pathway is assumed: Sennosides are oxidatively cleaved resulting in Rhein-8-glycosides which are subsequently enzymatically degraded to Rhein. Furthermore, during high humidity conditions, the enzymatic degradation to Sennidin

monoglycosides and further on to Sennidin takes place. In summary, according to Gobbel, dry-extracts are more stable than pulverized plant parts. Similarly, Senna leaves are more stable than Senna pods. Plant parts filled into wide-neck containers made of PE or in aluminium laminated bags are more stable than those which are filled in PE bags or are completely unpackaged. The used excipients may also have an influence on the stability of extract formulations. For example, sennoside A and B are incompatible with the excipients propyl paraben, sodium carbonate, stearic acid, citric acid, macrogols, sugars (lactose, glucose), and sugar alcohols (sorbitol) if in contact with water [106]. With this knowledge and a modification of the manufacturing processes a stability increase of the sennosides during storage may be achieved. The improvement of the stability of the sennosides in a spray-dried Senna extract is particularly important for *Sennae fructus*, because rhein, emodin, and aloe-emodin are discussed as degradation products and are suspected to be genotoxic [107].

1.5.   Objectives of this work

The objective of this work was to implement modern analytical methods to examine the decomposition regarding the active ingredients of a plant extract from the model plant Senna during the entire manufacturing process and to apply technological processes for an improvement of the finished herbal formulation. The plant Senna clearly shows that the current assay of the Ph. Eur. does not meet the present requirements for an appropriate stability test. Stability testing is an important procedure during pharmaceutical development and manufacturing, ensuring a constant product quality. Therefore, the formulation of dry extracts with defined properties should be required for the compliance with the quality standards in the pharmaceutical industry. One of the most common methods for the preparation of dry extracts is spray-drying. The formation of particles with defined particle properties is important for the resulting product properties. The variation of the spray-drying process conditions was made under consideration of economic aspects. To vary the concentration of the fluid extract or to increase the air flow rate is economically disadvantages in terms of energy consumption and yield. The products produced under the different conditions (atomizing gas pressure, inlet temperature, and pump feed rate) were characterized with regard to their physical properties such as moisture content, particle size, particle surface properties, and storage stability. Conditions of the drying process had to be adequately adjusted to allow the formation of particles which are resistant to hydrolysis, a reaction which is thought to be part of the degradation pathway. Under these conditions, the effect of moisture on the stability of the ingredients of Senna was investigated along with other stability-reducing factors of spray-dried Senna extracts.

Further aims of the present study were to obtain a low moisture content of the dry-

extracts, the reduction of the extract hygroscopicity as well as its known sticking tendency. For this purpose, different spray- and freeze-drying methods were plant to be compared regarding the extract preparation and properties. Moreover, the stability of the sennosides as active ingredients of *Sennae fructus* had to be investigated. In addition, the influence of the added amount of MD during spray-drying, freeze-drying, and fluidized bed granulation of *Sennae fructus* extract was to be evaluated. In this context, this study deals with the thermal analysis of the resulting extracts to examine the drug-excipient interactions and the extract stability in more detail.

The present study intended to develop a tablet formulation containing a high content of the hygroscopic spray-dried *Sennae fructus* extract. Therefore, the effectiveness of the moisture protection of an HMC materials and the suitability of the combination of both, the HMC materials and the aqueous enteric coating Eudragit® L 30 D-55 were another subject of this study. Different lipids were applied as HMC materials and compared in terms of their adequacy for HMC, their optimum coating amount, their reduction of hygroscopicity, and their compatibility with the enteric coating.

2.   Materials and Methods

2.1.   Materials

2.1.1.   Active pharmaceutical ingredients and excipients

The aqueous extract of *Sennae fructus* was obtained from roha arzneimittel (Bremen, Germany). The drying excipient Maltodextrin DE 19 (MD) was purchased from CSC Jäklechemie (Hamburg, Germany). The subcoating materials were medium chain triglyceride (MCT) purchased from Henry Lamotte Oils (Bremen, Germany), stearic acid (StA; Palmac 98-18) from Berg+Schmidt (Hamburg, Germany), Precirol® ATO 5 (Pr) and Compritol® 888 ATO (Cp) both from Gattefossé (Bad Krozingen, Germany). The outer enteric coating Eudragit® L 30 D-55 (EuL55) was received from Evonik (Darmstadt, Germany) and talcum from CSC Jäklechemie (Hamburg, Germany). Magnesium stearate was bought from Magnesia (Lüneburg, Germany). Fumed silica and microcrystalline cellulose were obtained from NRC (Hamburg, Germany). Sudan red 7B was purchased from Merck (Darmstadt, Germany).

2.1.2.   Reference substances

Sennoside A, sennoside B, rhein, physcion and chrysophanol were obtained from Carl Roth (Karlsruhe, Germany). Sennoside C, sennoside A1, rhein-8-glucoside and kaempferol were purchased from PhytoLab (Vestenbergsgreuth, Germany).

2.1.3.   Chemical reagents

Methanol was obtained from Honeywell (Erkrath, Germany), acetonitrile from VWR International (Hannover, Germany) and anhydrous formic acid was purchased from Sigma-Aldrich (Schnelldorf, Germany). Purified water was prepared with an Easypure II water purification system, type UVIID7401, Werner (Leverkusen,

Germany) with a Barnstead D3750 Hollow Fibre Filter, pore size 0.2 µm. Sodium chloride and potassium carbonate were obtained from Merck (Darmstadt, Germany). Triethyl citrate, sodium chloride, magnesium chloride, Combi Titrant 5, Combi Methanol for volumetric Karl-Fischer titration, and potassium carbonate were bought from Merck (Darmstadt, Germany).

2.2. Methods

2.2.1. Analysis of the ingredients of *Sennae fructus* extracts

2.2.1.1. *High performance liquid chromatography (HPLC)*

The HPLC investigations were carried out with a VWR Hitachi Chromaster at 30°C equipped with a photodiode array detector (Typ 5430) using a phenomenex Synergi Polar RP column (4.6 mm x 250 mm, 4.0 µm particle size) and a cartridge precolumn system (Polar-RP, 4 x 3.0 mm). According to the draft "Senna pods, Tinnevelly" of the European Pharmacopoeia (PA/PH/Exp.13A/T, 2015) each test solution was prepared by placing 0.025 g of the fructus extract into a 50 ml screw-cap bottle and adding 25.0 ml of a mixture of methanol and a sodium hydrogen carbonate solution of 1.0 g/l (70:30 v/v). Related to the powdered *Sennae fructus* 0.5 g (particle size: 355 µm) were placed into a 250 ml screw-cap bottle and 100.0 ml of a mixture of methanol and water (50:50 v/v) were added. Each test solution was sonicated for 30 min, shaken for 2 h and filtered through a membrane filter (ProFill™, pore size 0.45 µm). Sennoside B was dissolved in a mixture of methanol and purified water (50:50 v/v) leading to a reference solution with a concentration of 0.1 mg/ml. To investigate isomerization reactions, solutions of 1 mg/ml were prepared using the reference substances sennoside A, A1, B, and C. They were separately dissolved in a mixture of methanol and water (50:50 v/v) and heated in brown glass vials for 5 h in a water

bath at 80°C. Subsequently, HPLC-UV (DAD) analysis were performed with a mobile phase consisting of 1.275 % formic acid in purified water and acetonitrile at a flow rate of 1.0 ml/min and the following gradient: 0 min, 87:13 (v/v); 3 min, 87:13 (v/v); 40 min, 37:63 (v/v); 42 min, 37:63 (v/v); 50 min, 87:13 (v/v). The wave length of detection was 270 nm. The evaluation of the HPLC chromatograms was carried out under consideration of the residual moisture content of the samples. In the case of HPLC-MS coupling, it was advantageous to reduce the formic acid portion to 0.1 % in water and 0.1 % in acetonitrile. This did not disturb the HPLC separation and had only little influence on the retention times. Behind the HPLC column a flow splitter was mounted conducting the fifth part of the flow into the MS system while the rest passes the DAD.

2.2.1.2. *Electrospray ionization / mass spectrometry (ESI/MS)*

Mass spectra were recorded in positive ion mode on a TOF-MS fitted with a Dual ESI-Source. A gas temperature of 325°C, drying gas flow of 8 l/min, nebulizing gas pressure of 3 bar and a spray voltage of 4000 V were applied.

2.2.1.3. *Electrospray ionization tandem mass spectrometry (ESI/MS/MS)*

Mass spectra were recorded in positive ion mode at 200°C on a Q-TOF-MS with ESI-Source. A drying gas flow of 9 l/min, nebulizing gas pressure of 2 bar and spray voltage of 3000 V were selected. The target mass ranged from m/z 50 to 1300. To obtain MS/MS signals the CID (collision induced dissociation) energy was adjusted to 8000 V and the ISCID (in-source collision-induced dissociation) energy was set to 5000 V.

2.2.2. Preparation of spray-dried *Sennae fructus* extracts

Spray-drying was performed with an IWK lab spray-dryer type LZ 1 (Industrie-Werke Karlsruhe, Germany) equipped with an external peristaltic pump (Multifix, Germany). For each spray-drying run, 300 g of *Sennae fructus* dry extract (batch size two tons) was dissolved in 450 g of purified water, to obtain a 40 % (w/w) solution. During all spray-drying runs, the aspirator rate was kept constant at 100 m²/h. Three dependent variables (atomizing gas pressure, inlet temperature, pump feed rate) were varied according to a central composite face-centred (CCF) design with three factor steps. This design corresponds to a factorial design (the corner of a cube) together with centre and star points, resulting in 15 combinations of process conditions (Table 1).

Table 1: Overview of the experimental drying process conditions.

Sample #	Atomizing gas pressure [kg/cm²]	Inlet temperature [°C]	Pump feed rate [ml/min]
#1		180	40
#2		220	40
#3	0.5	180	80
#4		200	60
#5		220	80
#6		180	60
#7		200	60
#8	1.0	220	60
#9		200	40
#10		200	80
#11		180	40
#12		180	80
#13	1.5	200	60
#14		220	40
#15		220	80

The dryer was operated at an atomizing gas pressure of 0.5, 1.0, and 1.5 kg/cm², respectively, at a pump feed rate of 40, 60, and 80 ml/min, respectively and at an air inlet temperature of 180, 200, and 220°C, respectively.

2.2.3. Characterization of spray-dried *Sennae fructus* extracts

2.2.3.1. *Laser diffraction*

Particle size analysis of the spray-dried *Sennae fructus* extracts was carried out by laser diffraction. The laser diffraction sensor HELOS with a particle size range of 0.1 µm to 175 µm was used, equipped with the RODOS 12SR dry dispersing unit and the GRADIS gravity disperser for imaging and laser diffraction (equipment from Sympatec, Germany). The software PAQXOS, version 2.0, was used for particle size analysis.

2.2.3.2. *Mercury porosimetry*

The spray-dried samples were measured in the fully automated low pressure mercury porosimeter Pascal 140 (Porotec, Germany) and in the high pressure system Pascal 440 (Porotec, Germany). Data evaluation (particle size, total pore surface area, compressed volume) was based on the Washburn equation (Washburn, 1921). Each sample was degassed by applying a vacuum before measurement and subsequently covered with mercury. Finally, the dilatometer was slowly run to a pressure of 350 kPa. From the change in length of the mercury column, depending on the pressure, the macropore distribution is obtained. For the high pressure measurements (0.1 MPa to 200 MPa) the sample vessel was placed into the autoclave of the mercury porosimeter and overlaid with hydraulic fluid. This procedure gradually introduced the mercury into the pore system up to the maximum possible pressure of 200 MPa.

2.2.3.3. *Scanning electron microscopy (SEM)*

The morphology of the spray-dried particles was determined with the scanning electron microscope LEO 1525 Gemini (Zeiss, Germany). The samples were sputter-coated with gold-palladium and imaged under high vacuum. A magnification of 1,000 – 2,000 fold was achieved with an in-lens detector.

2.2.3.4. *Helium pycnometry*

The absolute densities ($\rho_{absolute}$) of the spray-dried particles were measured with a gas-displacement pycnometer (AccuPyc® 1330, Micromeritics Instruments, USA), applying helium as measuring gas.

2.2.3.5. *Surface area determination by Brunauer-Emmett-Teller (BET)*

The specific surface area of the spray-dried samples was measured using a Surfer analysis apparatus (Porotec, Germany) with nitrogen adsorption after drying of the samples (30°C, 2 h).

2.2.4. Preparation of *Sennae fructus* dry-extract formulations

2.2.4.1. *Spray-drying*

The aqueous extract of *Sennae fructus* was obtained by percolation of the cut pods with cold water, followed by short-term heating of the percolate and subsequent concentrating the thin extract with a falling-film vacuum evaporator up to a dry matter content of 40 %. Spray-drying of these aqueous *Sennae fructus* extracts was performed with an IWK lab spray-dryer type LZ 1 (Industrie-Werke Karlsruhe, Germany) equipped with a two-fluid nozzle. All spray-drying runs were carried out with aqueous solutions of 40 % *Sennae fructus* extracts. The air flow rate was kept constant at 100 m³/h. The selected atomizing gas pressure was adjusted to 1.0 kg/cm², the pump feed rate to 60 ml/min, and the inlet temperature to 200°C,

resulting in an outlet temperature of 105 - 110°C. The extract was spray-dried either without additives or after addition of MD at 5, 15, and 30 % referring to the dry matter of the extract (Table 2). The resulting particles (hollow spheres) had a size between 14 and 16 µm (d_{50}).

2.2.4.2. *Freeze-drying*

For freeze-drying, the aqueous *Sennae fructus* extracts were deep-frozen at -35°C with the freeze-drier Alpha 1-4 LSC (Christ, Germany) at a pressure of 0.035 mbar and the temperature was kept constant for 8 h. Primary drying was performed at -25°C for 15 h, followed by secondary drying at 30°C for 24 h. The resulting dry extracts were sieved with a mesh size of 1 mm. The extract was freeze-dried either without additives or after addition of MD at 5, 15, and 30 % (Table 2) as performed with the spray-dried extract.

2.2.4.3. *Fluidized bed granulation*

Fluidized bed granulation was performed with a Hüttlin Solidlab 1 (Bosch, Germany). *Sennae fructus* spray-dried extracts were granulated with the bottom-spray technique using a 15 % MD aqueous solution at different volumes leading to MD additions of 2.5, 5, and 15 % (Table 2). The granulator was operated at 80°C inlet temperature, 25 m³/h air volume flow, and 0.60 bar atomizing gas pressure. The resulting particles had a size between 16 and 20 µm (d_{50}).

Table 2: Different drying processes of aqueous *Sennae fructus* extracts with regard to the type of drying, granulation, and the addition of different amounts of MD.

Sample #	Drying Process	MD, added [%]
#1	spray	0
#2	spray	5
#3	spray	15
#4	spray	30
#5	spray + granulation	2.5
#6	spray + granulation	5
#7	spray + granulation	15
#8	freeze	0
#9	freeze	5
#10	freeze	15
#11	freeze	30

2.2.4.4. *Simultaneous TGA-DSC-MS analysis*

The thermal properties and the detection of the emerging decomposition gases upon heating of the spray-dried and freeze-dried samples were examined by combined thermogravimetric analysis (TGA) and differential scanning calorimetry (DSC; STA 449 F3 Jupiter® with SiC-Ofen, Netzsch, Germany) coupled with quadrupole mass spectrometry (MS; QMS 403 C Aëolos®, Netzsch, Germany). The temperature and enthalpy calibration were performed with In (tenfold), Sn, Bi, Zn, and CsCl. After several MS scans were recorded, the mass number 18 (H_2O+) and 44 (CO_2+) were representatively selected for analysis (70 eV). The samples were heated up under an argon 5.0 flow (20 ml/min) from room temperature to 350°C with a heating rate of 10°C/min. The experiments were performed in duplicate with the native extract, the spray-dried extract with 30 % MD, and the freeze-dried extract with 30 % MD.

2.2.5. Stability studies of *Sennae fructus* extracts and their formulations

2.2.5.1. *Determination of the stability during storage*

For the storage of the samples, polypropylene cans (Jaco, Kehl, Germany; length 55.5 5 ± 0.6 mm, inside radius 28.8 ± 0.1 mm, 30 ml) were filled with the differently prepared dried samples, closed with polyethylene caps (LyondellBasell, Rotterdam, The Netherlands), and stored in a desiccator above a saturated sodium chloride solution providing a relative humidity of 75 %. The desiccator was placed into an oven at 40°C for up to 12 months. Measurements of the sennoside contents were performed after 1, 2, 3, 4, 5, 6, 9, and 12 months by HPLC.

2.2.5.2. *Quantification of the water content*

After 12 months of storage, the residual moisture content of the dry extracts was determined gravimetrically by drying of each sample (1 g) in an oven at 105°C for 3 h. This residual moisture content was calculated as follows:

$$\text{Moisture content}[\%] = \frac{\text{Initial sample weight} - \text{Final sample weight}}{\text{Final sample weight}} \cdot 100 \qquad \text{(Eq. 2)}$$

2.2.5.3. *Measurement of the hygroscopicity*

The determination of the hygroscopicity was performed by storing the samples in an open vessel in a desiccator above saturated potassium carbonate solution providing a relative humidity of 43 % for 120 h. Moisture uptake was determined gravimetrically at predetermined time points (2, 4, 24, 26, and 120 h).

2.2.6. Preparation of moisture protected tablets with *Sennae fructus* extract

2.2.6.1. *Preparation of the moisture-sensitive tablet cores*

Moisture-sensitive tablet cores were prepared by compression of 200 mg of aqueous spray-dried *Sennae fructus* extract together with tableting excipients using a rotary tablet press (Fette P1200i, Fette Compacting, Schwarzenbek, Germany) to obtain tablets with a desired thickness of 5.1 ± 0.2 mm, a desired diameter of 10 ± 0.1 mm and a desired weight of 290 mg ± 10 mg. Tablet weight, thickness, diameter, and hardness of 20 tablets were determined by an automatic process with an Erweka Multicheck apparatus (Erweka, Heusenstamm, Germany).

2.2.6.2. *Hot-melt subcoating of the tablet cores*

For hot-melt subcoating *(*HMC) the moisture-sensitive tablet cores were coated in a traditional coating pan (Walter Brucks, Brüggen, Germany; diameter 350 mm) with lipids. The lipids used for HMC were medium chain triglycerides (MCT), stearic acid (StA), Precirol® ATO 5 (Pr), and Compritol® 888 ATO (Cp) at amounts of 5, 10, and 15 mg per tablet core corresponding to 1.5, 3, and 4.5 mg/cm^2 tablet surface with a calculated manufacturing surplus of 10 % (w/w). A batch of 2 kg of tablet cores were transferred to the coating pan and heated up during pan rotating until the temperature reached values above the drop point of the respective lipid (Table 3). Subsequently, each powdered lipid was then added in portions to the zone of the fastest movement of the tablet cores in the rotating pan with a scoop. The lipids melted immediately on the tablet core surfaces and were dispersed uniformly during rotation. Finally, the coated tablets were cooled down to room temperature (RT) under continuous rotation.

Table 3. Overview of the used HMC materials and their properties.

HMC materials	Lipid composition	HLB value	Drop point	Viscosity
Medium chain triglycerides (MCT) [108]	Triglycerides of caprylic and capric acid	7	-10°C	20°C: 30 mPa·s
Stearic acid (StA) [109]	C_{18} fatty acid	15	67 - 69°C	70°C: 10 mPa·s
Precirol® ATO 5 (Pr) [110]	Mono-, di-, triglycerides with saturated C_{16} and C_{18} fatty acids	2	53 - 57°C	60°C: 31 mPa·s
Compritol® 888 ATO (Cp) [111]	Mono-, di-, triglycerides of behenic acid	2	69 - 74°C	80°C: 25 mPa·s

To detect the distribution of the coating lipids on the tablet surfaces and their penetration into the tablet cores, the dye Sudan red 7 B was mixed with the lipids and afterwards dissolved in the melted lipids during the hot-melt coating of the tablet cores at a concentration of 50 mg/g lipid and detected with a stereo microscope (Discovery.V8, Zeiss, Cologne, Germany). The tablets were cut into two pieces and the lipid penetration depths were determined at the points marked in Fig. 1. Microscopic pictures were taken with a M420 Zoom macroscope (Wild Heerbrugg, Heerbrugg, Switzerland) equipped with a Canon EOS 70 d camera (Canon, Krefeld, Germany).

2.2.6.3. *Enteric coating of the produced tablets*

EuL55 was selected as enteric coating. This aqueous dispersion consists of an anionic copolymer based on methacrylic acid and ethyl acrylate. The ratio of free carboxyl groups to ester groups is 1:1. 20 % of the plasticizer triethyl citrate and 80 % of talc (based on the dry polymer weight) were added to this aqueous dispersion. Batches of 2 kg tablet cores, as well as subcoated tablets (10 mg HMC/core) were introduced into the fluidized bed coater Driacoater 500 (DRIAM Coating Technology, Eriskirch, Germany). The inlet temperature was kept constant at 45°C to reach a

product temperature of 30 - 33°C. The pressure of the spray gun was set to 2.0 bar, the air volume to 75 m³/min, and the pump feed rate to 20 ml/min. Sampling took place after both, 5 and 10 mg outer enteric coating per tablet, which corresponded to 1.5 and 3 mg/cm² tablet surface, respectively. The total film mass per tablet amounted to 20 mg, which included 10 mg of subcoating and 10 mg of enteric coating. The subsequent curing time was 30 min at 45°C.

2.2.6.4. *Moisture content and hygroscopicity of the tablets*

Karl-Fischer titration was performed for determination of the moisture content of all investigated tablet samples with a Mettler Toledo DL 18 coupled to a Mettler GA 44 printer and an AE 50 balance (Mettler-Toledo, Hamburg, Germany). The moisture content of the tablets was determined before and after the HMC process. The investigation of the hygroscopicity was performed by storing the tablets above three different aqueous salt solutions at RT: saturated magnesium chloride with a relative humidity (RH) of 33 %, saturated potassium carbonate with a RH of 43 %, and saturated sodium chloride with a RH of 75 %. Moisture uptake was determined gravimetrically at predetermined time points.

2.2.6.5. *Disintegration time of the tablets*

The disintegration test was performed with tablet cores, subcoated tablets, and enteric-coated tablets using the disintegration apparatus Erweka ZT3-2 (Erweka, Heusenstamm, Germany) according to the European Pharmacopoeia. The disintegration of tablet cores and the subcoated tablets was carried out with discs in distilled water at a temperature of 37°C. Examination of the enteric resistance of the enteric-coated tablets was performed after placing them into the acid medium (0.1 M HCl) without discs. Subsequently, the same samples were subject to a disintegration test with discs in a phosphate buffer pH 6.8 to simulate small intestinal conditions.

2.2.6.6. *Dissolution of the tablets*

In modification of the monograph of the European Pharmacopoeia, gastric resistance was tested in a disintegration tester for 2 h at 37°C in 0.1 M HCl before performing the dissolution tests. The in vitro dissolution tests were performed with the same tablets in 900 ml of phosphate buffer pH 6.8 at 37°C with the paddle apparatus of the European Pharmacopoeia at 100 rpm. Because of the high detection limits of the sennosides, 5 tablets per vessel were tested. After 15, 30, 45, and 60 min the content of the released sennosides were measured with HPLC.

3.   Results and Discussion

3.1.   Qualitative and quantitative analysis of *Sennae fructus*

3.1.1.   Identification of the ingredients of *Sennae fructus* extracts

HPLC-UV(DAD)-ESI/MS and HPLC-ESI/MS/MS analysis of *Sennae fructus* were conducted to reliably identify the peaks of the HPLC chromatograms presented in the draft monographs of the Pharmacopoeia [104]. The allocation was based on UV(DAD) spectra for the assignment to a specific substance class, on ESI/MS analysis to determine the molecular formula and on MS/MS investigations to identify characteristic structural fragments. Since the chemical composition of *Sennae fructus* is known, the assignment of the peaks to the constituents was possible. The chromatogram of a *Sennae fructus* extract showed good separation of 33 peaks (Fig. 10), consisting of 19 hydroxyanthracene derivatives, 8 flavonoids, 2 benzo-phenones, 3 naphthalenes and an unknown derivative (Table 4). Various compound groups could be identified in *Sennae fructus*, e.g.: anthraquinones, anthraquinone-glucosides, dianthrones, dianthrone-glucosides, dianthrone-diglucosides, benzo-phenones, flavonoids, flavonoide-glucosides, flavonoide-diglucosides, naphthalenes and naphthalene-glucosides. Their spectroscopic properties are discussed in the following.

3.1.1.1. *Anthraquinones*

The reference substances sennoside B, sennoside A1, sennoside A, sennoside C, rhein-8-glucoside, rhein, aloe emodin and chrysophanol were applied to confirm compound identification. Isomers such as sennidine A/B, sennidin-monoglucoside A/B, C/D and sennoside D/D1/C1 were not commercially available, i.e. the isomeric pairs could not be reliably assigned to the respective peaks.

Aloe emodin (Fig 10; Table 4, peak # 29):

UV maxima were detected at 253 and 431 nm, corresponding to the benzoyl group and at 430 nm (quinoid part) [112]. The ESI mass spectrum of this compound shows a prominent signal at m/z 271, representing the quasi-molecular ion [M+H]$^+$ with the molecular formula $C_{15}H_{10}O_5$. The dominating fragmentation process is the elimination of the substituent in position C3 at the second benzenoid ring, giving rise to an ion species at m/z 240. This specific fragment was observed in all ESI spectra of anthraquinone and dianthrone constituents containing a rhein and aloe emodin molecule, respectively. The breakdown of the tricyclic anthraquinone skeleton yields typical fragments at m/z 226 and 164, the formation of which remains unclear. These two characteristic ions could also be detected in the ESI spectra of the corresponding glucosylated anthraquinones and dianthrones. The MS/MS experiment on the [M+H]$^+$-ion showed fragments at m/z 239, 211, and 182, which by analogy with EI fragmentation may be explained as [(M+H) - CH$_3$OH]$^+$, [(M+H) - CH$_3$OH - CO]$^+$, and [(M+H) - CH$_3$OH - 2 CO]$^+$, respectively.

Rhein-8-glucoside (Fig 10; Table 4, peak # 15):

Absorption maxima at 260 and 411 nm give evidence for the presence of an anthranoid skeleton. In the ESI mass spectrum a signal at m/z 469 (molecular formula: $C_{21}H_{18}O_{11}$) representing the quasimolecular ion species [M+Na]$^+$ along with the base peak at m/z 285 suggests a rhein-8-glucoside structure. This prominent peak [(M+H) - glc]$^+$ is formed by cleavage of the glucosidic bond. The most intense signal in the high mass region is a fragment at m/z 421 [(M+H) - C$_2$H$_2$]$^+$ with about 43 % abundancy, presumably deriving from the ejection of acetylene after rearrangement. This neutral particle loss is energetically favoured and has been described for these aromatic compounds during EI ionization [113]. The strong peak

at m/z 270 is probably attributed to the unglucosylated rhein moiety, carrying no substituent in position C8. The abundant fragment m/z 240 $[(M+H) - glc - COOH]^+$ has already been mentioned earlier. Concerning the prominent ion species at m/z 255 several alternative fragmentation pathways can be considered.

Sennidin A/B (Fig 10; Table 4, peaks # 31, 32):

Sennidin A and B represent two isomeric dianthrone aglycones, exhibiting UV absorption maxima at 272 and 375 nm. Their ESI mass spectra are mainly characterized by two quasi-molecular ions at m/z 539 $[M+H]^+$ and m/z 561 $[M+Na]^+$ and a base peak at m/z 270, which is formed by cleavage of the central C9-C9´ single bond. H-rearrangement and successive bond cleavages of C8α-C9 and C1α-C9 leading to an entity of two substituted aromatic rings connected via the C10-carbonyl, may account for the fragment at m/z 256.

Sennidin-monoglucoside A/B (Fig 10; Table 4, peaks# 22, 23, 24):

These constituents bear a glucose residue at position 5´ of the sennidin A/B skeleton. The maxima of their UV absorption bands were at 251, 266, and 374 nm. In the ESI mass spectrum two quasi-molecular ions could be detected at m/z 718 and m/z 723 corresponding to $[M+NH_4]^+$ and $[M+Na]^+$, respectively. High resolution delivered the molecular formula $C_{36}H_{28}O_{15}$. After H-rearrangement and cleavage of the glucosidic bond the sugar moiety is removed. This results in a specific fragment of moderate intensity at m/z 539 $[(M+H)-glc]^+$. As already described for the corresponding aglycone, cleavage of the single bond C9-C9´ is the most favored fragmentation process and yields the base peak at m/z 270, representing an unglucosylated anthrone. Under EI conditions, a fragment at m/z 658 may be generated due to the loss of the neutral entity of CH_2CO with presumably C3 and C4 being involved. erhaps, a similar process is initiated by electrospray ionization

forming the ion species at m/z 681, which accounts for $[(M - CH_2CO)+Na]^+$. Concerning the abundant fragments at m/z 226, 240 and 256 please refer to the text on aloe emodin and sennidin A/B.

Sennoside B (Fig 10; Table 4, peak # 10):

This compound exhibits spectral properties of a homodianthrone bearing two sugar moieties. Its UV absorption maxima were encountered at 268 and 360 nm. The ESI mass spectrum shows an analogous fragmentation pattern to sennidin-mono-glucoside: quasimolecular ions were detected at m/z 880 $[M+NH_4]^+$ and 885 $[M+Na]^+$. Characteristic fragments deriving from successive sugar elimination were also observed at m/z 718 $[(M+NH_4) - glc]^+$ and m/z 539 $[(M+H) - 2glc]^+$, respectively. All these ion species were of minor intensity. As expected, the mass spectrum is dominated by the base peak at m/z 270 (unglucosylated monoanthrone moiety) resulting from the favoured single bond cleavage between C9 and C9´. In case of the heterodianthrones such as the sennosides C and D containing both a rhein and aloe emodin substructure, this fragmentation can produce two characteristic ion species, namely at m/z 270 and at m/z 256.

3.1.1.2. *Benzophenones*

Cassiaphenone B-2-glucoside (Fig 10; Table 4, peak # 3):

Chemically, this constituent is a benzophenone derivative with a glucose moiety attached. UV absorption maxima appear at 240, 275, and 321 nm. In the upper region of the ESI mass spectrum the ion species are observed at $[(M+H) - H_2O]^+$ at m/z 463, $[M+H]^+$ at m/z 481, $[M+NH_4]^+$ at m/z 498, and $[M+Na]^+$ at m/z 503, thus clearly determining the molecular mass of cassiaphenone B2-glucoside. All these ions are of low intensity. The spectrum is governed by two pronounced peaks: the signal at m/z 319, standing for the base peak, is formed by cleavage of the

glucosidic linkage, i.e. the ejection of the sugar residue. The second abundant fragment at m/z 209 is probably generated by elimination of the glucosylated aromatic ring because of an α-cleavage of the bond adjacent to the central carbonyl group connecting the two benzene rings. MS/MS experiments both on peak m/z 498 (quasi-molecular ion) and m/z 309 (aglycone) suggest that this structure may arise from the glycoside as well as from the non-sugar part. The less abundant ions at m/z 301 and m/z 191 may originate from fragments at m/z 319 and 209, respectively, by elimination of water.

3.1.1.3. *Flavonoids*

Quercetin-diglucoside (Fig 10; Table 4, peak # 4):

In the UV spectra of most flavonoids two major absorption maxima are found: The first maximum ranges from 240 to 285 nm and is caused by to the A-ring benzoyl system while the second one occurs in the range between 300 and 400 nm, originating from the B-ring cinnamoyl system [114]. For quercetin-diglucoside UV maxima at 258 and 356 nm were observed. In the ESI mass spectrum of quercetin-diglucoside two quasi-molecular ions are present: a base peak at m/z 627 $[M+H]^+$ and a second one at m/z 649 $[M+Na]^+$ being less abundant. High resolution resulted in the molecular formula $C_{27}H_{30}O_{17}$. In addition, the following characteristic fragment species of minor intensity are found: the peak at m/z 595 $[(M+H)-CH_2OH]^+$ results from elimination of the hydroxymethyl substituent of the terminal glucose moiety by α-cleavage. The successive loss of glucose leads to the ion species at m/z 465 $[(M+H)-glc]^+$ and m/z 303 $[(M+H)-2glc]^+$. The CID spectrum of $[M+H]^+$ is completely dominated by this last-mentioned fragment. Further ions are only detectable in traces. The species at m/z 285 presumably corresponds to the flavonoid aglycone bearing no substituent in position C-3 at the γ-pyrone ring. Maybe its decomposition

leads to the fragments at m/z 257 and 229 by successive elimination of CO. The ejection of this stable neutral particle is a well-known breakdown process of flavones under electron impact ionization [115]. The tiny fragments at m/z 145 and 127 are supposed to be products from the glucose fragmentation.

Vicenin-2 (Fig 10; Table 4, # 2):

This constituent is also a flavone in nature, representing a 6,8-di-C-glucosylapigenin. Vicenin-2 has gained importance in recent years because of new studies and discussions on anti-cancer effects in case of prostate cancer [116] and anti-glycation properties [117]. The UV spectrum of this compound shows maxima at 239, 271, and 333 nm. The molecular weight can easily be determined from the ESI mass spectrum exhibiting quasi-molecular ions at m/z 595 $[M+H]^+$, m/z 617 $[M+Na]^+$, and m/z 633 $[M+K]^+$. High resolution measurement provided the molecular formula $C_{27}H_{22}O_{12}$. Other fragments only occur with an abundance below 1%: the ions at m/z 489 and 475 presumably arise from a glucose degradation process, thus representing the species $[(M+H) - C_3H_6O_4]^+$ and $[(M+H) - C_4H_8O_4]^+$, respectively. The peak at m/z 447 may be assigned to a fragment that lost the sugar residue at position C-8 with leaving a CH_2-group. Such fragmentation has been described for C-glucosylflavones on electron impact ionisation [118]. Very small signals at m/z 559, 433, and 271 may indicate the loss of water and glucose, respectively, leading to the fragments $[(M+H) - 2H_2O]^+$, $[(M+H) - glc]^+$, and $[(M+H) - 2glc]^+$.

3.1.1.4. Naphthalenes

Substances belonging to this compound class exhibit an UV absorption band around 240 nm, a shoulder around 265 nm, and a weaker broad maximum between 300 - 340 nm.

Tinnevellin-glucoside (Fig 10; Table 4, # 20):

This constituent is of particular interest, since it serves as an analytical marker, characterizing extracts deriving from Cassia angustifolia plants. It is absent in Cassia acutifolia, which contains a different naphthalene derivative, 6-hydroxymusicin, as distinguishing feature. Tinnevellin-6-glucoside exhibits only minor fragmentations in its ESI mass spectrum. The $[(M+H)]^+$- base peak with the elemental composition $C_{20}H_{25}O_9$ at m/z 409 is accompanied by two less abundant quasi-molecular ions at m/z 431 $[(M+Na)]^+$ and m/z 447 $[(M+K)]^+$. The principal cleavage product is a fragment at m/z 247, indicating the elimination of the sugar moiety from the $[(M+H)]^+$- ion. The other quasi-molecular ions decompose in the same way, providing the peaks at m/z 269 $[(M+Na) - glc]^+$ and m/z 285 $[(M+K) - glc]^+$, respectively. The small peak at m/z 229 may formally be deduced from the $[(M+H)]^+$-species by splitting off glucose and water. The CID spectrum of the $[(M+H)]^+$-ion shows a prominent fragment at m/z 229, besides an abundant peak at m/z 247, thus giving rise to the assumption that this species may directly derive from the quasi-molecular ion. However, a parallel MS/MS experiment on the quasi-molecular ion of the aglycon tinnevellin at m/z 247 $[(M+H)]^+$ revealed that the m/z 229 species can also originate from the non-sugar part.
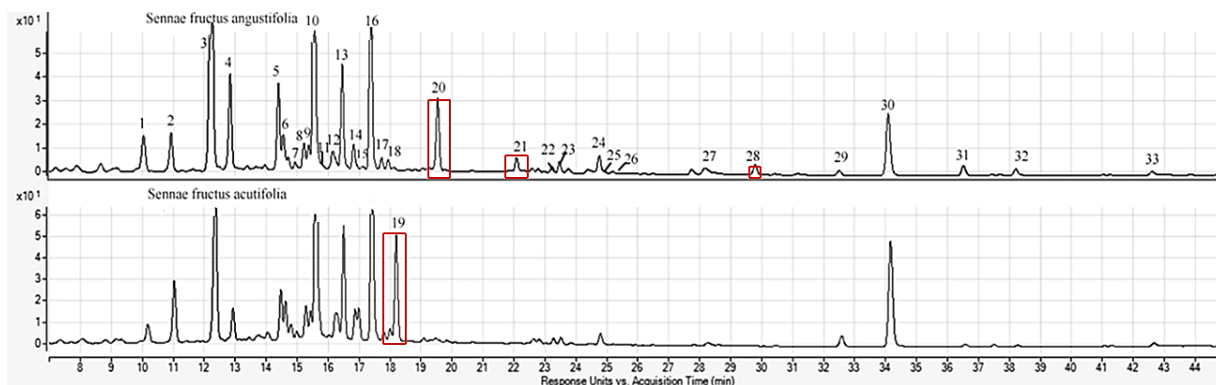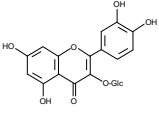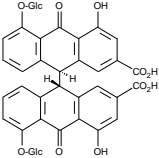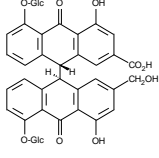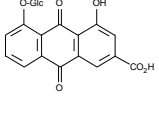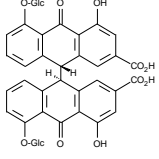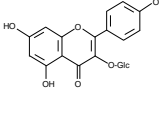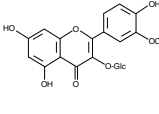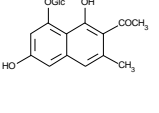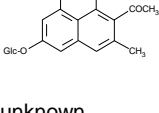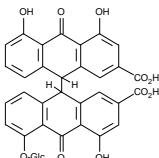

Fig. 10: HPLC-UV(DAD) chromatograms of *Sennae fructus* extracts recorded at 270 nm: A - *Sennae fructus* angustifolia, B - *Sennae fructus* acutifolia.

The peaks displayed in Figure 10 are described in detail in Table 4.
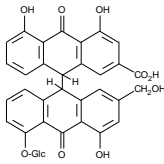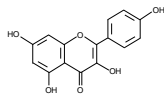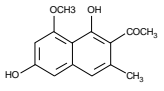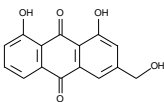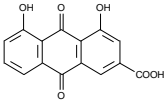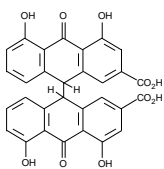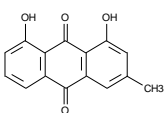
Table 4: Data obtained from the analysis of *Sennae fructus* extracts.

peak #	t_R [min]	Identity	Substance class	Structure	MW [g/mol] molecular formula	Identi-fication [1]	ESI pos $[m/z]^+$ [2]	MS/MS pos $[m/z]^+$ [3]
1	10.0	cassia-phenone A-2-glucoside	benzo-phenone-glucoside		466.42 $C_{21}H_{22}O_{12}$	[99]; UV; ESI; MS/MS	489, 467, 379, 305	484 → 305, 195; 305 →195
2	10.9	vicenin-2	flavonoid		594.52 $C_{27}H_{30}O_{15}$	[141]; UV; ESI; MS/MS	595, 617, 633, 475, 447	595 → 325, 379, 337, 307, 295
3	12.1	cassia-phenone B-2-glucoside	benzo-phenone-glucoside		480.40 $C_{21}H_{20}O_{13}$	[99]; UV; ESI; MS/MS	498, 463, 503, 319, 209, 191	498 → 209, 301, 319, 191 319 → 209, 301
4	12.8	quercetin-diglucoside	flavonoid		626.24 $C_{27}H_{30}O_{17}$	[139]; UV; ESI; MS/MS	627, 649, 595, 465, 303	627 → 303, 145, 127, 257, 465
5	14.4	kaempferol-diglucoside	flavonoid		610.52 $C_{27}H_{30}O_{16}$	[139]; UV; ESI; MS/MS	611, 633, 649, 449, 287	611 → 287, 145, 127, 329, 163 287 → 270, 224, 134, 130, 169
6	14.6	isorhamnetin-diglucoside	flavonoid		640.54 $C_{28}H_{32}O_{17}$	[139]; UV; ESI; MS/MS	641, 499, 478, 317, 611	641 → 317, 145, 127, 302, 285
7	15.1	aloe emodin-dianthron-diglucoside	hydroxy-anthracene		834 $C_{42}H_{42}O_{18}$	[139]; UV; ESI	857, 511, 256	511, 256, 852
8	15.2	sennoside D/D1/C1	hydroxy-anthracene		848.77 $C_{42}H_{40}O_{19}$	[137]; UV; ESI; MS/MS	871, 256, 240, 226, 195	525 → 256, 270; 256 → 224, 243, 169, 227, 211
9	15.4	sennoside D/D1/C1	hydroxy-anthracene	# 8	848.77 $C_{42}H_{40}O_{19}$	[137]; UV; ESI; MS/MS	871, 525	256 → 224, 243, 169, 227, 211
10	15.5	sennoside B	hydroxy-anthracene		862.74 $C_{42}H_{38}O_{20}$	[140]; Co; UV; ESI; MS/MS	880, 885, 718, 539, 270	539 → 270, 227, 224, 169, 211 270 → 256, 227, 224, 245, 169

11	15.7	sennoside D/D1/C1	hydroxy-anthracene	# 8	848.77 $C_{42}H_{40}O_{19}$	[137]; UV; ESI; MS/MS	866, 687, 270, 525, 256	$256 \rightarrow 224, 243, 169, 227, 211$ $866 \rightarrow 256, 270, 238, 181, 145$
12	16.2	quercetin-glucoside	flavonoid		464.38 $C_{21}H_{20}O_{12}$	[141]; UV; ESI; MS/MS	487, 465	$465 \rightarrow 303, 145, 127, 343, 367$
13	16.5	sennoside A1	hydroxy-anthracene		862.74 $C_{42}H_{38}O_{20}$	[139]; Co; UV; ESI; MS/MS	880, 539, 270	$270 \rightarrow 224, 227, 169, 211, 183$
14	16.8	sennoside C	hydroxy-anthracene		848.77 $C_{42}H_{40}O_{19}$	[137]; Co; UV; ESI; MS/MS	871, 525, 256	$525 \rightarrow 256, 270, 227, 238, 211$
15	16.9	rhein-8-glucoside	anthra-quinone-glucoside		446.37 $C_{21}H_{18}O_{11}$	[141]; Co; UV; ESI; MS/MS	469, 421, 285, 270, 255, 240	$285 \rightarrow 256, 227, 169, 224, 211$
16	17.4	sennoside A	hydroxy-anthracene		862.74 $C_{42}H_{38}O_{20}$	[140]; Co; UV; ESI; MS/MS	880, 539, 270	$880 \rightarrow 270, 454, 224, 196, 145$ $270 \rightarrow 256, 227, 224, 169, 211$
17	17.7	kaempferol-glucoside	flavonoid		448.66 $C_{22}H_{20}O_{11}$	[42]; ESI; MS/MS	449, 471, 287, 270	$449 \rightarrow 287, 145, 127, 227, 169;$ $287 \rightarrow 227, 169, 211, 183, 270$
18	17.9	isorhamnetin-glucoside	flavonoid		478.68 $C_{23}H_{22}O_{12}$	[42]; ESI; MS/MS	479, 449, 317	$479 \rightarrow 317, 302, 177, 145, 127$
19	18.2	6-hydroxy-musicin-8-glucoside	naphthalene		394.37 $C_{19}H_{22}O_{9}$	[136;99]; ESI; MS/MS	417, 395, 317, 233	$395 \rightarrow 233, 215, 299, 257, 145$ $233 \rightarrow 215$
20	19.5	tinnevellin-6-glucoside	naphthalene		408.40 $C_{20}H_{24}O_{9}$	[136;99]; UV; ESI; MS/MS	409, 431, 247, 229	$409 \rightarrow 247, 229, 205$
21	22.1	unknown	unknown	unknown	494	ESI; MS/MS	495	495
22	23.3	sennidinmono-glucoside A/B	hydroxy-anthracene		700.88 $C_{36}H_{28}O_{15}$	[99]; ESI; MS/MS	718, 681, 539, 270, 256, 240, 226	$718 \rightarrow 270, 227, 211, 169, 157$

23	23.5	sennidin-mono-glucoside A/B	hydroxy-anthracene	# 22	700.88 $C_{36}H_{28}O_{15}$	[99]; ESI; MS/MS	718, 723, 681, 539, 270, 256, 240, 226	539 → 270; 270 → 227, 211, 169, 157, 256
24	24.8	sennidin-mono-glucoside A/B	hydroxy-anthracene	# 22	700.88 $C_{36}H_{28}O_{15}$	[99]; ESI; MS/MS	723, 681, 539, 270, 211, 240, 226	718 → 270, 227, 211, 169, 123
25	24.9	sennidin-mono-glucoside C/D	hydroxy-anthracene		686 $C_{36}H_{30}O_{14}$	[99]; ESI; MS/MS	687, 525, 256, 270	256 → 213, 227, 169, 157, 123
26	25.2	sennidin-monoglucosid C/D	hydroxy-anthracene	# 25	686 $C_{36}H_{30}O_{14}$	[99]; ESI; MS/MS	687, 525, 256, 270	256 → 213, 227, 169, 157, 123
27	28.3	kaempferol	flavonoid		286.23 $C_{15}H_{10}O_6$	[99]; Co; UV; ESI; MS/MS	287, 271,	287 → 271, 157, 227, 169, 211
28	29.8	tinnevellin	naphthalene		246.54 $C_{14}H_{14}O_4$	[141]; UV; ESI; MS/MS	247, 269, 285	247 → 229, 157, 211, 169, 123
29	32.5	aloe emodin	anthra-quinone		270.24 $C_{15}H_{10}O_5$	[138]; Co; UV; ESI; MS/MS	271, 240, 226, 164	271 → 157, 227, 123, 169, 211
30	34.1	rhein	anthra-quinone		284.22 $C_{15}H_8O_6$	[138]; Co; UV; ESI	285, 240, 227	285
31	36.5	sennidin A/B	hydroxy-anthracene		538.46 $C_{30}H_{18}O_{10}$	[140]; ESI	539, 561, 270, 256, 240, 226	-
32	38.2	sennidin A/B	hydroxy-anthracene	# 31	538.46 $C_{30}H_{18}O_{10}$	[140]; ESI	539, 561, 270, 256, 240, 226	-
33	42.5	chrysophanol	anthra-quinone		254.24 $C_{15}H_{10}O_4$	[138]; Co; UV; ESI; MS/MS	254, 255, 277	254 → 157, 123, 169, 227, 211

[*1] [#] = compound already described for *Sennae fructus*; Co = coelution with reference substances;

UV = substance class assignment by DAD; ESI = detection of molecular formula (high resolution);

MS/MS = confirmation of fragmentation pattern.

[*2] quasimolecular ions and selected ions measured with ESI/MS.

[*3] fragments from the respective ion, marked with an arrow, five most intense signals observed with MS/MS.

3.1.2. Determination of the total hydroxyanthracene glycoside content

As described in the draft monographs the quantification of the bioactive anthraquinones is performed by determination of the sum of the total hydroxyanthracene glycosides. The HPLC/MS investigations on *Sennae fructus* extract furnished more detailed information about peaks which should be considered for calculation of the total content of hydroxyanthracene glycosides.

A number of 8 hydroxyanthracene glycosides could be identified in this HPLC chromatogram (Table 4). However, in the draft monographs only 6 hydroxy-anthracene glycosides are mentioned for the quantification of the total hydroxyl-anthracene glycosides. Unfortunately, these glycosides are not yet further specified. Therefore the two additional peaks found in the chromatograms of the present study cannot be allocated to the respective hydroxyanthracene glycosides. But most likely one of the two hydroxyanthracene glycosides is aloe emodin-dianthron-diglucoside. Although this substance does not appear to play a major role concerning its content but contributes to the overall pharmacologically effect of hydroxyanthracene glycosides. In comparison to rhein anthrone the stimulation of the laxative effect of the aloe emodin anthrone is less pronounced but it is assumed that both anthrones increase their purgative effects synergistically [119; 120; 121; 122].

One of the HPLC peaks mentioned in the draft monographs seems to be rhein-8-glycoside (Fig 10; Table 4, peak # 15), which function as active principle and toxicity is discussed in literature [123]. Moreover, its content varies depending on the kind of the sample preparation [98]. Therefore, including this anthraquinone glycoside into the total of hydroxyanthracene glycosides does not appear appropriate.

The determination of the total amount of these hydroxyanthracene glycosides seems more reasonable than to restrict quantification to solely sennoside A and sennoside B, as described in the Japanese Pharmacopoeia [124], because after thermal

treatment of the reference substances sennoside A, A1, B and C isomerizations could be detected by HPLC-UV(DAD)-ESI/MS. Such isomerizations have already been mentioned in the literature [125; 126] and it was found in this study that sennoside A is transformed into sennoside A1 and B, sennoside A1 to A and B and sennoside B to A1 and A. Therefore, the quantification of these single sennosides does not appear to be meaningful with regard to the quality of the herbal drug. Sennoside C partly transforms into 3 isomers – sennosides C1, D and D1 are assumed. This isomerization of sennoside C confirmed the assignment of the 3 isomers to the retention times as shown in Table 4.

In addition to the total hydroxyanthracene glycoside determination using the HPLC method of the monographs draft, it is possible to also identify other constituents for quantitative purposes intended for the evaluation of the toxicity or the shelf life as opposed to the Bornträger assay in the European Pharmacopoeia. Therefore, the maximally allowed levels of rhein and aloe emodin are determined according to the draft in Pharmeuropa [103,104]. In the past, these substances have often been discussed to be toxic or carcinogenic. Contradictory statements regarding to Senna were made: In animal studies, teratogenicity of rhein has been demonstrated [127], but could not be confirmed in humans [128]. Cytotoxicity of rhein could be detected in cell lines, leading to cell apoptosis [129]. However, in a long-term study with Senna in rats, carcinogenicity could not be proved [130].

In summary, especially by considering the low amounts of the anthraquinones detected in Senna, the constituents might not present a relevant genotoxic or carcinogenic risk for humans [131, 132, 133]. A long-term investigation of the contents of rhein and aloe emodin in various pharmaceutical dosage forms of senna could be helpful to monitor the contents of these anthraquinones in the dosage forms during the storage. Phytochemical differentiation between the two Senna species.

Historically, the distinction of the different Senna species is primarily based on the two main regions of origin for commercial trade – Africa and India. *Cassia angustifolia* was cultivated mainly in Tamil Nadu and Gujarat while cultivation of *Cassia acutifolia* was limited to the African Sahel with the main distribution area in northern Sudan [134]. In this country, the drugs are collected from wild plants, thus *Cassia acutifolia* plays a minor role in the world market, because it is not derived from cultivated plants such as *Cassia angustifolia* [135]. Currently, the main portion of *Sennae fructus* comes from newly developed cultivating areas in northern India, because of their lower level of aflatoxins. This plant material is labeled as *Cassia angustifolia*, but morphologically it shows different pod forms – one similar to *Cassia acutifolia* from Sudan and the other resembles *Cassia angustifolia* from southern India. *Cassia acutifolia* seems to exist in increasing quantities in northern India. Based on the European Pharmacopoeia the confirmation whether a mixture of the two species is present is only examined macroscopically. The result of this investigation is not always representative because of the different ripeness of *Sennae fructus* in the mixture. As the regions where Senna is cultivated increased during the last years, the analysis of the constituents becomes more important. To distinguish between the two Senna species in a mixture is possible phytochemically by the detection of two different naphthalenes as established by Lemli [136]. While *Sennae fructus acutifolia* contains 6-hydroxymusicin-glucoside *Sennae fructus angustifolia* is characterized by tinnevellin-6-glucoside. With the HPLC method presented in Pharmeuropa [103, 104] two additional peaks can be found in the extract of *Sennae fructus angustifolia* in comparison to that one of *Sennae fructus acutifolia*: the non-glycosylated Tinnevellin and an unknown derivate (Table 4).

Currently, the two *Sennae fructus* monographs specify that not more than 1 % foreign matter including parts of other plants is present. This is difficult to meet

because of the extending regions of cultivated Senna particularly in northern India. As *Sennae fructus* may consist of mixtures of two Cassia species, which are difficult to distinguish macroscopically, a combination of the two monographs resulting in one *Sennae fructus* monograph with suitable analytical assays is recommended. A practical solution for the use of Senna pods, which are currently defined in the European Pharmacopoeia with different contents of total hydroxyanthracene glycosides, should be considered for industrial processing and dispensing in pharmacy.

3.1.3. Conclusions

The HPLC method, which is in discussion for the modified monographs of *Sennae fructus* in the European Pharmacopoeia, showed numerous well-separated constituents of *Sennae fructus* extracts. A number of 32 compounds could be identified and assigned to the corresponding chromatogram peaks. Because of possible isomerizations of the sennosides the quantification should include all 8 detectable sennosides to obtain realistic data of the bioactive anthraquinones. Thus, the calculation of only 6 sennosides as described in the draft monographs [103,104] for quantification of the total hydroxyanthracene glycosides and including rhein-8-glucoside should be reconsidered. In addition, the elaboration of a combined monograph instead of two separate monographs of *Sennae fructus* has to be discussed and suitable analytical assays need to be added.

3.2. Stability-relevant analysis of the spray-dried *Sennae fructus* extracts

3.2.1. Effect of the spray-drying conditions on the moisture content

The loss on drying of the spray-dried *Sennae fructus* extracts obtained under various process conditions resulted in significant differences (Fig. 11). The lowest loss on drying amounted to 5.2 ± 0.3 % obtained under the following conditions: atomizing gas pressure 1.5 kg/cm^2, inlet temperature 220°C, pump feed rate 40 ml/min. The sample with the highest loss on drying (6.6 ± 0.1 %) was obtained with 0.5 kg/cm², 180°C, and 80 ml/min. Thus, the total difference in the moisture content of the spray-dried samples amounted to 1.4 ± 0.4 %. An increase of the atomizing gas pressure from 0.5 kg/cm² to 1.5 kg/cm² led to a moisture reduction of 12.3 %. A decrease of the temperature from 220°C to 180°C as well as a rise of the pump feed rate from 40 ml/min to 80 ml/min resulted in a moisture increase of 6.1 %. In summary, spray-dried *Sennae fructus* extracts resulted in reduced moisture contents at high atomizing gas pressures, high inlet temperatures, and low pump feed rates. Interestingly, the atomizing gas pressure had the most significant effect on the moisture content. During the spray-drying process, the heat and mass transfer define the resulting powder properties. The crucial influence of atomizing gas pressure results from generating large surface areas over which heat and mass transfer takes place. Also, the inlet temperature influences directly this transfer in the spray-dried droplets because of the higher moisture evaporation and thus higher moisture gradients inside the droplets at higher inlet temperatures [142]. This result is consistent with other findings [12, 143]. Araruna et al. [144] studied the influence of the pump feed rate, the inlet temperature and the air flow rate on the moisture content of the powder. They observed the highest influence by varying the pump feed rate. This observation is in accordance with a study by Kurozawa, Park, & Hubinger [145] who found that higher pump feed rates reduce the contact time

between the feed and the drying air resulting in a lower driving force for water evaporation, thus obtaining powders with higher moisture content.
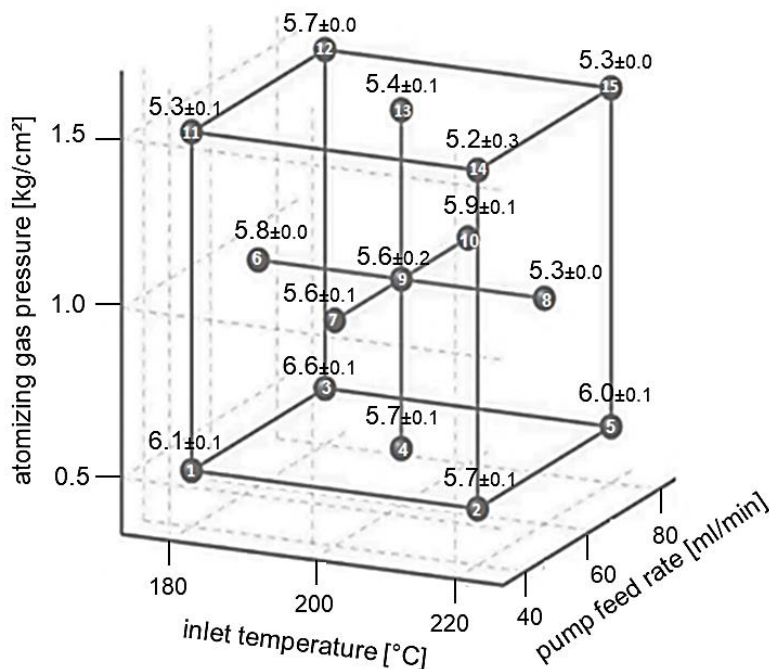
Fig. 11: Illustration of the experimental drying variables according to the central composite face-centered (CCF) design. The dependence of the moisture content of the spray-dried samples on the different spray drying conditions may be obtained from the loss on drying [%], displayed by the numbers above the spheres. The numbers (#1-#15) within the spheres represent the different process parameters which are listed in detail in Table 1. Means ± SD, n=3, ANOVA: $F_{(14,30)}=32$, $p<0.05$.

3.2.2. Particle size analysis

Particle size analysis was carried out by laser diffraction and mercury porosimetry. The curves profiles shown in Fig. 12 illustrate the particle distributions of the spray-dried *Sennae fructus* extracts. The respective drying variables (#1-#15) attributable to the individual particle size distribution curves are listed in Table 1. Spray-drying

with an atomizing gas pressure of 0.5 kg/cm² (curves #1-#5) resulted in *Sennae fructus* extract particles with mean $d_{50\%}$ values between 16.6 and 19.7 µm (laser diffraction) and between 14 and 21 µm (mercury porosimetry). Particles with a mean $d_{50\%}$ values between 13.2 and 14.2 µm (laser diffraction) and between 10 and 12 µm (mercury porosimetry) were obtained by an atomizing gas pressure of 1.0 kg/cm² (curves #6-#10) while particles with a mean $d_{50\%}$ values between 8.9 and 11.1 µm (laser diffraction) and between 7 and 9 µm (mercury porosimetry) were generated by an atomizing gas pressure of 1.5 kg/cm² (curves #11-#15). This data is shown in detail in Table 5.
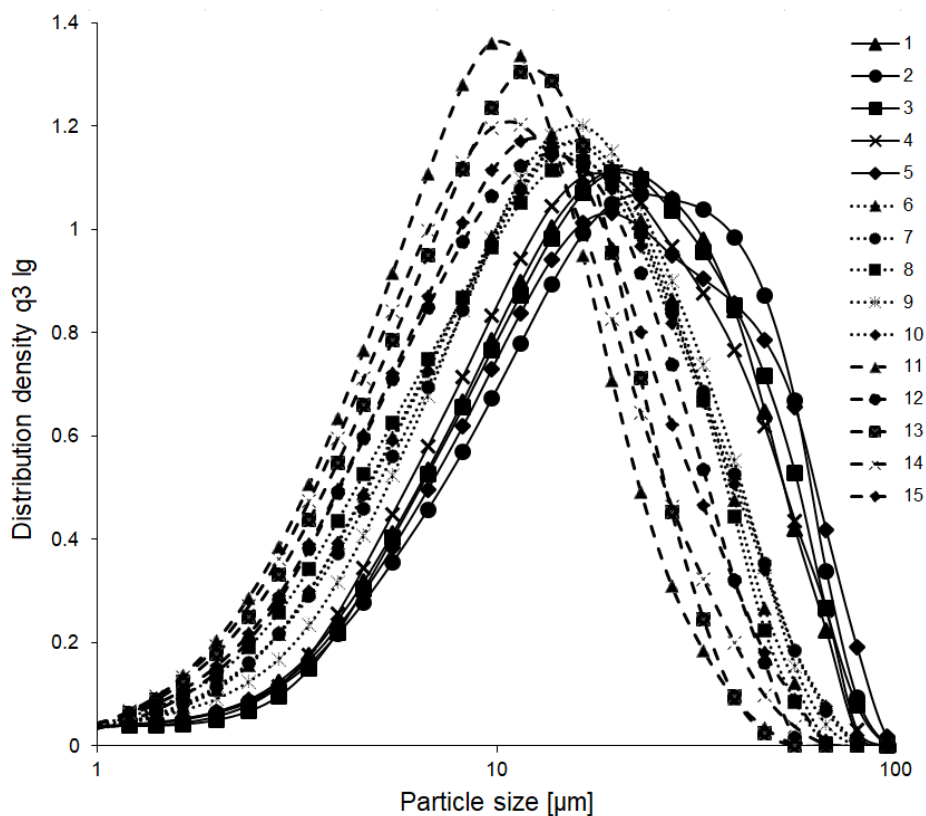
Fig. 12: Averaged particle size distribution profiles (n = 3) of the spray-dried *Sennae fructus* extracts obtained by different spray drying conditions determined by laser diffraction. Particle size is given in µm. Numbering of the distribution curves refers to numbering in Table 1.

A comparison of the particle sizes measured by laser diffraction with the data obtained from measurements by mercury porosimetry led to different results with regard to the exact particle sizes. A cause may be the different extent of aggregation resulting from the high degree of pulverization of the particles. The data in both, Fig. 12 and Table 5, demonstrate that the atomizing gas pressure has the largest influence on the particle size distribution. The particle size can nearly be doubled by reducing the atomizing gas pressure, this is shown by comparing the $d_{50\%}$ values of samples #1 - #5 and those of samples #11 - #15. A comparison of the $d_{90\%}$ results at the respective atomizing gas pressure of samples #1 - #5, #6 - #10, and #11 - #15 shows dependencies of the inlet temperature on the particle size.

Table 5. Particle size analysis by laser diffraction, given as $d_{10\%}$, $d_{50\%}$, and $d_{90\%}$; Means ± SD, n = 3. With mercury porosimetry only $d_{50\%}$ values were determined.

Sample #	Process conditions for the spray-dried (refer to Table 1)	Particle size Laser diffraction [µm]			Particle size Mercury porosimetry [µm]
		$d_{10\%}$	$d_{50\%}$	$d_{90\%}$	$d_{50\%}$
#1	180°C; 40 ml/min	5.3 ± 0.1	17.8 ± 0.4	43.4 ± 0.7	15
#2	220°C; 40 ml/min	5.5 ± 0.0	19.7 ± 0.3	49.0 ± 1.1	18
#3	0.5 kg/cm²; 180°C; 80ml/min	5.5 ± 0.0	18.1 ± 0.1	46.9 ± 0.8	15
#4	200°C; 60 ml/min	5.2 ± 0.2	16.6 ± 0.5	43.4 ± 1.0	14
#5	220°C; 80 ml/min	5.4 ± 0.0	19.0 ± 0.4	52.1 ± 1.0	21
#6	180°C; 60 ml/min	4.1 ± 0.1	13.3 ± 0.1	32.8 ± 0.6	10
#7	200°C; 60 ml/min	4.1 ± 0.0	13.6 ± 0.1	34.6 ± 0.1	12
#8	1.0 kg/cm²; 220°C; 60 ml/min	4.3 ± 0.0	13.5 ± 0.3	34.6 ± 0.6	12
#9	200°C; 40 ml/min	4.5 ± 0.1	14.2 ± 0.1	34.5 ± 0.5	11
#10	200°C; 80 ml/min	4.1 ± 0.0	13.2 ± 0.1	34.2 ± 0.2	11
#11	180°C; 40 ml/min	3.2 ± 0.0	8.9 ± 0.0	20.3 ± 0.2	9
#12	180°C; 80 ml/min	3.4 ± 0.1	10.5 ± 0.1	22.0 ± 0.5	9
#13	1.5 kg/cm²; 200°C; 60 ml/min	3.3 ± 0.1	9.9 ± 0.3	22.2 ± 0.5	9
#14	220°C; 40 ml/min	3.3 ± 0.0	9.6 ± 0.2	23.7 ± 0.8	8
#15	220°C; 80 ml/min	3.5 ± 0.0	11.1 ± 0.0	28.2 ± 0.0	7

These results are similar to those described by Reiniccius [146], Tonon, Brabet, & Hubinger [12] and Chegini & Ghobadian [13], who observed that a low atomizing gas pressure generates large droplets. Moreover, during the first drying phase the high inlet temperature leads to a fast formation of a solid ring. Subsequently, the inner moisture evaporates and produces a large expansion of the hollow spheres. Thus, at higher inlet temperatures large porous particles were obtained.
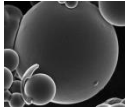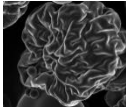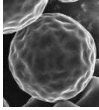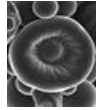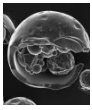
3.2.3.   Effect of the spray-drying conditions on the particle morphology

The influence of the three dependent process parameters atomizing gas pressure, inlet temperature, and pump feed rate on the particle morphology was studied by SEM, and the results are summarized in Table 6. Particle surfaces and particle shapes were investigated and two types of particle surfaces could be distinguished: smooth and wrinkled. Concerning the particle shapes resembling golf ball, doughnut, and shard could be differentiated. Morphological changes of single component maltodextrin particles during the spray-drying process were examined by Almilla-Beltràn, Chanona-Pérez, Jiménez-Aparicio, & Gutiérrez-López [147]. They explored relationships between the particle structure and the inlet temperature of the spray-drying device. In the present study, dealing with a plant-based multicomponent system such as a dry extract of *Sennae fructus* showed that the formation of smooth particles was favored in case of high inlet temperatures (e.g. 220°C) and does not seem to be influenced by different atomizing gas pressures and pump feed rates (Table 6).

In contrast, low inlet temperatures (e.g. 180°C) prevent the generation of smooth particles. This presumably results from the fact that if the above-mentioned solid ring has been formed, the particles stop to expand. At a high drying temperature, the particle diameter increases as a result of the temperature increase and internal

vaporization. This demonstrates that the surfaces of the dried plant particles are a function of the drying temperature and the evaporation rate. Similar results were observed by Vicente, Pinto, Menezes, & Gasper [148] and Lin & Gentry [149].

Table 6. Particle morphologies, displayed as SEM images, observed in dependence of the three process parameters atomizing gas pressure, inlet temperature, and pump feed rate. x indicates the predominant form of the present particle type. (x) could not clearly be determined.

Sample #	Process conditions	Particle surfaces		Particle shapes		
	atomizing gas pressure; inlet temperature; pump feed rate	smooth	wrinkled	golf ball	doughnut	shard
#1	0.5 kg/cm²; 180°C; 40 ml/min		x			x
#2	0.5 kg/cm²; 220°C; 40 ml/min	x				x
#3	0.5 kg/cm²; 180°C; 80 ml/min		x	x		
#4	0.5 kg/cm²; 200°C; 60 ml/min	x	x	(x)	x	
#5	0.5 kg/cm²; 220°C; 80 ml/min	x				x
#6	1.0 kg/cm²; 180°C; 60 ml/min		x	x		
#7	1.0 kg/cm²; 200°C; 60 ml/min	x		(x)	x	
#8	1.0 kg/cm²; 220°C; 60 ml/min	x	x			
#9	1.0 kg/cm²; 200°C; 40 ml/min		x		x	x
#10	1.0 kg/cm²; 200°C; 80 ml/min	x		x		
#11	1.5 kg/cm²; 180°C; 40 ml/min		x			
#12	1.5 kg/cm²; 180°C; 80 ml/min	x		x		
#13	1.5 kg/cm²; 200°C; 60 ml/min	x	x	x	x	
#14	1.5 kg/cm²; 220°C; 40 ml/min	x	x		x	x
#15	1.5 kg/cm²; 220°C; 80 ml/min	x	x		x	

According to the data in Table 6, it has to be mentioned that a high atomizing gas pressure (1.5 kg/cm²) generates very small droplets during the drying process, which still needs to be investigated in more detail. Thus, sometimes unexpected results concerning particle surfaces and shapes can be observed. Wrinkled particles with a small quantity of hollow spheres can be found in the case of low drying temperatures

(e.g. 180°C) along with atomizing gas pressures of 0.5 and 1.0 kg/cm², respectively. If the inlet temperature is adjusted to 220°C, wrinkled particles may only be obtained in the case of high atomizing gas pressures such as 1.0 or 1.5 kg/cm². Regarding the particle surface it is remarkable that the existence of a golf ball surface is clearly correlated to temperatures of 180-200°C in combination with pump feed rates ranging from 60-80 ml/min (Table 6). Presumably, this surface results from a rather low temperature which does not inflate the particles as much as in the case of a smooth surface as observed on a sphere. Additionally, the relatively high pump feed rate is responsible for a high portion of solid per droplet, leading to a more stable shell of the hollow spheres. The two remaining particle structures developing during the spray-drying process of *Sennae fructus* were doughnut and shard. As shown in Table 6, these two structures exhibited no clear relationships with the spray-drying conditions. Doughnut-like particles have also been described by Nandiyanto & Okuyama [150] and Iskandar, Gradon, & Okuyama [10]. If the shell, which is formed during the first drying phase, is impermeable to water vapor, the particle inflates by increasing internal vapour pressure. After cooling, a negative pressure is created which causes a shrinking of the shell resulting in a loss of the structural stability of the particles. Finally, particles with a shard-like structure resulting from hollow spheres by collapsing were encountered. A low pump feed rate and a high inlet temperature seem to be crucial for their generation. Because of the low particle density in the spray droplets, hollow spheres with thinner shells are formed. During drying in the air stream the inner pressure in spheres decreases, i.e. the thin shells will not resist the interior vapor pressure, which results in fragmentation of the particles. Similar relationships were published by Lin et al [149] and Maa, Constantino, Nguyen, & Hsu [151].

3.2.4. Effect of the particle morphology on the dry extract properties

To further specify the structure and properties of the spray-dried samples, their densities were determined by helium pycnometry. The resulting values are significantly different and are summarized in Table 7.

Table 7. Densities of the individual *Sennae fructus* spray-dried extract samples measured with helium pycnometry in dependence on the three process parameters atomizing gas pressure, inlet temperature, and pump feed rate. The density of a micronized sample was determined to estimate the true density. Means ± SD, n = 3, ANOVA: $F_{(14,30)} = 89$, $p<0.05$; Bonferroni´s post-hoc test: group #2, #5, #7, and #12 significant higher than group #1, #3, #11, and #13.

Sample #	Process conditions atomizing gas pressure; inlet temperature; pump feed rate	Density helium pycnometry [g/cm³]
#1	0.5 kg/cm²; 180°C; 40 ml/min	1.468 ± 0.002
#2	0.5 kg/cm²; 220°C; 40 ml/min	1.318 ± 0.007
#3	0.5 kg/cm²; 180°C; 80 ml/min	1.446 ± 0.002
#4	0.5 kg/cm²; 200°C; 60 ml/min	1.420 ± 0.007
#5	0.5 kg/cm²; 220°C; 80 ml/min	1.331 ± 0.003
#6	1.0 kg/cm²; 180°C; 60 ml/min	1.414 ± 0.010
#7	1.0 kg/cm²; 200°C; 60 ml/min	1.329 ± 0.005
#8	1.0 kg/cm²; 220°C; 60 ml/min	1.394 ± 0.007
#9	1.0 kg/cm²; 200°C; 40 ml/min	1.402 ± 0.005
#10	1.0 kg/cm²; 200°C; 80 ml/min	1.394 ± 0.009
#11	1.5 kg/cm²; 180°C; 40 ml/min	1.449 ± 0.006
#12	1.5 kg/cm²; 180°C; 80 ml/min	1.370 ± 0.014
#13	1.5 kg/cm²; 200°C; 60 ml/min	1.422 ± 0.014
#14	1.5 kg/cm²; 220°C; 40 ml/min	1.408 ± 0.004
#15	1.5 kg/cm²; 220°C; 80 ml/min	1.410 ± 0.004
		true density (micronized sample): 1.511 ± 0.016

These differences indicate that the data do not represent true densities, because the enclosed cavities could not be reached by the helium gas. Interestingly, a comparison with the SEM images suggests that the fraction of inaccessible hollow spheres for helium is higher for example for the samples #2, #5, #7, and #12 than for the samples #1, #3, #11, and #13. These results correspond to the fact that samples with smooth and round particles include a high fraction of the hollow spheres with lower densities than the wrinkled collapsed structures. The densities of these structures were similar to their true density which was determined by measurement of a micronized sample. Density values depending on the particle morphology and helium permeability have also been described by Maas [152] for α-lactose monohydrate. Additional information on the particle properties are provided by the evaluation of BET measurements and again mercury porosimetry measurements. Table 8 shows a selection of 6 samples with 3 samples selected from the high fraction of hollow spheres (#2, #5, and #7) and 3 selected from the low fraction of hollow spheres (#1, #3, and #11).

From these samples, the surface areas and the compressed volumes were determined. The BET surface area differs from that measured with mercury intrusion. On the one hand, the internal pores cannot be detected by BET measurements and no meaningful surface properties can be deduced from the obtained results because of the dominating meso- and macropores. On the other hand, during mercury porosimetry measurements, the hollow spheres do not withstand the pressure applied and collapse. This collapse leads to an increase in the surface, which allows the measurement of both, the inner and outer side of spheres resulting in the high total pore surface area (Table 8). Thus, more detailed information may be obtained using mercury porosimetry as compared to BET measurements concerning the surface structure of the different types of particles.

Table 8. BET-surface area of the spray-dried particles as well as total pore surface area and compressed volume measured with mercury porosimetry illustrated for samples #1, #3, and #11 (wrinkled particles), as well as samples #2, #5, and #7 (hollow spheres). Means ± SD, n = 2, BET-surface area: ANOVA: $F_{(5,6)} = 0.4$, $p > 0.05$. Total pore surface area: ANOVA: $F_{(5,6)} = 15$, $p < 0.05$; Bonferroni´s post-hoc test: group #1, #3, and #11 significant lower than group #2, #5, and #7. Compressed Volume: ANOVA: $F_{(5,6)} = 19$, $p < 0.05$; Bonferroni´s post-hoc test: group #2, #5, #7, and #12 significant higher than group #1, #3, #11, and #13.

Sample #		Process conditions atomizing gas pressure; inlet temperature; pump feed rate	BET-surface area BET [m²/g]	Total pore surface area	Compressed Volume
				mercury porosimetry [m²/g]	
#1	wrinkled	0.5 kg/cm²; 180°C; 40 ml/min	0.8 ± 0.3	15.4 ± 3.5	0.1 ± 0.1
#3		0.5 kg/cm²; 180°C; 80 ml/min	0.8 ± 0.5	14.4 ± 0.2	0.2 ± 0.1
#11		1.5 kg/cm²; 180°C; 40 ml/min	1.0 ± 0.0	15.5 ± 4.9	1.0 ± 0.9
#2	hollow	0.5 kg/cm²; 220°C; 40 ml/min	0.6 ± 0.2	28.6 ± 1.3	9.3 ± 0.0
#5		0.5 kg/cm²; 220°C; 80 ml/min	0.7 ± 0.0	23.2 ± 1.2	7.2 ± 3.7
#7		1.5 kg/cm²; 200°C; 60 ml/min	0.6 ± 0.5	30.9 ± 1.6	11.1 ± 0.8

It may be derived from the data in Table 5 that the size of the wrinkled particles (samples #1, 3#, and #11) is about half as large as that of the smooth hollow particles (samples #2, #5, and #7). This fact is also confirmed by the higher volume of the hollow spheres which are more compressible than the wrinkled particles.

To evaluate the hygroscopicity of the spray-dried *Sennae fructus* extracts, their loss on drying was compared directly after the drying process with that after 6 and 12 months of storage, respectively (Table 9). The moisture content of the dried extracts with high density and wrinkled particle surfaces (samples #1, #3, and #11) increases more pronounced during the first 6 months than the samples containing a higher

portion of hollow and smooth particles (samples #2, #5, and #7). These results confirm the assumption that differences in the particle morphology affect the hygroscopicity. After 6 months the loss on drying of the samples #1, #3, and #11 as well as the samples #2, #5, and #7 was still different. However, after 12 months of storage the water content of the two sample groups was similar, because the limit of moisture saturation was achieved. This influenced the characteristic surface structure of the particles.

Table 9. Loss on drying of spray-dried *Sennae fructus* extract particles measured after different time periods of storage shown with the samples #1, #3, and #11 as well as the samples #2, #5, and #7 in dependence of the three process parameters atomizing gas pressure, inlet temperature, and pump feed rate. Means ± SD, n = 3, Loss on drying after 6 months of storage: ANOVA: $F_{(5,12)}$ = 80, $p < 0.05$; Bonferroni´s post-hoc test: group #2, #5, and #7 significant different from group #1, #3, and #11. Loss on drying after 12 months of storage: ANOVA: $F_{(5,12)}$ = 13, $p < 0.05$; Bonferroni´s post-hoc test: group #2, #5, and #7 not significant different from group #1, #3, and #11.

Sample #	Process conditions atomizing gas pressure; inlet temperature; pump feed rate	Loss on drying after spray-drying [%]	Loss on drying after 6 months storage [%]	Increase within 6 months storage [%]	Loss on drying after 12 months storage [%]	Increase within 6 and 12 months storage [%]
#1	0.5 kg/cm²; 180°C; 40 ml/min	6.1 ± 0.1	7.1 ± 0.1	1.0 ± 0.2	8.6 ± 0.1	1.5 ± 0.2
#3	0.5 kg/cm²; 180°C; 80 ml/min	6.6 ± 0.1	8.0 ± 0.9	1.4 ± 1.0	8.9 ± 0.5	0.9 ± 1.4
#11	1.5 kg/cm²; 180°C; 40 ml/min	5.3 ± 0.1	5.8 ± 0.1	0.5 ± 0.2	8.0 ± 0.2	2.2 ± 0.3
#2	0.5 kg/cm²; 220°C; 40 ml/min	5.7 ± 0.1	6.0 ± 0.1	0.3 ± 0.2	8.2 ± 0.1	2.2 ± 0.2
#5	0.5 kg/cm²; 220°C; 80 ml/min	6.1 ± 0.1	6.4 ± 0.0	0.3 ± 0.1	8.5 ± 0.1	2.1 ± 0.1
#7	1.5 kg/cm²; 200°C; 60 ml/min	5.6 ± 0.2	5.8 ± 0.2	0.2 ± 0.4	7.6 ± 0.2	1.8 ± 0.4

3.2.5. Effect of the dry extract properties on the storage stability of the sennosides

The differently prepared samples of spray-dried *Sennae fructus* extracts (Table 1) were stored for 12 months at 40°C and 75 % RH and the decrease of the sennoside contents was monitored monthly by HPLC analysis [153].

Table 10. Total sennoside contents of different spray-dried samples of *Sennae fructus* (refer to Table 1) during a storage period of 12 months at 40°C and 75 % RH. The values measured by HPLC represent the total sennoside content in percentage based on the initial value. Means, RSD < 0.8 %, n=4, ANOVA significant $p<0.05$; [1] nonsignificant Bonferroni´s post-hoc test.

sample #	months of storage atomizing gas pressure; inlet temperature; pump feed rate	1[1] [%]	2[1] [%]	3 [%]	4 [%]	5 [%]	6 [%]	9 [%]	12 [%]
#1	0.5 kg/cm²; 180°C; 40 ml/min	100.7	100.7	96.5	94.8	91.6	84.7	80.4	66.9
#2	0.5 kg/cm²; 220°C; 40 ml/min	99.7	99.7	99.3	95.8	92.8	87.4	84.4	74.2
#3	0.5 kg/cm²; 180°C; 80 ml/min	100.9	97.7	96.2	95.1	90.3	81.5	75.5	58.9
#4	0.5 kg/cm²; 200°C; 60 ml/min	99.2	98.8	98.7	96.8	92.6	86.7	84.6	70.5
#5	0.5 kg/cm²; 220°C; 80 ml/min	98.3	97.2	97.5	96.0	92.5	88.4	83.2	68.5
#6	1.0 kg/cm²; 180°C; 60 ml/min	100.6	97.2	95.6	95.4	92.2	86.0	83.0	68.0
#7	1.0 kg/cm²; 200°C; 60 ml/min	99.7	100.1	98.3	96.6	94.9	87.9	85.4	72.0
#8	1.0 kg/cm²; 220°C; 60 ml/min	100.2	100.2	95.2	94.8	92.9	86.5	82.1	69.4
#9	1.0 kg/cm²; 200°C; 40 ml/min	99.2	99.4	96.3	94.7	92.0	83.5	80.0	67.4
#10	1.0 kg/cm²; 200°C; 80 ml/min	100.6	100.1	97.8	95.7	92.2	85.9	81.6	66.4
#11	1.5 kg/cm²; 180°C; 40 ml/min	99.6	99.7	97.4	94.9	92.1	85.9	83.3	68.6
#12	1.5 kg/cm²; 180°C; 80 ml/min	100.3	100.3	99.1	96.1	92.4	86.3	82.6	69.5
#13	1.5 kg/cm²; 200°C; 60 ml/min	98.7	98.7	98.7	96.3	92.8	88.1	81.8	66.9
#14	1.5 kg/cm²; 220°C; 40 ml/min	99.9	100.3	99.9	98.2	94.1	86.0	83.4	69.4
#15	1.5 kg/cm²; 220°C; 80 ml/min	97.6	97.3	93.6	93.3	91.6	86.3	84.1	70.2
mean of all values [%]		99.7	99.2	97.3	95.6	92.5	86.1	82.4	68.5
range of all values [%]		3.3	3.5	6.3	4.9	5.6	6.9	9.9	15.2

During the first 2 months of storage, no statistically significant degradation of the sennosides could be observed. After 5 months of storage the mean value of the total sennoside contests of all 15 samples amounted to 92.5 %, which was below the required limit of 95 % (Table 10).

The most pronounced degradation of the sennosides (up to 58.9 %) occurs in sample #3 (0.5 kg/cm²; 180°C; 80 ml/min), which has the highest moisture content (Fig. 11). To study the influence of the moisture content on the degradation of the sennosides, the samples with the maximum range of moisture content (Fig. 11) were examined after 6 and 12 months, respectively. After 6 months, a stronger influence of moisture on the stability of the ingredients was observed than after 12 months. In accordance with the results of the hygroscopicity determined by the loss on drying (Table 9), the water content of spray-dried samples was similar and thus the effect of moisture on the stability was decreased.
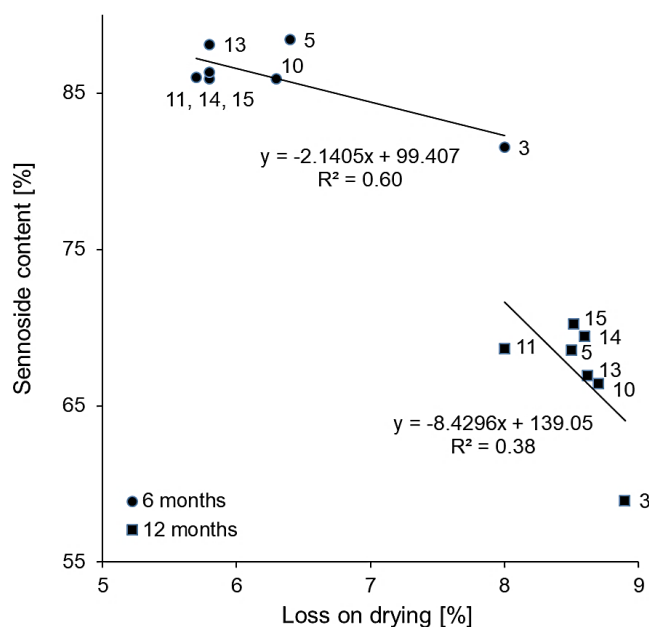

Fig. 13: Relationship between loss on drying and sennoside content after 6 and 12 months of storage, respectively (refer to Fig. 11 and Table 10). Sample numbering refers to Table 1.

Samples with similar moisture content were investigated with regard to correlation between the density of the spray-dried particles and the sennoside stability (Fig. 13). As shown before, the density depends on the surface morphology. Density measurements revealed that inner volume of the hollow spheres cannot be reached by helium, and probably the same is true for atmospheric oxygen. The data in Fig. 13 led assume that if only a small portion of the particle surface is accessible to water and oxygen, degradation of the sennosides takes place to a lower extent.
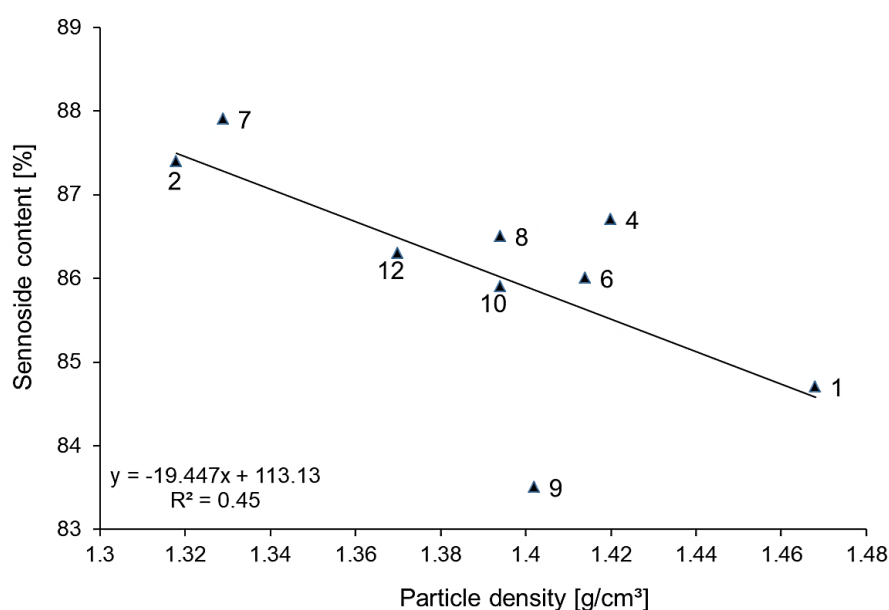
Fig. 14: Relationship between the particle density and the sennoside content after 6 months of storage (refer to Table 7 and 10). Sample numbering refers to Table 1.

It may be derived from Fig. 11 and Table 4 that the particle morphology and the moisture content of spray-dried samples is influenced by the inlet temperature of the spray-drying process. Thus, this process condition also exerts an effect on the degradation of the sennosides in spray-dried particles. In Fig. 15 the observation that a high inlet temperature leads to a positive influence on the stability of the sennosides is illustrated. A high inlet temperature also affects the dryness of the samples as well as the particle morphology positively (Fig. 11 and Table 6).
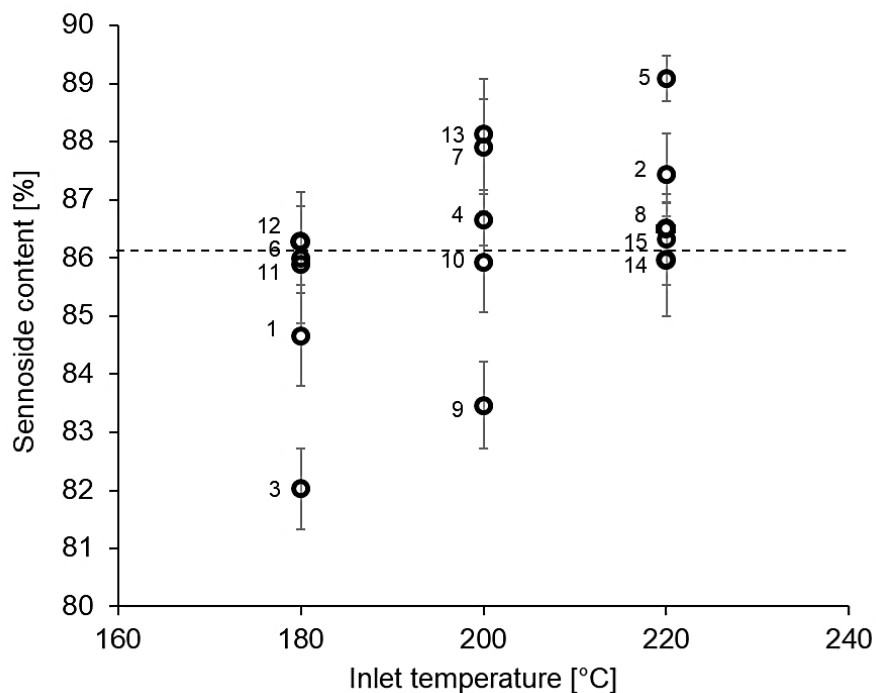
Fig. 15: Sennoside contents in the spray-dried extracts of *Sennae fructus* after 6 months of storage with respect to different inlet temperatures; Means ± SD, n=4. The dashed line symbolizes the mean sennoside content of all investigated samples.

3.2.6. Conclusions

To summarize the results of the present study, the moisture content, the particle size distribution, the particle morphology, the surface area, the density, and the hygroscopicity of *Sennae fructus* extracts may be influenced by varying the process conditions atomizing gas pressure, inlet air temperature, and pump feed rate during the spray-drying process. The moisture content may be reduced by increasing the inlet temperature, decreasing the pump feed rate and increasing the atomizing gas pressure, which has the most significant effect. An increase in the particle size is achieved by reducing the atomizing gas pressure and by increasing the inlet air temperature. Different particle morphologies such as smooth or wrinkled particle surfaces as well as golfball, doughnut, and shard particle shapes result from these spray-drying conditions. The formation of smooth particles is mainly observed in the

case of high inlet temperatures. The measured densities, hygroscopicities, and surface areas may be used as measurable quantities to further describe and support the microscopically determined particle morphologies. The different particle properties influence their storage stability. Therefore, a high inlet temperature is crucial for dryness and smooth particle surfaces with low densities and consequently for improvement of the stability of the sennosides.

These relationships support the understanding of the production process of herbal spray-dried extracts to achieve defined particle properties for improvement of the product quality. This is especially necessary, as the required stability tests have to be performed with all formulations, including herbals. For further stability improvements of *Sennae fructus* extracts, the choice of packaging material and the addition of drying adjuvants may be considered.

3.3. Stabilization and destabilization of *Sennae fructus* extract formulations

3.3.1. Influence of the drying processes on the sennoside content

The information weather the applied temperatures during spray-drying and freeze-drying have an effect on a potential thermal degradation of ingredients of a formulation is necessary for the selection of the best drying process. E. Desobry et al. demonstrated that the application of different drying processes led to varying stabilities of the resulting products, whereby with freeze-drying the least pronounced degradation was observed with ß-carotene [154]. To study the thermal sensitivity of the sennosides, all samples obtained by the different drying process were analysed by HPLC directly after preparation. No significant difference could be established between the content of the sennosides of the spray-dried and the freeze-dried extracts (Table 11, samples #1 and #8). Apparently, the content of the sennosides was not influenced by the applied heat or cold. As expected, the addition of different amounts of MD (5, 15, and 30 %) before drying led to a corresponding decrease of the content of the sennosides in the spray-dried (Table 11, samples #2 - #4) and the freeze-dried samples (Table 11, sample #9 - #11) as a result of dilution. This data is in good accordance with the content of sennosides obtained by theoretical calculation based on the amount of added MD (Table 11, column 4). It has to be mentioned that no segregation took place during the spray- and freeze-drying process. Presumably, the *Sennae fructus* extracts and MD are present in a matrix after drying. In contrast, during granulation of the native spray-dried extracts with MD solution the calculated MD contents after drying (Table 11, sample #5 - #7, column 4) were lower than the expected values indicating production losses or an inhomogeneity of the granules.

Table 11. Influence of the different drying processes on the sennoside content as well as the MD content (added and calculated) of the investigated samples (means ± SD, n = 3). Samples #1 (spray) and #8 (freeze) served as 100 % values, respectively.

Sample #	Sennoside content [%]	MD, added [%]	MD, calculated [%]
#1	8.59 ± 0.11	0 (spray)	0
#2	8.15 ± 0.05	5 (spray)	5.19 ± 1.32
#3	7.31 ± 0.06	15 (spray)	14.90 ± 1.19
#4	6.05 ± 0.06	30 (spray)	29.63 ± 0.98
#5	8.51 ± 0.16	2.5 (granulation)	0.96 ± 1.38
#6	8.40 ± 0.14	5 (granulation)	2.18 ± 1.37
#7	7.38 ± 0.12	15 (granulation)	14.07 ± 1.20
#8	8.79 ± 0.12	0 (freeze)	0
#9	8.32 ± 0.11	5 (freeze)	5.37 ± 1.05
#10	7.34 ± 0.02	15 (freeze)	16.48 ± 0.94
#11	6.18 ± 0.04	30 (freeze)	29.73 ± 0.96

3.3.2.   Moisture uptake during storage of the *Sennae fructus* extract formulations

The aim of this study was to investigate the effect of different drying technologies and the addition of MD on the hygroscopicity of the prepared samples. The influence of MD on the degree of moisture uptake was examined by Tonon et al. who discovered the hygroscopicity of açai powder decreased with increasing amount of MD. Moreover, samples with low moisture content were more susceptible to moisture uptake, because of the pronounced difference in moisture between the powder surface and the relative humidity [12]. For a comparable determination of the

moisture sensitivity in the present study, the initial moisture level before storage of all samples were adjusted to a moisture content of 3.5 ± 0.2 %.
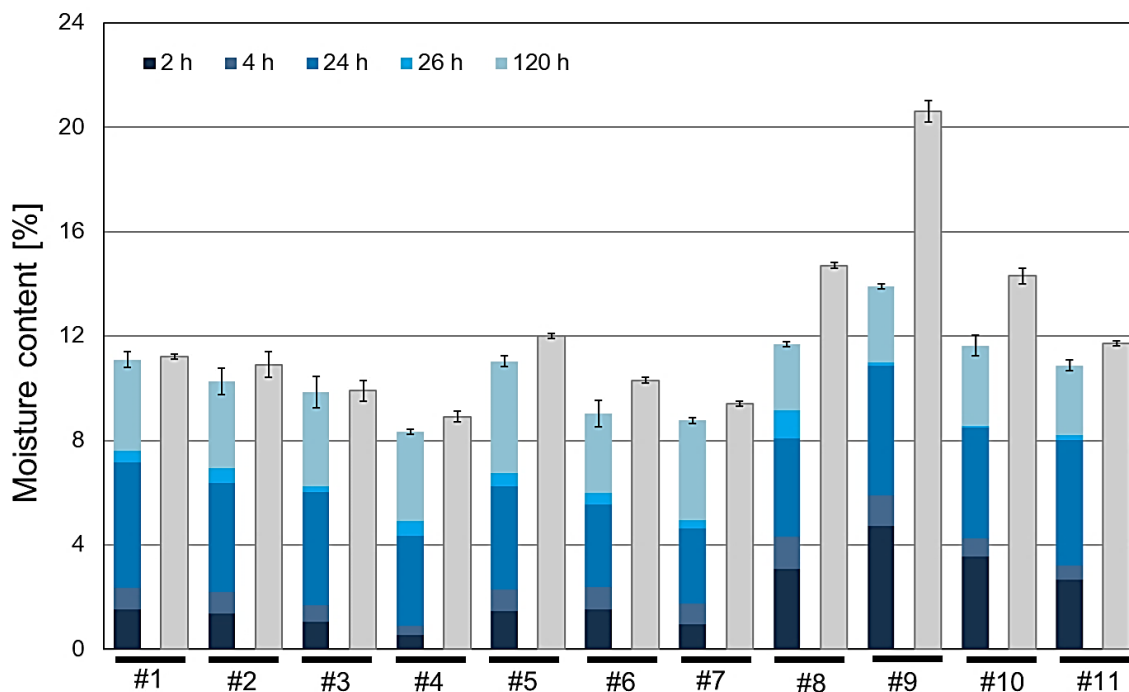
Fig. 16: Dependency of the moisture uptake on the sample composition at 40°C and 75 % relative humidity. The sample numbers correspond to those in Table 2. Light grey bars: Moisture content after 12 months of storage. Blue bars: Results of the hygroscopicity measurements; moisture uptake after 2, 4, 24, 26, and 120 h of the different samples (means ± SD, n = 3).

The determination of the residual moisture content after 12 months of storage revealed that the spray-dried extracts (Fig. 16, sample #1 - #4, light grey bars) absorbed less moisture than the freeze-dried extracts (Fig. 16, samples #8 - #11, light grey bars). Increasing the MD level of the spray-dried extracts from 5 % to 30 % (Fig. 16, sample #2 - #4, light grey bars) resulted in a decrease of the moisture uptake. A similar moisture protecting effect of MD was observed with the freeze-dried extracts (Fig. 16, samples #10 and #11, light grey bars) except for the extract with 5 % MD (Fig. 16, sample #9, light grey bars). These results were confirmed by

the data of the hygroscopicity measurements (Fig. 16, blue bars). If MD is sprayed onto the native spray-dried extracts during fluidized bed granulation, a comparable effect can be registered: an increase of the addition of MD results in a better moisture protection (Fig. 16, samples #5 - #7). In this context, it is remarkable that in the case of the extract granulated with MD (e.g. with 15 % MD) the same protection against humidity may be achieved as by addition of higher amounts of MD (e.g. 30 % MD) to the spray-dried extract (Fig. 16, samples #4 and #7). The data of the hygroscopicity measurement and the total amount of moisture uptake over time allowed the examination of the rate of moisture uptake. For this purpose, all samples were compared with regard to the time needed to reach 50 % of their total moisture (Table 12). It was observed that the freeze-dried samples absorbed moisture about twice as fast as the spray-dried samples.

Table 12: Rate of moisture uptake of the extract formulations displayed as the time needed to reach 50 % of their total moisture. The sample numbers correspond to those in Table 2.

Sample #	Time needed for a 50 % moisture uptake [h]
#1	17
#2	18
#3	19
#4	23
#5	20
#6	17
#7	23
#8	9
#9	6
#10	9
#11	11

It was also evident that the addition of MD induced a delayed uptake of moisture, except for the freeze-dried powder with 5 % MD. An explanation for these unexpected results might be that during freeze-drying, especially with sugar derivatives a structural collapse may occur depending on the composition, the freezing temperature, and the moisture behaviour of the samples [155]. The probability of a collapse is increased by a higher concentration of unfrozen water during the drying process caused by a high water binding tendency. If the effects (which are different for every formulation) reach a critical level, changes in the viscosity and porosity during the transition to the rubbery state may occur [156]. The freeze-dried extract with a content of 5 % MD showed an increased stickiness which led to caking possibly as a result of the collapse phenomenon.

3.3.3.   Analysis of *Sennae fructus* extracts by simultaneous TGA-DSC-MS

In this study, simultaneous TGA-DSC-MS provided profound information on the thermal degradation and thermal stability of the spray-dried and freeze-dried *Sennae fructus* extracts. This analysis allowed correlating the sample weight loss with enthalpy changes and with the emerging decomposition gases. The coupling of these techniques was necessary to successfully study the complex composition of a plant extract characterized by numerous thermal processes in comparison to a single substance. Investigations on isolated active constituents such as sennoside A and B in combination with commonly used pharmaceutical excipients have already been performed by Verloop et al. [106] using DSC and HPLC methods. They found out, that in the presence of water many excipients may not be used. In contrast, in the present study whole extract formulations of *Sennae fructus* were the subject of investigation. With simultaneous TGA-DSC-MS measurements the different morphology of the spray-dried hollow spheres and the freeze-dried material became

apparent in the DSC thermograms. In this connection, it has to be mentioned, that endothermic peaks corresponded to the evaporation of the surface and capillary water which caused several MS signals of m/z 18 (Table 13). In case of the spray-dried samples, the water evaporation started more than 10°C below the water evaporation temperature of the freeze-dried samples, which may be explained by the tendency of the spray-dried formulations to bind water less tightly than the freeze-dried samples. By studying the thermal degradation of the extract formulations of *Sennae fructus* the exothermic DSC peaks and the TGA weight loss were identified as CO_2 with the MS value of m/z 44 in the emerged decomposition gas. For other ion species with low molecular weight, which were also generated during the decomposition process of dried *Sennae fructus* extracts, only low intensities could be detected and were not displayed for the sake of clarity.

Table 13: Thermoanalytical data of spray-dried and freeze-dried *Sennae fructus* extracts with and without MD. The peaks of the exothermic (exo) processes were determined by DSC measurements. The peaks of the masses 18 and 44 were identified as water (amu 18) and CO_2 (amu 44) in the emerged decomposition gas by MS. Mass data were analysed using the first derivative (ion current per minute).

Drying process	Thermo-analytical event	Extract of *Sennae fructus* [°C]	Extract with 5 % MD [°C]	Extract with 15 % MD [°C]	Extract with 30 % MD [°C]
Spray-drying	Peak exo	181	186	194	207
	m/z 44	178	179	189	211
	m/z 18	85; 152; 169	87; 150; 171	89; 156; 177	85; 160; 188
Freeze-drying	Peak exo	195	180	189	202
	m/z 44	194	177	175, 193	196
	m/z 18	99; 138; 161; 197	99; 148; 171; 196	98; 146; 175; 195	110; 153; 198

In Fig. 17 it is illustrated that the decomposition of the spray-dried samples (C) was detected at increasing temperatures with increasing MD content. As examples, with the native extract (sample #1) the decomposition was measured at 178°C and with the extract formulation with 30 % MD (sample #4) at 211°C, demonstrated by the ion trace m/z 44. To summarize, MD appears to improve the thermal stability of the spray-dried *Sennae fructus* extract. Freeze-dried samples in general showed a similar tendency but with an inconsistent decomposition and samples of this drying type containing 15 % MD (sample #10) indicated an additional decomposition step. The native freeze-dried extract decomposed late in comparison to the formulations with MD. Overall, the freeze-dried samples appeared thermally more unstable.
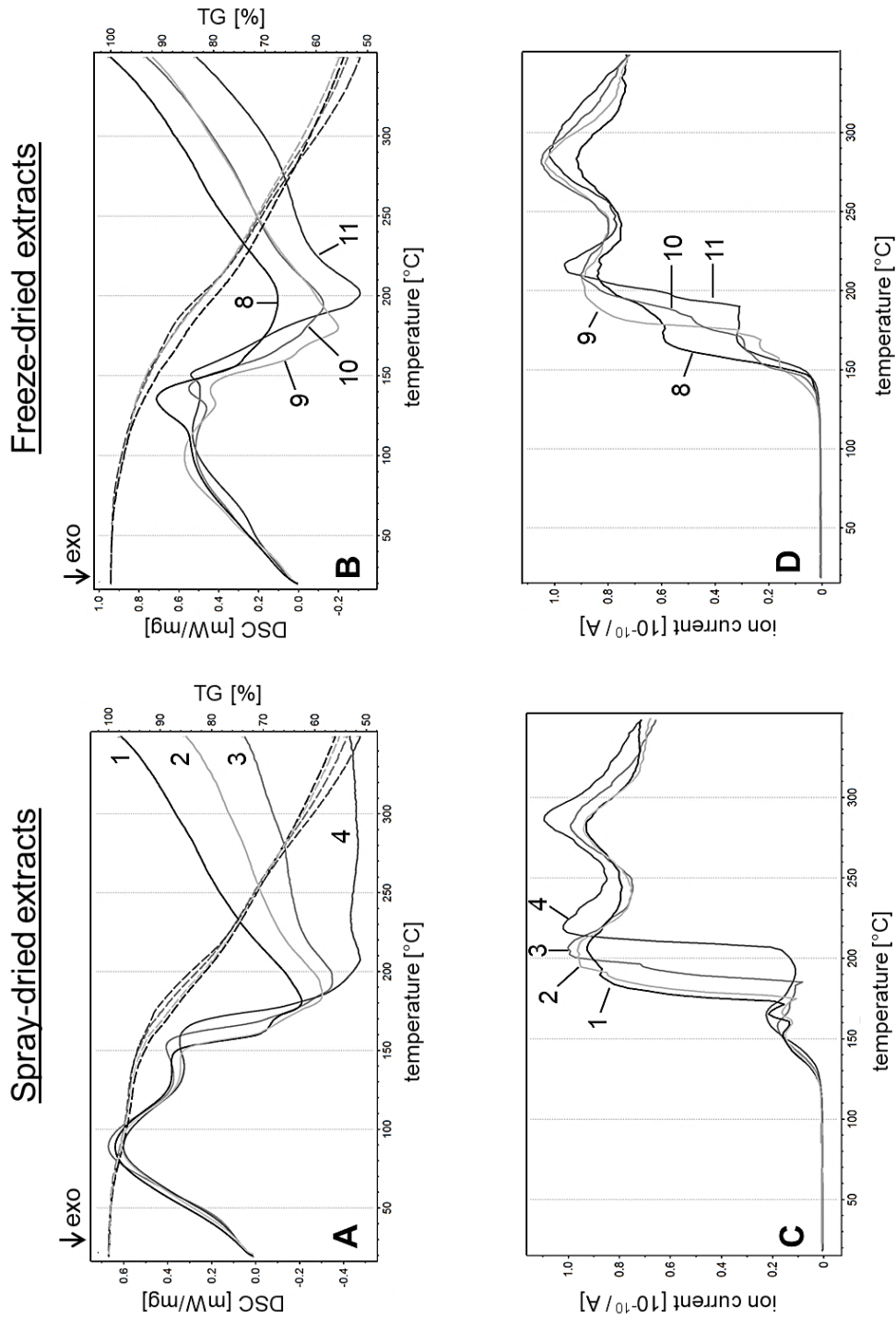
Fig. 17: TGA and DSC thermograms of spray-dried (A) and freeze-dried (B) *Sennae fructus* extracts without MD (samples #2 - #4 and #9 - #11) and with MD (samples #1 and #8) and with MD (samples #2 - #4 and #9 - #11). In addition, the corresponding MS traces (m/z 44) of the emerged decomposition gases of spray-dried (C) and freeze-dried (D) *Sennae fructus* extracts are displayed.

3.3.4.   Storage stability of the sennosides in S*ennae fructus* extract formulations

The *Sennae fructus* extract formulations (Table 2) were stored for 12 months at 40°C and 75 % RH and the decrease of the sennoside contents were measured by HPLC [120]. The aim was to investigate if the drying method and the amount of added MD have an effect on the storage stability of the sennosides. Already after the first month, differences between the formulations were detected. The sennoside content of the native freeze-dried samples and the freeze-dried samples with 5 % MD was reduced to less than 90 % already after 1 month of storage (Fig. 18).
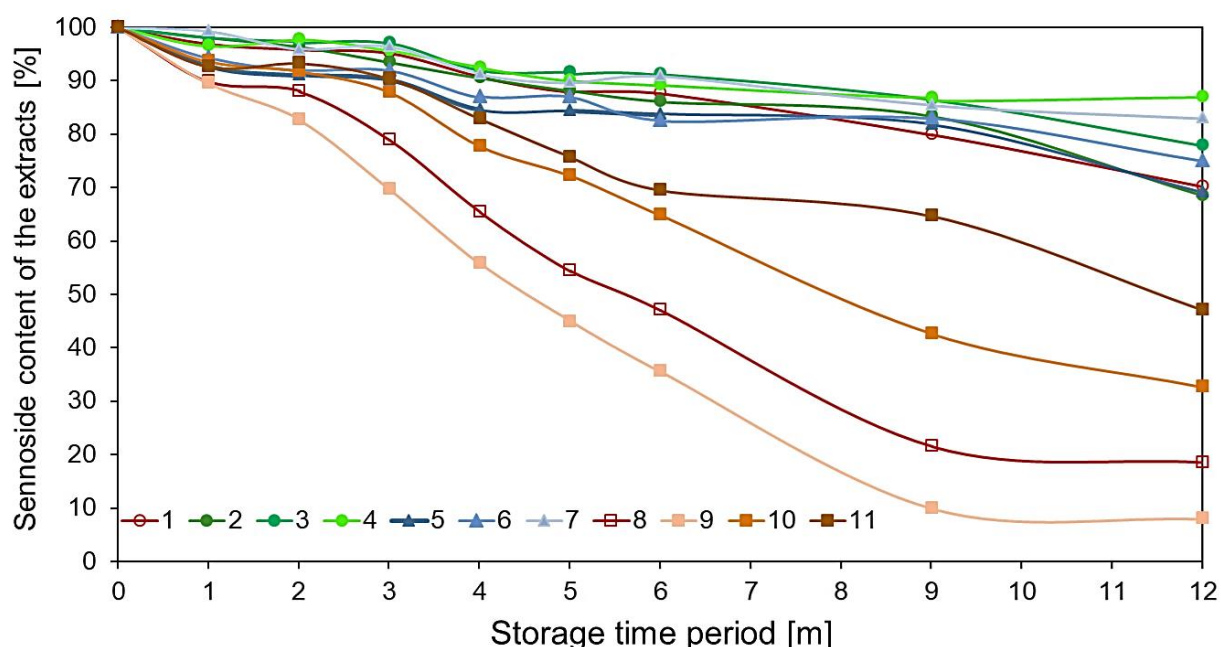
Fig. 18: Sennoside content (in percentage of the initial value) of the 11 samples (see Table 2) measured by HPLC after 1, 2, 3, 4, 5, 6, 9, and 12 months of storage at 40°C and 75 % RH (means, RSD < 2.5 %, n = 3).

In contrast, the sennoside content of spray-dried *Sennae fructus* extracts containing 30 % MD and spray-dried samples granulated with 15 % MD were reduced to less than 90 % only after 7 months of storage. Surprisingly, the largest decrease in the sennoside content after all storage time periods was observed with the freeze-dried

sample containing 5 % MD (sample #9, 8 %). An explanation for this result may be the structural collapse during freeze-drying induced by an interaction of the sample composition, the freezing temperature, and the moisture content. A collapse influences the microstructure of the freeze-dried extracts and may affect the stability of the active compounds [155]. The most stable samples were #4 (spray-dried with 30 % MD; 87 % sennosides) and #7 (granulated with 15 % MD; 83 % sennosides) as shown in Fig. 18. The addition of MD resulted in an improvement of the sennoside stability in the spray-dried samples of 24 % (sample #4: 87 % sennosides compared to sample #1: 70 % sennosides), in the granulated samples of 19 % (sample #7: 83 % sennosides compared to sample #1: 70 % sennosides), and in the freeze-dried samples of 154 % (sample #11: 47 % sennosides compared to sample #8: 18.5 % sennosides) after 12 months of storage. Obviously, the effect of MD addition is most evident in the freeze-dried samples which are more susceptible to decomposition. As mentioned before (Section 2), if MD is applied to spray-dried extracts by granulation, already a small amount is sufficient in contrast to simultaneous spray-drying with MD. However, in all cases MD exerted a positive influence on the stability of the sennosides.

3.3.5. Conclusions

In general, spray-drying and freeze-drying of *Sennae fructus* extracts did not lead to a thermal degradation of the sennosides; neither the applied heat nor the cold had a negative influence. Furthermore, the addition of MD before spray-drying and freeze-drying caused no production loss or inhomogeneity in contrast to the addition of MD during fluidized bed granulation. The investigation of the moisture content, which is a stability-reducing factor, provided comparable results of the hygroscopicity test and the moisture content after 12 months of storage for all investigated samples. The

freeze-dried samples absorbed more moisture than the spray-dried extracts and twice as fast. For the spray-dried extracts the hygroscopicity decreased with increasing content of MD. A granulation of the spray-dried extract with a low MD content turned out to be of advantage, because the protection against humidity was similar to that of spray-dried extracts with a high MD content. However, the freeze-dried extracts with MD delayed the moisture uptake in comparison to the native extract, except for the sample with 5 % MD. The simultaneous TGA-DSC-MS measurements allowed two different types of bound water to be identified in the samples. The surface water of the freeze-dried extracts needed higher temperatures to evaporate than the water in the spray-dried extracts, which was less strongly bound. These simultaneous measurements enable the correlation of the sample weight loss, the enthalpy changes and the amount of evolved CO_2. It became clear, that the thermal decomposition was delayed with increasing MD content in the samples. Similar to the hygroscopicity measurements, the freeze-dried samples showed irregularities in their decomposition reactions. These results were also confirmed by the measurement of the stability of the sennosides under accelerated conditions with HPLC over 12 months in which the most stable samples were the spray-dried extract with 30 % MD and the spray-dried extract granulated with 15 % MD. The freeze-dried sample with 5 % MD showed deviations from all the other samples in all measurements. A structural collapse during freeze-drying may affect the water uptake behaviour, thermal degradation, and storage stability.

In summary, spray-dried extracts were more stable than freeze-dried extracts. The addition of MD resulted in a stability improvement of all extracts. Lower amounts of MD were necessary if applied onto the surface of the native extract during fluidized bed granulation. The freeze-dried samples showed an increased hygroscopicity and

a reduced stability. Advantages of the addition of MD are most evident in the more decomposed freeze-dried products.

A combination of hygroscopicity measurements, simultaneous TGA-DSC-MS analysis, and accelerated storage stability studies are recommended to evaluate the stability of a plant extract. In further studies, other plant extracts and excipients as well as other aspects such as caking tendency, flow behaviour or water solubility of the extracts should be investigated.

3.4. Effect of coatings on moisture protection of *Sennae fructus* extract tablets

3.4.1. Characterization of the subcoated moisture-sensitive tablets

To protect a moisture-sensitive tablet core during further processing steps and storage from water permeation, tablets containing spray-dried *Sennae fructus* extract were dry-coated using HMC. For this purpose, HMC materials of different physicochemical properties (Table 3) were used. Different amounts of these lipophilic materials were applied to the tablets to achieve an optimal relationship between moisture protection and required disintegration time by determination of the surface distribution, the lipid penetration, and the tablet hygroscopicity.

3.4.1.1. *Interactions of the hot-melt coatings with the tablet cores*

The selected HMC materials MCT, StA, Pr, and Cp differ by their drop points and their lipophilic properties (Table 3). According to their viscosity and their interfacial tension, these differences also caused deviations in the penetration depth and the degree of tablet surface coverage. All HMC materials had in common that at the measuring positions 1 and 5 (Fig. 19) deeper penetration depths of the lipids were detected than close to the tablet edges. The maximum penetration depth was observed with 15 mg of MCT, resulting in a nearly complete impregnation of the tablet directly after the coating process. An analysis, which was performed several days later, resulted in a tablet core completely soaked with MCT. StA, Pr, and Cp showed a similar penetration behaviour concerning the changes in the penetration depths which are big between 5 and 10 mg and smaller between 10 and 15 mg (Table 14).
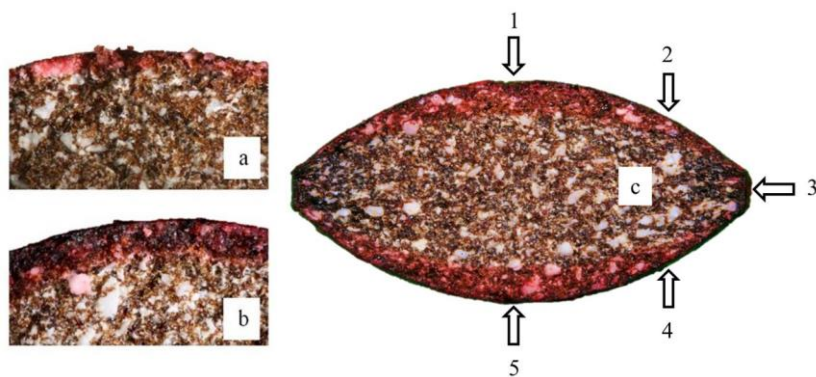
Fig. 19: Illustration of the penetration depth of the colour-traced subcoating into the tablet core; 5 mg of Cp (a), 15 mg of Cp (b). Total cross-section of a tablet subcoated with 10 mg of colour-traced StA (c), displaying the different penetration depths of the HMC substance into the tablet core at the marked measuring positions.

The tendency of deeper penetration of StA and Cp may be attributed to their slightly lower viscosity at the respective process temperature compared to Pr. In comparison to the other HMC materials, the penetration of StA was less pronounced at the edge of the tablet than at the tablet curvature. This phenomenon was probably caused by the low viscosity of StA being responsible for the rapid penetration into the tablet core.

What the surface coverage is concerned, with all HMC materials an incomplete surface coverage was observed by microscopic examination at an applied amount of only 5 mg. However, if 10 mg of the materials were applied, a complete surface coverage was observed.

Table 14. Penetration depth of the different HMC materials with their various amounts, determined at the measuring positions displayed in Fig. 19. Means ± SD, n = 3.

HMC materials	Measuring positions	5 mg [µm]	10 mg [µm]	15 mg [µm]
MCT	1	1320 ± 160	1440 ± 240	1840 ± 180
	2	1040 ± 80	1430 ± 180	1610 ± 170
	3	1290 ± 140	1410 ± 320	1900 ± 240
	4	1240 ± 200	1420 ± 150	1870 ± 150
	5	1470 ± 110	1600 ± 280	1960 ± 170
StA	1	370 ± 120	740 ± 30	830 ± 30
	2	180 ± 50	540 ± 40	610 ± 60
	3	210 ± 60	440 ± 20	430 ± 140
	4	200 ± 90	370 ± 100	380 ± 20
	5	420 ± 110	660 ± 30	810 ± 100
Pr	1	190 ± 20	647 ± 30	670 ± 150
	2	150 ± 50	470 ± 50	570 ± 110
	3	180 ± 80	457 ± 70	550 ± 100
	4	180 ± 70	445 ± 70	570 ± 40
	5	200 ± 60	685 ± 125	710 ± 70
Cp	1	330 ± 130	652 ± 60	790 ± 100
	2	290 ± 80	565 ± 110	690 ± 50
	3	250 ± 50	515 ± 150	610 ± 50
	4	260 ± 50	525 ± 50	660 ± 40
	5	300 ± 90	694 ± 80	800 ± 60

3.4.1.2. Disintegration times of the subcoated tablets

From the results in Table 15 it is apparent that the tablet cores disintegrated in 9.3 ± 2.0 min. All tablets with hot-melt subcoating showed a time delay of disintegration, which was dependent on the applied amount of subcoating. As already mentioned above, in the case of an application of 5 mg of HMC material, the subcoated tablets showed an only partially coated tablet surface because of an insufficient quantity of the HMC material. Therefore, it becomes clear, why nearly all HMC formulations with a quantity of 5 mg disintegrated simultaneously. Except for MCT, the disintegration

time of all tablets coated with 10 mg HMC material, at least doubled compared to the tablet cores. All tablet formulations with 15 mg of HMC material led to a further delay of the disintegration time and some of them did not even meet the requirements of the European Pharmacopoeia: StA and Cp proved to be unsuitable for tablet subcoating and MCT remained critical with its disintegration time of 22.8 ± 7.6 min.

Table 15. Influence of the HMC materials on the disintegration times according to Ph. Eur. of the subcoated tablets prepared with 5, 10, and 15 mg of lipid, respectively (disintegration medium: distilled water). Means ± SD, n = 3.

Tablet samples	Disintegration time [min]
Plain tablet cores	9.3 ± 2.0
Tablet cores subcoated with MCT 5 mg	13.0 ± 1.7
Tablet cores subcoated with MCT 10 mg	15.7 ± 2.1
Tablet cores subcoated with MCT 15 mg	22.8 ± 7.6
Tablet cores subcoated with StA 5 mg	13.2 ± 3.2
Tablet cores subcoated with StA 10 mg	22.3 ± 5.0
Tablet cores subcoated with StA 15 mg	39.0 ± 5.5
Tablet cores subcoated with Pr 5 mg	14.7 ± 3.2
Tablet cores subcoated with Pr 10 mg	19.8 ± 2.5
Tablet cores subcoated with Pr 15 mg	21.5 ± 2.9
Tablet cores subcoated with Cp 5 mg	13.5 ± 1.9
Tablet cores subcoated with Cp 10 mg	18.5 ± 2.5
Tablet cores subcoated with Cp 15 mg	32.7 ± 4.7

Tablets coated with MCT showed a different behaviour concerning disintegration, which can be explained by soaking of the tablet core with MCT because of the liquid state of this lipid. As a tendency of disintegration of the HMC materials StA and Cp were similar but differed from Pr. The lipophilic properties and the penetration into the tablet core seem to be influencing factors.

3.4.1.3. Moisture protection of the tablet cores by hot-melt coatings

The aim of this investigation was to compare the influence of the type and amount of the selected HMC materials on the hygroscopicity of the tablet cores and the subcoated tablets. The possibility to form a barrier that protects the active ingredients from moisture has already been studied by Achanta et al. [157]. In this study it was shown, that the storage temperature and the thickness of the investigated hot-melt coating affected the behaviour of the moisture absorption of the coating. In the present study, the water uptake of the tablet cores and the subcoated tablets was investigated at 33, 43, and 75 % RH at RT. After 7 d of storage at these conditions the moisture penetration into the tablet cores slowed down significantly because of the applied HMC materials (Fig. 20).
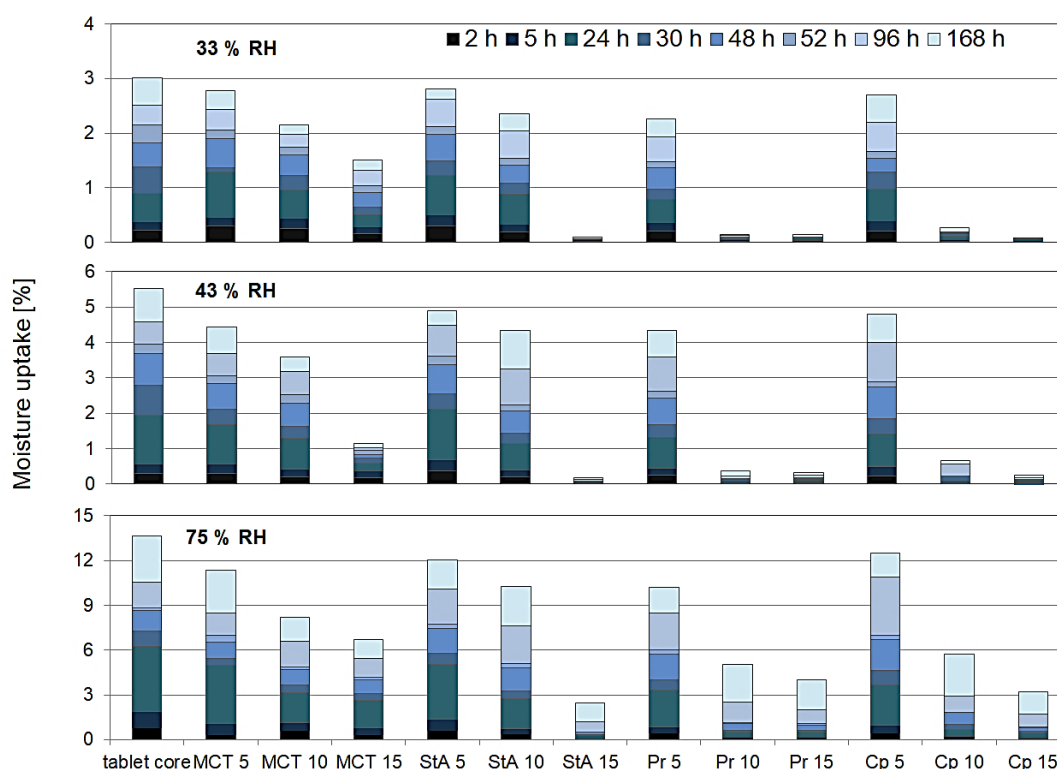

Fig. 20. Comparison of the hygroscopicities of the tablet cores with tablets subcoated with 5, 10, and 15 mg of HMC materials. Moisture uptake refers to the initial tablet weight, measured at 33, 43, and 75 % RH. Means, RSD < 0.5 %, n = 3.

As expected, with increasing amount of applied HMC materials a more pronounced reduction of moisture uptake occurs. The maximum decrease of hygroscopicity compared with the tablet cores was 97 % at 33 % RH (15 mg Cp and StA), 97 % at 43 % RH (15 mg StA), and 82 % at 75 % RH (15 mg StA). In general, the tablet cores subcoated with 5 mg HMC materials exhibited a similarly high moisture uptake as the tablet cores themselves, presumably again because of an incomplete coating. With regard to the subcoatings consisting of 10 mg lipids, the moisture uptake of the tablet cores subcoated with MCT and StA was comparable and amounted to a 20 - 30 % lower moisture uptake after 7 d of storage at all humidity conditions in relation to the tablet cores. However, these two HMC materials were not as efficient as the Pr and Cp subcoatings at 10 mg which both resulted in a 90 - 95 % lower moisture uptake at 33 / 43 % RH and a 60 % lower moisture uptake at 75 % RH compared to the cores.

According to the lipophilic fraction of the applied HMC materials (HLB values see Table 3), the following order of their moisture permeability was expected: StA > MCT > Pr = Cp. This order was confirmed with tablet cores subcoated with 10 mg HMC materials. An amount of 15 mg StA resulted in a significant lower moisture uptake compared to MCT, roughly reaching the level of Pr and Cp. From these data the rate of moisture uptake was determined for the condition of 75 % RH at RT (Fig. 21), because only under these conditions a precise measurement of samples with low moisture uptake was possible. In Fig. 21 it is demonstrated that generally tablet cores, all MCT subcoated tablets, and tablets subcoated with 5 mg StA absorb moisture most quickly at the beginning. The rates of moisture uptake of tablets coated with 10 mg StA, 5 mg Pr, and 5 mg Cp are superimposed and showed a reduced moisture uptake compared to the initially mentioned samples.
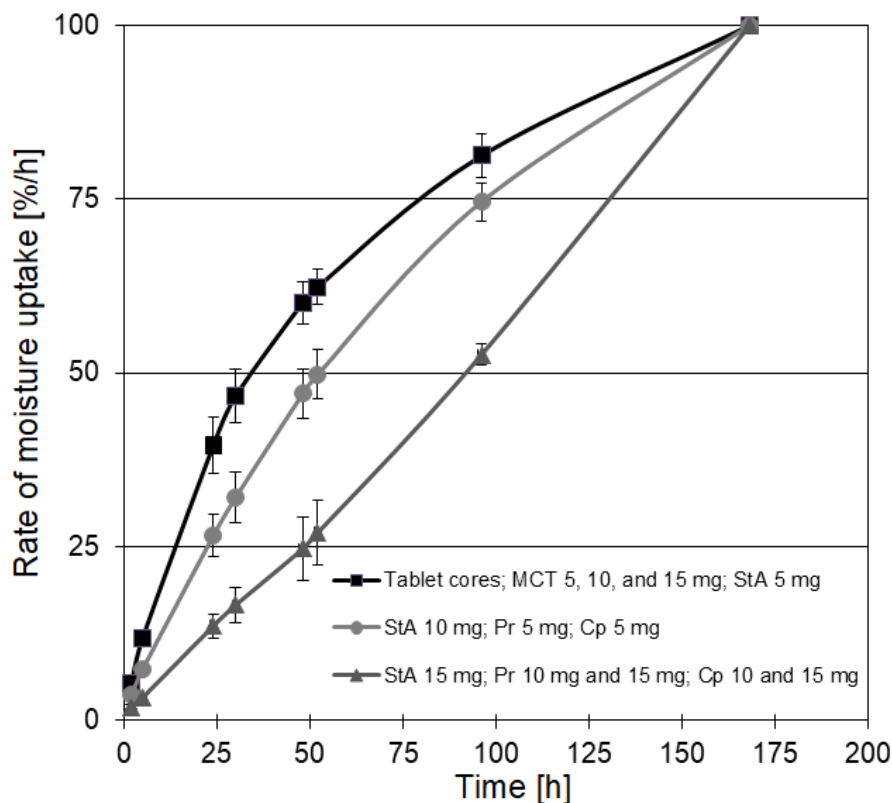
Fig. 21. Rate of moisture uptake of tablets subcoated with 5, 10, and 15 mg of the selected HMC materials at 75 % RH/RT (means ± SD, n = 3).

Tablet cores subcoated with high quantities of StA, Pr, and Cp behaved similar concerning the moisture absorption rate, which was represented by the lowest curve in Fig. 21. The differences between these three groups of tablets may be illustrated by comparing their time periods necessary for a total moisture uptake of 50 %: the first group needed 30 h, the second group 48 h, and the third group 96 h. The rates of their moisture absorption corresponded to their lipophilic characteristics (Table 3) as well as to their penetration data of the HMC materials into the tablet cores.

Because of the good balance between applied amount of HMC material, disintegration time, and adequate reduction of moisture uptake, an amount of 10 mg of subcoating material was chosen for all subsequent enteric formulations.

3.4.1.4. Influence of the coatings on the tablet properties

In Table 16 the changes of the tablet properties caused by the applied HMC materials regarding weight, thickness, diameter, and hardness is summarized. Each tablet surface was coated with 10 mg HMC material considering a calculated manufacturing overage of 10 %. The weights of the tablet cores subcoated with MCT and Pr were in good accordance with the applied 10 mg of both materials per tablet. The lower increase of the average weight of the tablet cores by subcoating with StA and Cp may be explained by the higher drop points of these HMC materials. These higher drop points caused longer heat-up times and induced a higher moisture loss in the tablet cores. During the subcoating procedure with Cp the cores lost 1.8 % moisture (means ± 0.1, n=2) referring to the initial moisture content of 4.5 % resulting in a final moisture content of 2.7 % and with StA the cores lost 1.5 % moisture (means ± 0.2, n=2) resulting in a final moisture content of 3.0 %. Generally, longer process times also led to an increase of the abrasion of the tablet cores, which was confirmed by the tablet thickness and diameter presented in Table 16.

Table 16. Weight, thickness, diameter, and hardness of the tablet cores and subcoated with 10 mg of MCT, StA, Pr, and Cp, respectively. Means ± SD, n=20.

Tablet samples	Weight [mg]	Thickness [mm]	Diameter [mm]	Hardness [N]
Plain tablet cores	287 ± 5	5.04 ± 0.03	9.96 ± 0.02	69 ± 14
Tablet cores subcoated with MCT 10 mg	297 ± 4	5.01 ± 0.02	9.95 ± 0.01	69 ± 11
Tablet cores subcoated with StA 10 mg	292 ± 6	5.02 ± 0.04	9.92 ± 0.01	97 ± 9
Tablet cores subcoated with Pr 10 mg	297 ± 3	4.95 ± 0.03	9.94 ± 0.02	112 ± 14
Tablet cores subcoated with Cp 10 mg	292 ± 6	4.97 ± 0.04	9.93 ± 0.02	95 ± 11

Apart from abrasion, the penetration of the HMC materials into the pores of the tablet cores may be responsible for the lack of an increase in thickness and diameter of the

subcoated tablets. The hardness of the subcoated tablets corresponds to that of the tablet cores after application of MCT and increased after application of StA, Pr, and Cp. The highest average increase in tablet hardness was observed with Pr (62 % increase, Table 16).

In summary it could be shown, that HMC with any of the selected HMC materials does not affect the tablet properties negatively with regard to subsequent processing steps. Interestingly, a positive impact of the solid HMC materials on the hardness of the tablets could be observed.

3.4.2.   Combination of the hot-melt coating and the enteric polymer coating

The spray-dried aqueous *Sennae fructus* extract is highly hygroscopic. The principal active constituents are dimeric dianthrone glycosides. They act as prodrugs, which are hydrolysed by enzymes from intestinal bacteria and are reduced to the active monoanthrones, finally causing the laxative effect in the intestine. Therefore, an outer enteric coating of the tablets is necessary such as EuL55. The combination of a hot-melt subcoating and an outer coating has already been discussed for a model drug by Tiwari et al. [158]. It was found out that this approach resulted in a more pronounced sustained release of the drug through the polymer coating, and reduced the interaction between the polymer coating and the active compound. In the present study, tablet cores subcoated with 10 mg HMC materials (MCT, StA, Pr, and Cp) and subsequently coated with different amounts (5 and 10 mg) of the enteric polymer EuL55 were investigated. It was mainly focused on changes of the disintegration and dissolution times, as well as the moisture protection. In contrast to the studies by Yang, Lu, and Tang [83], the combination of sub- and outer coating is not intended to cause a sustained drug release.

3.4.2.1. *Disintegration and dissolution times of the enteric-coated tablets*

Tablet cores as well as tablets subcoated with 10 mg of HMC material were coated with 10 mg of enteric polymer (EuL55). All tablet formulations exhibited a good robustness against 0.1 M hydrochloric acid for 2 h and disintegrated within 1 h in the disintegration medium pH 6.8 (Table 17). In contrast to the enteric-coated tablet cores, all subcoated enteric formulations showed a delayed disintegration. Tablet cores coated with both, the subcoating materials MCT and StA as well as with the enteric polymer disintegrated about 50 % later compared to the enteric-coated tablet cores without subcoating. The tablet cores subcoated with Pr and Cp resulted in a disintegration time twice as long as that of the EuL55 coated tablets without subcoating.

Table 17. Disintegration (means ± SD, n = 3) and dissolution times $t_{80\%}$ (means ± SD, n = 2) of tablets with 10 mg of hot-melt subcoating and 10 mg of enteric coating in phosphate buffer pH 6.8 after testing for gastric resistance in 0.1 M HCl for 2 h according to Ph. Eur.

Tablet cores		Disintegration time [min]	$t_{80\%}$ [min]
subcoated	enteric-coated		
-	EuL55 10 mg	15.0 ± 1.6	18 ± 2
MCT 10 mg	EuL55 10 mg	22.9 ± 3.7	20 ± 1
StA 10 mg	EuL55 10 mg	24.8 ± 4.6	46 ± 3
Pr 10 mg	EuL55 10 mg	29.2 ± 2.0	49 ± 2
Cp 10 mg	EuL55 10 mg	31.6 ± 2.7	51 ± 2

The less prolonged disintegration time of the tablet cores subcoated with MCT and EuL55 may be caused by the deep penetration of MCT into the tablet cores. In contrast, with the StA subcoating, the less prolonged disintegration time may be

caused by its comparably low lipophilicity (Table 3). The disintegration results of the tablet cores with Pr and Cp subcoatings as well as the enteric coating may be explained by the similar penetration into the tablet cores and their equal HLB values. Similar relationships are also evident in the dissolution results. However, it is noticeable that the StA-, Pr-, and Cp subcoated and additionally enteric-coated tablets showed a significantly delayed dissolution (Table 17). Clear differences between the disintegration times are recognizable. One explanation for this observation may be the lack of mechanical stress by the dissolution paddles compared to the discs in the glass tubes of the disintegration apparatus. Nevertheless, the 80 % release of the sennosides from all samples was below 60 min.

3.4.2.2 Moisture protection by combined subcoating and enteric coating

Recently, it was shown that film coatings such as EuL55 are able to reduce moisture absorption by tablet cores [69]. The aim of this present investigation was to examine the influence of the consecutive application of hot-melt subcoating and enteric coating on the hygroscopicity of the respective tablets. Therefore, 10 mg of HMC material was chosen for all tablet cores. As illustrated in Fig. 22, not in all cases the moisture absorption was reduced by a coating with EuL55. Surprisingly, the tablet cores subcoated with MCT and enteric-coated with EuL55 did not show any improvement with regard to the hygroscopicity compared to the enteric-coated tablet cores without subcoating. The maximum reduction in hygroscopicity in comparison to the tablet cores (Fig. 20) amounted to 98 % at 33 % RH/RT (Cp 10 + EuL55 10), to 96 % at 43 % RH/RT (Cp 10 + EuL55 10), and to 85 % at 75 % RH/RT (Pr 10 + EuL55 10), respectively (Fig. 22). Considering the tablet cores coated with 10 mg of EuL55, it was remarkable that after 7 d (at 75 % RH/RT) moisture absorption could be reduced from 13.6 to 5.4 %. Tablet cores subcoated with StA and Cp,

respectively, and coated with either 5 or 10 mg of EuL55 led to similar results. Only with the Pr subcoating, no matter whether 5 or 10 mg of EuL55 were applied, the reduction of the hygroscopicity was even higher than with the plain EuL55 coating at an amount of 10 mg.
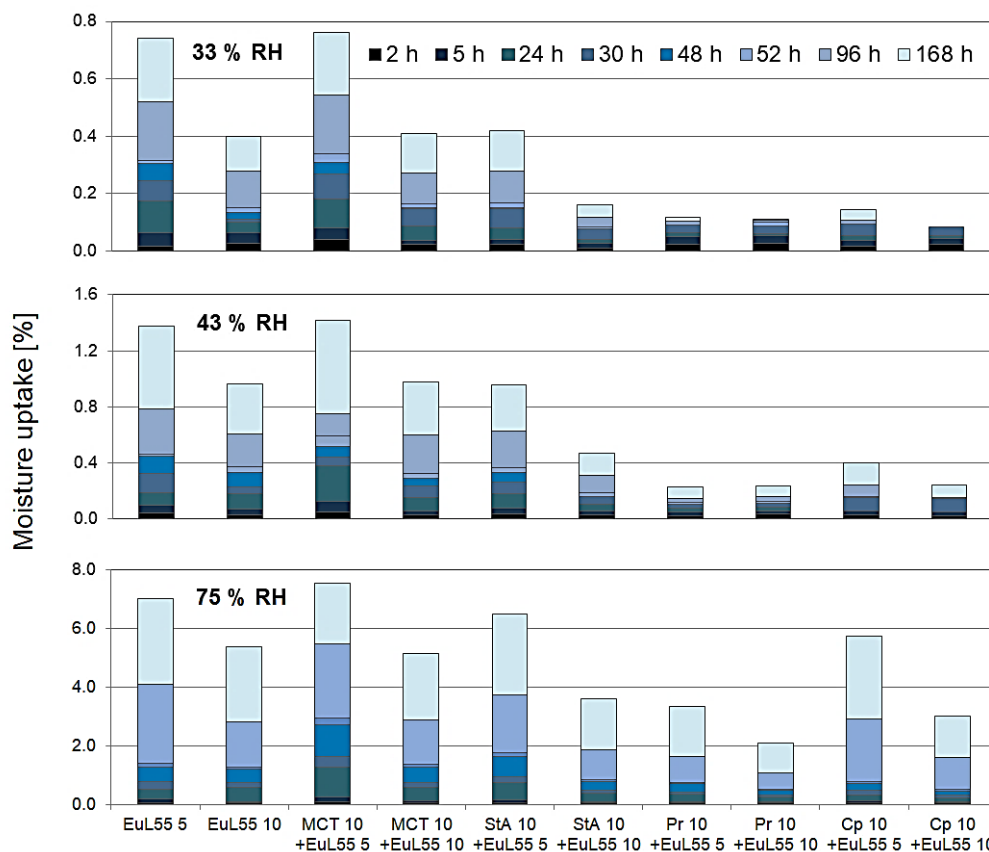

Fig. 22: Hygroscopicity of the tablet cores and the tablets subcoated with HMC materials both enteric-coated with 5 mg and 10 mg EuL55, respectively. Moisture uptake was measured at 33, 43, and 75 % RH. Means, RSD < 0.4 %, n = 3.

From the hygroscopicity data the rate of moisture uptake was determined for the condition of 75 % RH at RT (Fig. 23), because only under these conditions a precise measurement of samples with low moisture uptake was possible as already mentioned above. With regard to the rate of moisture uptake over time, it was noticed that tablets only coated with 5 mg of EuL55 and those additionally subcoated

with MCT absorb moisture more quickly than all the other coating combinations of analyzed tablets (Fig. 23). All tablet cores subcoated with Cp and coated with EuL55 showed a lower rate of moisture uptake particularly during the first 50 h.
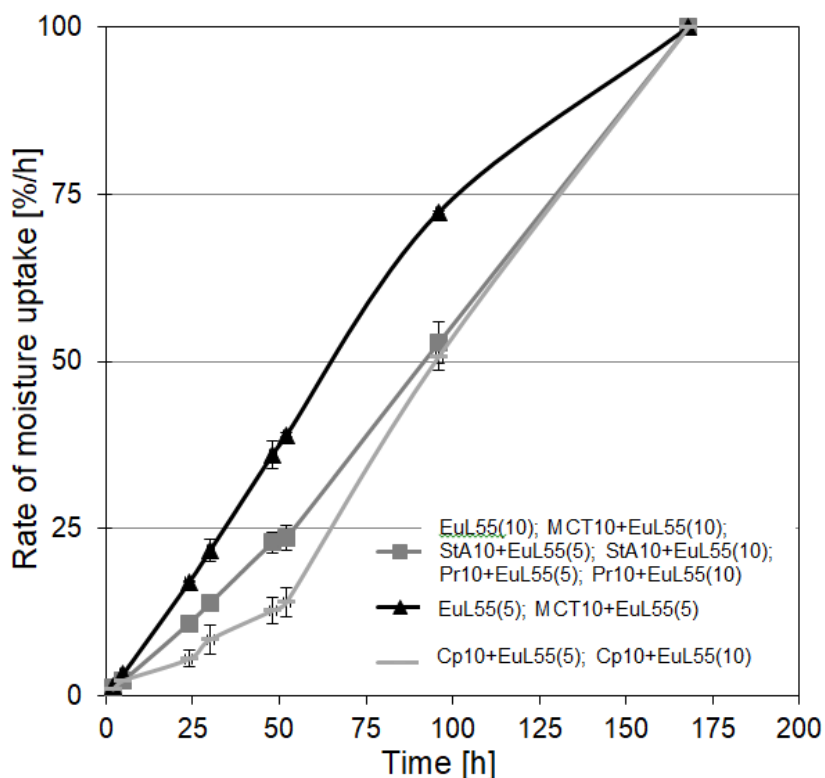

Fig. 23: Rate of moisture uptake of tablets subcoated with 10 mg of the investigated HMC materials and coated with EuL55 (5 and 10 mg) at 75 % RH/RT. For comparison, the results of tablets only coated with EuL55 are displayed (means ± SD, n = 3).

It is assumed that the enteric coating prevented direct moisture exposure to the subcoated tablet cores, which allowed the detection of even slight changes in the rate of moisture uptake. Apparently, the longer chain length of the behenic acid in Cp compared to the stearic acid in StA and Pr affected the rate of moisture uptake during the first hours.

3.4.3   Conclusions

In the present study it was shown that hot-melt coating is a successful technique for the application of a subcoating to tablet cores serving as a barrier against moisture permeation into hygroscopic tablet cores. The extract of *Sennae fructus*, representing a potent herbal laxative, was selected as hygroscopic model formulation. For HMC the following materials were tested as subcoatings: MCT, StA, Pr, and Cp. MCT as subcoating was able to reduce the hygroscopicity of the tablet cores without affecting the tablet properties such as tablet hardness. In addition no heat was necessary for application of this liquid subcoating leading to a short process time. However, MCT as subcoating may only be beneficial for protecting the tablet cores during the process of aqueous enteric coating, but not for tablet cores coated with both, MCT and EuL55. With tablets subcoated with StA and Cp, respectively, similarly high temperatures were necessary, which led to a longer process time. It is notable, that Cp as subcoat in combination with EuL55 reduced the rate of moisture uptake and also prolonged the disintegration and dissolution time of the coated tablets. For Pr subcoated tablets, it is advantageous that the process time was reduced because of the comparably low melting point. The Pr subcoating led to a high protection of the tablet cores against hygroscopicity, which even increased in combination with EuL55 to an almost complete protection against moisture and a pronounced reduction of the rate of moisture uptake. Interestingly, Pr applied as a subcoating to the tablet cores and subsequently coated with a low amount EuL55 was more efficient with regard to the protection against hygroscopicity than tablet cores coated solely with a high amount of EuL55. For a rapid determination of the hygroscopicity of the tablet cores the disintegration test may partly be suitable as the hygroscopicity data correspond to the disintegration results allowing the detection of reduced moisture permeability. In further studies,

the long-term stability of hygroscopic Sennae fructus extract as well as the aging of the HMC materials during storage should be investigated. Moreover it should be examined weather the results obtained from these studies may be transferred to other hygroscopic dry plant extracts.

4. References

[1]   European Commission. Commission Directive 2003/63/EC of 25 June 2003 amending Directive 2001/83/EC of the European Parliament and of the Council on the Community code relating to medicinal products for human use. *Official Journal of the European Union.* **2003**, L159, 46-94.

[2]   Committee for Proprietary Medicinal Products. Guideline on stability testing: Stability testing of existing active substances and related finished products. CPMP/QWP/122/02, 2003.

[3]   Committee for Proprietary Medicinal Products. Note for Guidance on in-use stability testing of human medicinal products. CPMP/QWP/2934/99, 2001.

[4]   Committee on Herbal Medicinal Products. Guideline on quality of herbal medicinal products/traditional herbal medicinal products. EMA/HMPC /201116/2005 Rev. 3, 2018.

[5]   Committee on Herbal Medicinal Products. Guideline on specifications: test procedures and acceptance criteria for herbal substances, herbal preparations and herbal medicinal product/traditional herbal medicinal products. EMA/HMPC/162241/2005 Rev. 2, 2011.

[6]   European Commission, Enterprise and Industry Directorate-Gerneral. EU Guidelines to Good Manufacturing Practice Medicinal Products for Human and Veterinary Use, Quality Control; Part I, Ch. 6. Vol. 4. EudraLex, Brussels, Belgium, 2014.

[7]   Henda, S. S. An overview of extraction techniques for medicinal and aromatic plants. In *Extraction Technologies for Medicinal and Aromatic Plants*; Handa, S. S.; Khanuja, S. P. S.; Longo, G.; Rakesh, D. D., Ed.; International Centre for Science and high Technology: Trieste, 2008.

[8]   Gharsallaoui, A.; Roudaut, G.; Chambin, O.; Voilley, A.; Saurel, R. Application of spray-drying in microencapsulation of food ingredients: An overview. *Food Res. Int.* **2007**, 40, 1107-1121.

[9]   Griesing, J. M., Untersuchung der Trocknungskinetik und Strukturausbildung von Vinylacetat-Ethylen-Copolymerdispersionen in akustisch levitierten Einzeltropfen. Ph.D. Dissertation, University Hamburg, Germany, 2015.

[10]   Iskandar, F.; Gradon, L.; Okuyama, K. Control of the morphology of nanostructured particles prepared by the spray drying of a nanoparticle sol. *J. Colloid Interface Sci.* **2003**, 265, 296-303.

[11]   Kurozawa, L.; Park, K. J.; Hubinger, M. Spray Drying of Chicken Meat Protein Hydrolysate: Influence of Process Conditions on Powder Property and Dryer Performance. *Drying Techn.* **2011**, 29, 163-173.

[12]   Tonon, R. V.; Brabet, C.; Hubinger, M. D. Influence of process conditions on the physicochemical properties of açai (Euterpe oleraceae Mart.) powder produced by spray-drying. *J. Food Eng.* **2008**, 88, 411-8.

[13]   Chegini, G. R.; Ghobadian, B. Effect of spray-drying conditions on physical properties of orange juice powder. *Drying Techn.* **2007**, 23, 657-668.

[14]   Qian, L.; Zhang, H. Controlled freezing and freeze drying: a versatile route for porous and micro-/nano-structured materials. *J. Chem. Technol. Biotechnol.* **2010** , 86(2), 172-184.

[15]   Rey, L.; May, J. C. Freeze drying/lyophilization of pharmaceutical and biological products, 3rd ed; Informa Healthcare: New York, 2010.

[16]   Oetjen G. W.; Haseley, P. Freeze-Drying. Wiley-VCH Verlag: Weinheim, 2004.

[17]   Altmann, R. Die Elementarorganismen und ihre Beziehungen zu den Zellen, von Veit and Comp.: Leipzig, 1894.

[18]   Greaves, R. I. N.; Fry, R. M. The survival of bacteria during and after drying. *J. Hyg.* **1951**, 49 (2-3), 220-246.

[19]   Flosdorf, E. E., Stokes, F. J., and Mudd, S., J. Am. Med. Assoc. 115, 1095-1097 (1940).

[20]   Padma Ishwarya, S.; Anandharamakrishnan, C; Stapley, A. G. F. Spray-freeze-drying: A novel process for the drying of foods and bioproducts. *Trends Food Sci. Technol.* **2015**, 41(2), 161-181.

[21]   Song, J. G.; Lee, S. H.; Han, H.-K. Biophysical evaluation of aminoclay as an effective protectant for protein stabilization during freeze-drying and storage. *Int. J. Nanomedicine.* **2016**, 11, 6609–6619.

[22]   Jafari, S.-M.; Mahdavi-Khazaei, K.; Hemmati-Kakhki, A. Microencapsulation of saffron petal anthocyanins with cress seed gum compared with Arabic gum through freeze drying. *Carbohydr. Polym.* **2016**, 140, 20-25.

[23]   Ferrari, C. C. Storage stability of spray-dried Blackberry powder produced with maltodextrin or gum arabic. *Drying Techn.* **2013**, 31, 470-478

[24]   Goula, A. M.; Adamopoulos, K. G. Effect of maltodextrin addition during spray drying of tomato pulp in dehumidified air: II. Powder properties. *Drying Techn.* **2008**, 26, 726-737.

[25]   Franks, F. Thermomechanical properties of amorphous saccharides: their role in enhancing pharmaceutical product stability. *Biotechnol. Genet. Eng. Rev.* **1999**, 16(1), 281-292.

[26]   Huntington, D. H. The influence of the spray drying process on product properties. *Drying Technol.* **2004**, 22, 1261-1287.

[27]   Lee Y. K.; Ganesan P.; Baharin B. S.; Kwak H-S. Characteristics, stability, and release of Peanut Sprout extracts in powdered microcapsules by spray drying. *Drying Technol.* **2015**. 33, 1991-2001.

[28]   Carneiro, H. C. F.; Tonon, R. V.; Grosso, C. R. F.; Hubinger, M. D. Encapsulation efficiency and oxidative stability of flaxseed oil microencapsulated by spray drying using different combinations of wall materials. *J. Food Eng.* **2013**, 115, 443-451.

[29]   Goula, A. M.; Adamopoulos, K. G. Effect of maltodextrin addition during spray drying of tomato pulp in dehumidified air: II. Powder properties. *Drying Technol.* **2008**, 26, 726-737.

[30]   Jaya, S.; Das, H. Effect of maltodextrin, glycerol monostearate and tricalcium phosphate on vacuum dried mango powder properties. *J. Food Eng.* **2004**, 63, 125-134.

[31]   Rodríguez-Hernández G. R.; González-García, R.; Grajales-Lagues, A.; Ruiz-Cabrera, M. A.; Abud-Archila, M. Spray-drying of Cactus Pear Juice (Opuntia streptacantha): Effect on the physicochemical properties of powder and reconstituted product. *Drying Technol.* **2005**, 23, 955-973.

[32]   Sonner, C.; Maa, Y. F.; Lee, G. Spray-freeze-drying for protein powder preparation: Particle characterization and a case study with trypsinogen stability. *J. Pharm. Sci.* **2002**, 91(10), 2122-2139.

[33]   Edwards, D.A.; Hanes, J.; Caponetti, G.; Hrkach, J.; Ben-Jebria, A.; Eskew, M. L.; Mintzes, J.; Deaver, D.; Lotan, N.; Langer, R. Large Porous Particles for Pulmonary Drug Delivery. *Science.* **1997**, 276(5320), 1868-1871.

[34]   Stoklosa, A. M.; Lipasek, R. A.; Taylor, L. S.; Mauer, L. J. Effects of storage conditions, formulation, and particle size on moisture sorption and flowability of powders: A study of deliquescent ingredient blends. *Food Res. Int.* **2012**, 49(2), 783-791.

[35]   Ryzak, M.; Bieganowski, A. Methodological aspects of determining soil particle-size distribution using the laser diffraction method. *J. Plant Nutr.* **2011**, 174(4), 624-633.

[36]   Sympatec, Technical information, HELOS, 2017.

[37]   Lang, G. Histotechnik, Praxislehrbuch für die Biomedizinische Analytik, 2rd ed.; Springer-Verlag: Wien, 2013.

[38]   Thermofisher, Technical information, Scanning Electron Microscopy Explained, 2019.

References

[39]   Kühl, S.; Linnemann, A. Grundlagen der Licht- und Elektronenmikroskopie; Eugen Ulmer: Stuttgart, 2018.

[40]   Giesche, H. Mercury Porosimetry: A General (Practical) Overview. *Part. Syst. Charact.* **2006**, 23(1), 1-11.

[41]   *Washburn, E. W.* The Dynamics of Capillary Flow. *Phys. Rev. **1921**, 17, 273–283.*

[42]   Hasanuzzaman, M.; Rashid, A.; Olabi, A. G. Characterization of Porous Glass and Ceramics by Mercury Intrusion Porosimetry. *Reference Module in Materials Science and Materials Engineering.* **2017**.

[43]   Brunauer, S.; Emmett, P. H.; Teller, E. Adsorption of Gases in Multimolecular Layers. *J. Am. Chem. Soc.* **1938**, 60(2), 309-319.

[44]   Fagerlund, G. Determination of specific surface by the BET method. *Matériaux et Construction.* **1973**. 6(3), 239–245.

[45]   Lowell, S.; Shields, J.E.; Thomas, M. A.; Thommes, M. Characterization of Porous Solids and Powders: Surface Area, Pore Size and Density; Springer Science+Business: New York, 2004.

[46]   Kim, K. C.; Yoon, T. U.; Bae, Y. S. Applicability of using CO_2 adsorption isotherms to determine BET surface areas of microporous materials. *Microporous and Mesoporous Mater.* **2016**, 224, 294-301.

[47]   Weber, J.; Bastick, M. Influence de la température sur la détermination de la masse volumique de divers carbones par pycnométrie dans l'helium. *Bulletin de la Société Chimique de France.* **1968**, 7, 2702–2706.

[48]   Neimark, A. V.; Ravikovitch, P. I. Calibration of pore volume in adsorption experiments and theoretical models. *Langmuir.* **1997**, 13, 5148-5160.

[49]   Viana, M.; Jouannin, P.; Herry, C.; Chulia, D. About pycnometric density measurements. *Talanta.* **2002**, 57(3), 583-593.

[50]   Micromeritics, Technical information, AccuPycII Pycnometer.

[51]   Götz, E. Modulare Keramik-Komposite mit periodischer Mikrostruktur. Ph.D. Dissertation, University of Erlangen-Nürnberg, Germany, 2014.

[52]   Goppel, M. Stabilitätsuntersuchungen pflanzlicher Zubereitungen am Beispiel von Baldrian- und Senna- Trockextrakten. Ph.D. Dissertation. University of Regensburg. 2003.

[53]   Vaughn, S. F.; Berhow, M. A. Glucosinolate hydrolysis products from various plant sources: pH effects, isolation, and purification. *Ind. Crops Prod.* **2005**, 21, 193-202.

[54]   Giovanelli, G.; Paradiso, A. Stability of Dried and Intermediate Moisture Tomato Pulp during Storage. J. Agric. *Food Chem.* **2002**, 7277-7281.

[55]   Dabbagh, H. A.; Azami, F. Experimental and theoretical study of racemization, stability and tautomerism of vitamin C stereoisomers. *Food Chem.* **2014**, 164, 355-362.

[56]   Brown, B. R.; Phil, D. The mechanism of thermal decarboxylation. *Quarterly Reviews, Chemical Society.* **1951**, 2.

[57]   Toscano, G.; Colarieti, M. L.; Greco, G. Oxidative polymerization of phenols by a phenol oxidase from green olives. *Enzyme Microb.Techn.* **2003**, 33(1), 47-54.

[58]   Jackson, K.; Young, D.; Pant, S. Drug-excipient interactions and their effect on absorption. *Pharm. Sci. Technol. Today.* **2000**, 3, 336-3.

[59]   Gutch, P. K.; Jitendra, S.; Alankar, S.; Anurekha, J.; Ganesan, K. Thermal analysis of interaction between 2-PAM chloride and various excipients in some binary mixtures by TGA and DSC. *JTAC.* **2013**, 111(3), 1953-1958.

[60]   Van Dooren, A. A. Design for Drug-Excipient Interaction Studies. *Drug Dev. Ind. Pharm.* **1983**, 9, 43-55.

[61]   Aigner, Z.; Heinrich, R.; Sipos, E.; Farkas, G.; Ciurba, A.; Berkesi, O.; Szabó-Révész, P. Compatibility studies of aceclofenac with retard tablet excipients by means of thermal and FT-IR spectroscopic methods. *J. Thermal Anal.* **2011**, 104, 265-271.

[62]   Bozdağ-Pehlivan, S.; Subaşi, B.; Vural, I.; Unlü, N.; Capan, Y. Evaluation of drug-excipient interaction in the formulation of celecoxib tablets. *Acta Pol. Pharm.* **2011**, 68, 423-433.

[63]   Bruni, G.; Amici, L.; Berbenni, V.; Marini, A.; Orlandi, A. Drug-Excipient Compatibility Studies. Search of interaction indicators. *J. Thermal Anal.* **2002**, 68, 561-573.

[64]   Charlton, B.; Newton, J. M. Theoretical estimation of punch velocities and displacements of single-punch and rotary tablet machines. *J Pharm. Pharmacol.* **1984**, 36(10).

[65]   Kása, P.; Bajdik, J.; Zsigmond, Z.; Pintyee-Hódi, K. Study of the compaction behavior and compressibility of binary mixtures of some pharmaceutical excipients during direct compression. *Chem. Eng. Process.* **2009**, 48(4), 859-863.

[66]   Patel, S.; Kaushal, A. M.; Bansal, A. K. Compression Physics in the Formulation Development of Tablets. *Crit. Rev. Ther. Drug.* **2006**, 23(1), 1-65.

[67]   Ankit, G.; Bilandi, A.; Kataria, M. K.; Neetu, K. Tablet Coating techniques: Concepts and recent trends. *Int. Res. J. Pharm.* **2012**, 3(9), 50-58.

[68]   Joshi, S.; Petereit, H. U. Film coating for taste masking and moisture protection. *Int. J. Pharm.* **2013**, 457(2), 395-406.

[69]   Mwesigwa, E.; Basit, A. W.; Buckton, G. Moisture sorption and permeability characteristics of polymer films: implications for their use as barrier coatings for solid dosage forms containing hydrolysable drug substances. *J. Pharm. Sci.* **2008**, 97, 4433-4445.

[70]   Abbaspour, M. R.; Sharif Makhmalzadeh, B.; Jalali, S. Study of free-films and coated tablets based on HPMC and microcrystalline cellulose, aimed for improve stability of moisture-sensitive drugs. *Jundishapur J. Nat. Pharm. Prod.* **2010**, 5, 6-17.

[71]   Hagenmaier, R. D.; Shaw, P. E. Moisture permeability of edible films made with fatty acid and hydroxypropyl methyl cellulose. *J. Agric. Food. Chem.* **1990**, 38(9), 1799-1803.

[72]   Hoshino, T.; Kashimoto, N.; Kasuga, S. Effects of Garlic Preparations on the Gastrointestinal Mucosa. *J. Nutr.* **2001**, 31, 1109-1113.

[73]   Bonetta, A.; Di Pierro, F. Enteric-coated, highly standardized cranberry extract reduces risk of UTIs and urinary symptoms during radiotherapy for prostate carcinoma. *Cancer Management Res.* **2012**, 281-286.

[74]   Ramchander, A. M.; Middha, A.; Jalwal, P. Formulation and evaluation of enteric coated tablets of Senna for the treatment of constipation. *The Pharma Innovation Journal.* **2017**, 6, 263-267.

[75]   Unna, P. G. Keratinierte Pillen. *Pharm. Zentrahlle.* ***1884,*** 25, 577.

[76]   Deshpande, T. M.; Quadir, A.; Obara, S.; Ibrahim, A.; Hoag, S. W. Developing a stable aqueous enteric coating formulation with hydroxypropyl methylcellulose acetate succinate (HPMCAS-MF) and colloidal silicon dioxide as anti-tacking agent. *Int. J. Pharm.* **2018**, 524(1-2), 108-116.

[77]   Macchi, E.; Zema, L.; Maroni, A.; Gazzaniga, A.; Felton, L. A. Enteric-coating of pulsatile-release HPC capsules prepared by injection molding. *Eur. J. Pharm. Sci.* **2015**, 70, 1-11.

[78]   Jog, R.; Unachukwu, K.; Burgess, D. J. Formulation design space for stable, pH sensitive crystalline nidedipine nanoparticles. *Int. J. Pharm.* **2016**, 514(1), 81-92.

[79]   Krishnaiah, Y. S. R.; Satyanarayana, S.; Rama Prasad, Y.V. Studies of Guar Gum Compression-Coated 5-Aminosalicylic Acid Tablets for Colon-Specific Dug Delivery. *Drug Dev. Ind. Pharm.* **1999**, 25, 651-657.

[80]   Chan, E. S.; Zhang, Z. Bioencapsulation by compression coating of probiotic bacteria for their protection in an acidic medium. *Process Biochem.* **2005**, 40, 3346-3351.

[81]   Kablitz, C. D.; Urbanetz, N. A. Characterization of the film formation of the dry coating process. *Eur. J. Pharm. Biopharm.* **2007**, 7, 449-457.

[82]   Qiao, M.; Zhang, L.; Ma, Y.; Zhu, J.; Xiao, W. A novel electrostatic dry coating process for enteric coating of tablets with Eudragit® L100-55. *Eur. J. Pharm. Biopharm.* **2013**, 83, 293-300.

[83]   Yang, Z. Y.; Lu, Y.; Tang, X. Pseudoephedrine hydrochloride sustained-release pellets prepared by a combination of hot-melt subcoating and polymer coating. *Drug Dev. Ind. Pharm.* **2008**, 34, 1323-1330.

[84]   Sinchaipanid, N.; Junyaprasert, V.; Mitrevej, A. Application of hot-melt coating for controlled release of propranolol hydrochloride pellets. *Powder Technol.* **2004**, 141, 203-209.

[85]   Haak, D.; Koeberle, M. Hot melt coating for controlling the stability, release properties and taste of solid oral dosage forms. *Techno Pharm.* **2014**, 4, 258-263.

[86]   Sudke, S. G.; Sakarakar, D. M. Lipids – An Instrumental Excipient in pharmaceutical Hot-Melt Coating. *Int. J. Pharm. Tech. Res.* **2013**, 5, 607-621.

[87]   Barthelemy, P.; Laforet, J. P.; Farah, N.; Joachim, J. Compritol 888 ATO: An innovative hot-melt coating agent for prolonged-release drug formulations. *Eur. J. Pharm. Biopharm.* **1999**, 47: 87-90.

[88]   European Directorate for the Quality of Medicines. Senna leaf, monograph 0206. *Pharmacopoea Europaea.* 8.3 ed. France: Strasbourg, 2013.

[89]   European Directorate for the Quality of Medicines. Senna pods, Alexandrian, monograph 0207. *Pharmacopoea Europaea.* 8.3. ed. France: Strasbourg, 2013.

[90]   European Directorate for the Quality of Medicines. Senna pods, Tinnevelly, monograph 0208. *Pharmacopoea Europaea.* 8.3. ed. France: Strasbourg, 2013.

[91]   European Directorate for the Quality of Medicines. Senna leaf dry extract, standardized, monograph 1261. *Pharmacopoea Europaea.* 8.3. ed. France: Strasbourg, 2013.

[92]   Gärtner G, Kochendörfer G, Kolbusch P. Nutzungsmöglichkeiten ausgewählter Trockenzonenpflanzen in Entwicklungsländern. Forschungsbericht des Bundesministeriums für wirtschaftliche Zusammenarbeit. München:Weltforum Verlag, 1982.

[93]   Steinegger, E.; Hänsel, R. Lehrbuch der Pharmakognosie und Phytopharmazie, 4th ed. Springer-Verlag: Berlin, 1988.

[94]   Kinjo, J.; Ikeda, T.; Watanabe, K.; Nohara, T. An anthraquinone glycoside from Cassia angustifolia leaves. *Phytochem.* **1994**, 37, 1685-1687.

[95]   Schultze, W.; Jahn, K.; Richter, R. Volatile constituents of the dried leaves of Cassia angustifolia and C.acutifolia (Sennae folium). *Planta Med.* **1996**, 62, 540-543.

[96]   Korulkin, D.; Muzychkina, R. A. Biosynthesis and Metabolism of Anthraquinone Derivatives. *World Academy of Science, Engineering and Technology.* **2014**, 8(7).

[97]   Akao, T.; Che, Q. M.; Kobashi, K.; Yang, L.; Hattori, M.; Namba, T. Isolation of a human intestinal anaerobe, Bifidobacterium sp. strain SEN, capable of hydrolyzing sennosides to sennidins. *Appl. Environ. Microbiol.* **1994**, 60, 1041-1043.

[98] Meilhammer, B. Untersuchungen zur Hydroxyanthracenfreisetzung aus Abführtees unter haushaltsnahen Extraktionsbedingungen. Ph.D. Dissertation, Uniersity of Regensburg, Germany, 2003.

[99] Terreaux, C.; Wang, Qi.; Loset, J.-R. ; Ndjoko, K. ; Grimminger, W.; Hostettmann, K. Complete LC/MS analysis of a Tinnevelly senna pod extract and subsequent isolation and identification of two new benzophenone glucosides. *Planta Med.* **2002**, 68, 349-354.

[100] Sun, S.W.; Su, H.T. Validated HPLC method for determination of sennosides A and B in senna tablets. *J. Pharm. Biomed. Anal.* **2002**, 29, 881-894.

[101] Shreedhara, C.; Ghosh, A.; Shetty, R.; Kumar, V.; Sanghai, D. Quantification of Sennosides by reverse phase high performance liquid chromatography coupled with electro spray ionization tandem mass spectrometry in unani formulations. *Int. J. Pharmacogn Phytochem. Res.* **2013**, 4(4), 224-226.

[102] Rosenthal, I.; Wolfram, E.; Meier, B. A HPLC method to determine sennoside A and sennoside B in Sennae fructus and Sennae folium. *Pharmeuropa Bio & Scientific Notes.* **2014**, 92-102.

[103] PA/PH/Exp. 13A/T. Senna Pods, Alexandrian (0207). *Pharmeuropa.* **2015**, 175-180.

[104] PA/PH/Exp.13A/T. Senna Pods, Tinnevelly (0208). *Pharmeurope.* **2015**, 181-186.

[105] De Hoffmann, E. Mass spectrometry, in: Kirk, R.E.; Othmer D. (Eds.), Encyclopedia of Chemical Technology, John Wiley & Sons, Inc., 2005.

[106] Verloop, Q.; Marais, A.F.; de Villiers, M.M.; Liebenberg, W. Compatibility of sennoside A and B with pharmaceutical excipients. *Pharmazie.* **2004**, 59, 728-730.

[107] EFSA Panel of Food Additives and Nutrient Sources added to Food. Safety of hydroxyanthracene derivatives for use in food. *EFSA Journal.* **2008**, 16, 5090.

[108]   Olionatura. Information MCT-Oil, 2019.

[109]   Severino, P.; Pinho, S. C.; Souto, E. B.; Santana, M. H. A. Polymorphism, crystallinity and hydrophilic-lipophilic balance of stearic acid and stearic acid-capric/caprylic triglyceride matrices for production of stable nanoparticles. *Colloids Surf.* **2011**, 86(1), 125-130.

[110]   Gattefossé, Precirol® ATO 5, Product form.

[111]   Gattefossé, Compritol® 888 ATO, Product form.

[112]   Kock, G. Synthese, Charakterisierung und antioxidative Eigenschaften von vinylog verlängerten Flavonoiden. Ph. D. Dissertation, University of Düsseldorf, Germany, 2008.

[113]   Beynon, I. H.; Williams, A. E. Mass Spectra of Various Quinones and Polycyclic Ketones. *Appl. Spectroscopy.* **1960**, 14(6), 156-160.

[114]   Harbone, J. B.; Mabry, T. J.; Mabry, H. The Flavonoids. Springer Science+Business Media: Dordrecht, 1975; p. 46.

[115]   Harbone, J. B.; Mabry, T. J.; Mabry, H. The Flavonoids. Springer Science+Business Media: Dordrecht, 1975; p. 82.

[116]   Negaprashantha, L. D.; Vatsayayan, R.; Singhal, J.; Fast, S.; Roby, R.; Awasthi, S. Anti-cancer effects of novel flavonoid vicenin-2 as a single agent and in synergistic combination with docetaxel in prostate cancer. *Biochem. Pharmacol.* **2011,** 82(9), 1100-1109.

[117]   Islam, M. N.; Ishita, I. J.; Jung, H. A.; Choi, J. S. Vicenin 2 isolated from Artemisia capillaris exhibited potent anti-glycation properties. *Food Chem. Toxicol.* **2014,** 69, 55-62.

[118]   Harbone, J. B.; Mabry, T. J.; Mabry, H. The Flavonoids. Springer Science+Business Media: Dordrecht, 1975; p. 118.

[119] Nakajima, K.; Yamauchi, K.; Kuwano, S. Isolation of a new aloe-emodin dianthrone diglucoside from senna and its potentiating effect on the purgative activity of sennoside A in mice. *J. Pharm. Pharmacol*. **1985**, 37(10), 703-706.

[120] Yagi, T.; Yamauchi, K.; Kuwano, S. The synergistic purgative action of aloe-emodin anthrone and rhein anthrone in mice: synergism in large intestinal propulsion and water secretion. *J. Pharm. Pharmacol*. **1997,** 49(1), 22-25.

[121] Yamauchi, K.; Shinano, K.; Nakajima, K.; Yagi, T.; Kuwano, S. Metabolic activation of sennoside C in mice: synergistic action of anthrones. *J. Pharm. Pharmacol*. **1992,** 44(12), 973-976.

[122] Fairbaim, J.W.; Moss, M. J. The relative purgative activities of 1,8-dihydroxyanthracene derivatives. *J. Pharm. Pharmacol*. **1970**, 22(8), 584-593.

[123] Hietala, P.; Marvola, M.; Parviainen, T.; Lainonen, H. Laxative potency and acute toxicity of some anthraquinone derivatives senna extracts and fractions of senna extracts. *Pharmakol. Toxicol*. **1987,** 61, 153-156.

[124] Senna Leaf. *Japanese Pharmacopoeia.* 16th ed. Japan, 2011.

[125] Rosenthal, I.; Wolfram, E.; Meier, B.. A HPLC method to determine sennoside A and sennoside B in Sennae fructus and Sennae folium. *Pharmeuropa Bio & Scientific Notes.* **2014,** 92-102.

[126] Tanaka, H.; Murata, R.; Yoshida, A.; Hayashi, S. Analytical studies on the active constituents in crude drugs. V. The structure of sennoside G, a new glucoside from senna. *Chem. Pharm. Bull.* **1982**, 30(5), 1550-1556.

[127] Hu, Y.; Zeng, C.; Liao, F.; Tan, H.; Wu, L.; Liu, X. Embryotoxicity and Teratogenicity of Rhein. *J. Health Sci.* **2014**, 2, 180-184.

[128] Ács, N.; Bánhidy, F.; Puhó, E. H.; Czeizel, A. E. Senna treatment in pregnant women and congenital abnormalities in their offspring—A population-based case–control study. *Reprod. Toxicol.* **2009**, 28(1), 100–104.

[129] van Gorkom, B. A. P.; Himmer-Bosscha, H.; de Jong, S.; van der Kolk, D. M.; Kleibeuker, J. H.; de Vries, E. G. E. Cytotoxicity of rhein, the active metabolite of sennoside laxatives, is reduced by multidrug resistance-associated protein 1. *Br. J. Cancer.* **2002,** 86(9), 1494-1500.

[130] Mitchell, J. M.; Mengs, U.; McPherson, S.; Zijlstra, J.; Dettmar, P.; Gregson, R.; *et al.* An oral carcinogenicity and toxicity study of senna (Tinnevelly senna fruits) in the rat. *Arch. Toxicol.* **2006,** 80(1), 34-44.

[131] Heidemann, A.; Miltenburger, H. G.; Mengs, U. The genotoxicity status of senna. *Pharmacol.* **1993,** 47(1), 178-186.

[132] Heidemann, A.; Völker, W.; Mengs, U. Genotoxicity of aloeemodin in vitro and in vivo. *Mutat. Res.***1996**, 367(1),123-133.

[133] Krumbiegel, G.; Schulz, H. U. Rhein and aloe-emodin kinetics from senna laxatives in man. *Pharmacol.* **1993**, 47(1), 120-124.

[134] Gärtner, G.; Kochendörfer, G.; Kolbusch, P. Nutzungsmöglichkeiten ausgewählter Trockenzonenpflanzen in Entwicklungsländern. Forschungsbericht des Bundesministeriums für wirtschaftliche Zusammenarbeit. Weltforum Verlag:München, 1982.

[135] Sticher O, Steinegger E. In: Hänsel R. *Pharmakognosie-Phytopharmazie.* Heidelberg; 1999. p. 456-464.

[136] Lemli, J.; Cuveele, J.; Verhaen E. Chemical Identification of Alexandrian and Tinnevelly Senna. *Planta Med.* **1983,** 49(9), 36-37.

[137] Schmid, W.; Angliker, E. Sennosid C, ein neues Glucosid aus Cassia angustifolia. *Helv. Chim. Acta.* **1965,** 48, 1911-1921.

[138] Crellin, J. K.; Fairbaim, J. W.; Friedmann, C. A.; Ryan, H. A. New glycosides from senna. *J. Pharm. Pharmacol.* **1961**, 13, 639-640.

[139] Kinjo, J.; Ikeda, T.; Watanabe, K.; Nohara, T. An anthraquinone glycoside from Cassia angustifolia leaves. *Phytochem.* **1994,** 37, 1685-1687.

[140]   Stoll, A.; Becker, B.; Kussmaul. Die Isolierung der Anthraglykoside aus Sennadrogen. *Helv. chim. acta.* **1950**, 32, 1892-1903.

[141]   Farag, M. A.; Porzel, A.; Mahrous, E. A.; El-Massry, M. M.; Wessjohann, L. A. Integrated comparatice metabolite profiling via MS and NMR techniques for Senna drug quality control analysis. *Anal. Bioanal. Chem.* **2015**, 407, 1947-1949.

[142]   Singh, A.; Van den Mooter, G. Spray drying formulation of amorphous solid dispersions. *Adv. drug deliv. rev.* **2015**, 100, 27-50.

[143]   Quek, S. Y.; Chok, N. K.; Swedlund, P. The physicochemical properties of spray-dried watermelon powders. *Chem. Eng. Process.* **2007**, 46, 386-392.

[144]   Araruna, S. M.; Silva, A. H.; Canuto, K. M.; Silveira, E. R.; Leal, L. K. A. M. Influence of process conditions on the physicochemical characteristics of cumaru (*Amburana cearensis*) powder produced by spray drying. *Revista Brasileira de Farmacognosia.* **2013**, 23,132-137.

[145]   Kurozawa, L.; Park, K. J.; Hubinger, M. Spray Drying of Chicken Meat Protein Hydrolysate: Influence of Process Conditions on Powder Property and Dryer Performance*. Drying Techn.* **2011**, 29, 63-173.

[146]   Reineccius, G. A. Multiple-core encapsulation; The spray drying of food ingredients. In: Vilstrup P (Ed.). Microencapsulation of Food Ingredients. Leatherhead Food RA Publishing, Leatherhead, England, 2001.

[147]   Almilla-Beltrán, L.; Chanona-Pérez, J. J.; Jiménez-Aparicio, A. R.; Gutiérrez-López, G. F. Description of morphological changes of particles along spray drying. *J. Food Eng.* **2005**, 67, 179-84.

[148]   Vicente, J.; Pinto, J.; Menezes, J.; Gaspar, F. Fundamental analysis of particle formation in spray drying. *Powder Technol.* **2013**, 247, 1-7.

[149]   Lin, J. C.; Gentry, J. W. Spray Drying Drop Morphology: Experimental Study. *Aerosol Sci. Techn.* **2003**, 37, 15-32.

[150]   Nandiyanto, A. B. D.; Okuyama, K. Progress in developing spray-drying methods for the production of controlled morphology particles: From the nanometer to submicrometer size ranges. *Adv. Powder Techn.* **2011**, 22, 1-19.

[151]   Maa, Y. F.; Costantino, H. R.; Nguyen, P. A.; Hsu, C. C. The effect of operating and formulation variables on the morphology of spray-dried protein particles. *Pharm.l Dev. Techn.* **1997**, 2, 213-23.

[152]   Maas S. G. Optimierung trägerbasierter Pulverinhalte durch Modifikation der Trägeroberfläche mittels Sprühtrocknung. Ph.D. Dissertation, University of Düsseldorf, Germany, 2009.

[153]   Zier, K.; Schultze, W.; Sakmann, A.; Leopold, C. S. Sennae fructus Analysis an devaluation of the new draft monographs for the European Pharmacopoeia. *Pharmind.* **2006**, 11, 1650-60.

[154]   Desobry, S. A.; Netto F. M.; Labuza, T. P. Comparison of spray-drying, drum-drying and freeze-drying for ß-Carotene encapsulation and preservation. *J. Food Sci.* **2006**, 62, 1159-1162.

[155]   Harnkarnsujarit, N.; Charoenrein S.; Roos Y. H. Microstructure formation of maltodextrin and sugar matrices in freeze-dried systems. *Carbohydr. Polym.* **2012**, 88, 734-742.

[156]   Meister, E. Methodology, data interpretation and practical transfer of freeze-dry microscopy. Dissertation, Friedrich-Alexander-Universität Erlangen-Nürnberg, Erlangen-Nürnberg, Germany, 2009.

[157]   Achanta, A. S.; Adusumilli, P. S.; James, K. W.; Rhodes, C. T. Hot-Melt Coating: Water sorption behavior of excipient films. *Drug. Dev. Ind. Pharm.* **2001**, 27, 241-250.

[158]   Tiwari, R.; Murthy, R. S. R.; Agarwal, S. K. The influence of hot melt subcoat and polymer coat combination on highly water soluble sustained release multiparticulate formulation. *Int. J. Drug. Delivery.* **2013**, 5, 131-136.

Appendix

A Curriculum vitae

Lebenslauf entfällt aus datenschutzrechtlichen Gründen

B Conference contributions and publications

In context with this work, the following contributions have been presented at

conferences and journal articles have been published.

Conference contributions - oral presentations

Auswertung massenspektrometrischer Untersuchungen des Senna-
Monographie Entwurfes. Fachgruppe Phytopharmazie und Naturstoffe, 2017,
zhaw Zürich, Schweiz.

Conference contributions - poster presentations

Moisture content and particle morphology of spray-dried Sennae fructus
extracts: A stability study, Meeting of the American Association of
Pharmaceutical Scientists 2017, San Diego, USA.

Addition of maltodextrin to Sennae fructus extracts during spray-drying,
fluidized bed granulation, and freeze-drying, 11th PBP World Meeting 2018,
Granada, Spain.

Hot-melt coating for highly moisture-sensitive tablets, 3rd European Conference
on Pharmaceutics 2019, Bologna, Italy.

Journal articles with authors contributions and reference chapters.

Title	Journal	Authors	Contribution to the work	Percentage	Reference chapters
Sennae fructus. Analysis and evaluation of the new draft monographs for the European Pharmacopoeia	Pharmaceutical Industry	Zier, K.I. Schultze, W. Sakmann, A. Leopold, C.S.	Project plan, experiments, data analysis, publication Supervisor Supervisor Supervisor	100 %	2.2.1, 3.1
Factors influencing the properties and the stability of spray-dried Sennae fructus extracts	Drug Development and Industrial Pharmacy	Zier, K.I. Schultze, W. Leopold, C.S.	Project plan, experiments, data analysis, publication Supervisor Supervisor	100 %	2.2.1, 2.2.3, 2.2.5, 3.2
Stabilizing and destabilizing effects of drug-excipient interactions in spray-dried, freeze-dried, and granulated Sennae fructus extracts	Drying Technology	Zier, K.I. Schultze, W. Sazama, U. Fröba, M. Leopold, C.S.	Project plan, experiments, data analysis, publication Supervisor Data acquisition Supervisor Supervisor	95 % 5 %	2.2.1, 2.2.2, 2.2.4, 2.2.5, 3.3
Combination of a hot-melt subcoating and an enteric coating for moisture protection of hygroscopic Sennae fructus tablets	Pharmaceutical Development and Technology	Zier, K.I. Schultze, W. Leopold, C.S.	Project plan, experiments, data analysis, publication Supervisor Supervisor	100 %	2.2.4, 2.2.6, 3.4

C Hazardous materials

Substance	Supplier	Danger symbol	Hazard statements	Precautionary statements
Acetonitrile	VWR, Hannover, Germany		H225, H302+H312+H332, H319	P210, P280, P305+338+351
Anhydrous formic acid	Sigma-Aldrich, Schnelldorf, Germany		H226, H290, H302, H314, H331	P210, P280, P303+361+353, P304+340, P305+351+338
Chrysophanol	Carl Roth, Karlsruhe, Germany		H315, H319	P264, P280, P302+352, P305+351+338, P332+313, P337+313, P362+364
Combi Titrant 5	Merck, Darmstadt, Germany		H360, H315, H318, H351, H372	P201, P280, P302+352, P305+351+338

Methanol	Honeywell, Erkrath, Germany		H225, H301+H311+331, H370	P210, P270, P280, P303+361+353, P304+340, P308+311
Physcion	Carl Roth, Karlsruhe, Germany		H315, H319, H335	P261, P305+351+338
Rhein	Carl Roth, Karlsruhe, Germany		H315, H319, H335	P305+351+338
Rhein-8-glycoside	PhytoLab, Vesten-bergsgreuth, Germany		H315, H319, H335	P302+352, P305+351+338
Sennoside A1	PhytoLab, Vesten-bergsgreuth, Germany		H302	P264, P270, P301+312+330, P501

D Acknowledgements

This thesis was prepared at the University of Hamburg, at the Department of Chemistry in the division of Pharmaceutical Technology on the initiative and under supervision of Professor Dr. Claudia S. Leopold.

First of all, I would like to thank Prof. Dr. Leopold for the chance to be a member of her research group. Her guidance and support made it possible for me to work on a topic that was of great interest to me. I deeply appreciate her provided freedom in my research and thank her for the inspiring scientific discussions.

Furthermore, I wish to express my sincere appreciation to PD Dr. Wulf Schultze. I really enjoyed his motivation, his effort for the joint research project, and the helpful discussions during all the last years.

Moreover, I would like to show my deep appreciation to Dr. Philip Berghöfer, who has the substance of a genius. He has given this research project a soul. Without his admiration for the plant Senna and his experiences, the goal of this project would not have been realized. I would also like to thank him and Dr. Jörg Rutz for their understanding, trust, and the opportunity to combine flexible work and research.

Additionally, I am grateful to Prof. Dr. Sascha Rohn for evaluating this thesis. Furthermore, I would like to thank Prof. Dr. Christian Stark and Dr. Ulrich Riederer for being members of the examination committee.

I also wish to show my gratitude to Dr. Albrecht Sakmann, who has been tolerant and supportive and gave me constructive comments. Petra Borbe and Kai Braunschweig are thanked for their assistance with regard to TGA, HPLC analysis, spray-drying, and granulation. Special thanks to Kai Braunschweig for his support, which was often helpful because of the distance between Bremen and Hamburg.

In addition, I thank Dr. Maria Riedner and her team for the friendly welcome in their lab and their help regarding the MS measurements. Her support was especially in my first research year invaluable.

Also, I owe a very important debt to Uta Sazama and Prof. Dr. Michael Fröba for the assistance with simultaneous TGA-DSC-MS measurements, their meticulous comments were an enormous help to me.

Furthermore, I would like to acknowledge my colleagues from the working group of Pharmaceutical Technology, it was a pleasure to work and to take a rest from work with you. I especially thank Dr. Ina Petry and Alexander Kalies for the good times during the conference journeys.

I would like to thank Steffen Wirth, Katharina Holzapfel, Alexander Kalies, Cristian Kulcitki, and Hendrik Küllmar for proof reading of this thesis. Special thanks go also to my former colleagues Dr. Anna Novikova and Dr. Claudia Al-Karawi for their great support and the productive scientific discussions.

I am deeply grateful to all my family and friends for their endless understanding, their support in all situations, and patience during the last years. Their encouragement significantly contributed to the success of this work.

Declaration on oath / Eidesstattliche Versicherung

Hiermit versichere ich an Eides statt, die vorliegende Dissertation selbst verfasst und keine anderen als die angegebenen Hilfsmittel benutzt zu haben. Die eingereichte schriftliche Fassung entspricht der auf dem elektronischen Speichermedium. Ich versichere, dass diese Dissertation nicht in einem früheren Promotionsverfahren eingereicht wurde.

Datum, Unterschrift